INFORMATION TO USERS

This material was produced from a microfilm copy of the original document. While the most advanced technological means to photograph and reproduce this document have been used, the quality is heavily dependent upon the quality of the original submitted.

The following explanation of techniques is provided to help you understand markings or patterns which may appear on this reproduction.

1. The sign or "target" for pages apparently lacking from the document photographed is "Missing Page(s)". If it was possible to obtain the missing page(s) or section, they are spliced into the film along with adjacent pages. This may have necessitated cutting thru an image and duplicating adjacent pages to insure you complete continuity.

2. When an image on the film is obliterated with a large round black mark, it is an indication that the photographer suspected that the copy may have moved during exposure and thus cause a blurred image. You will find a good image of the page in the adjacent frame.

3. When a map, drawing or chart, etc., was part of the material being photographed the photographer followed a definite method in "sectioning" the material. It is customary to begin photoing at the upper left hand corner of a large sheet and to continue photoing from left to right in equal sections with a small overlap. If necessary, sectioning is continued again – beginning below the first row and continuing on until complete.

4. The majority of users indicate that the textual content is of greatest value, however, a somewhat higher quality reproduction could be made from "photographs" if essential to the understanding of the dissertation. Silver prints of "photographs" may be ordered at additional charge by writing the Order Department, giving the catalog number, title, author and specific pages you wish reproduced.

5. PLEASE NOTE: Some pages may have indistinct print. Filmed as received.

University Microfilms International
300 North Zeeb Road
Ann Arbor, Michigan 48106 USA
St. John's Road, Tyler's Green
High Wycombe, Bucks, England HP10 8HR

77-17,968

CHON, Chun-Su, 1942-
DYNAMIC RESPONSE OF FRICTION PILES.

The University of Michigan, Ph.D., 1977
Engineering, civil

Xerox University Microfilms, Ann Arbor, Michigan 48106

PLEASE NOTE:

The following dissertation contains computer print-outs that have light and indistinct print. Filmed as received.

UNIVERSITY MICROFILMS.

DYNAMIC RESPONSE OF FRICTION PILES

by

Chun-Su Chon

A dissertation submitted in partial fulfillment
of the requirements for the degree of
Doctor of Philosophy
(Civil Engineering)
in The University of Michigan
1977

Doctoral Committee:

Professor Frank E. Richart, Jr., Co-Chairman
Professor Richard D. Woods, Co-Chairman
Professor Samuel K. Clark
Professor Donald H. Gray
Professor E. Benjamin Wylie

To My Wife

ACKNOWLEDGEMENTS

The author would like to express his sincerest appreciation to Professor Frank E. Richart, Jr. and Professor Richard D. Woods for their continued guidance and encouragement throughout this study. Sincere appreciation is also extended to his Committee members Professor Donald H. Gray, Professor E. Benjamin Wylie, and Professor Samuel K. Clark for their interests and advice during the investigation.

This study was funded by the National Science Foundation, Grant No. GK-35789. This financial assistance from the National Science Foundation is gratefully acknowledged. The author is also grateful for the teaching assistantships and other financial assistance granted by the Civil Engineering Department of the University of Michigan.

The author wishes to extend his sincere appreciations to his colleagues in Soil Dynamics at the University of Michigan, D. G. Anderson, F. Somogyi, N. F. Allen, for their continuous interest and assistance in the performance of the tests. The author also wishes to extend his sincere appreciation to technical personnel at G. G. Brown Laboratory in particular, H. G. Chalmers, L. E. North,

and D. Hutchings for their assistance in machining and electronic services required for the preparation of the tests.

Finally, the author wishes to thank his wife, Young-Hee, for her patience and sacrifice during the past four years.

TABLE OF CONTENTS

DEDICATION..... ii

ACKNOWLEDGEMENTS..... iii

LIST OF TABLES..... ix

LIST OF FIGURES..... x

LIST OF APPENDICES..... xv

NOMENCLATURE..... xvi

CHAPTER

I. INTRODUCTION..... 1

A. Background..... 1
B. Objective..... 1
C. Approach..... 2

II. REVIEW OF PREVIOUS WORK..... 3

A. Resistance of Piles to Static Horizontal Load..... 3
B. Response of Piles to Dynamic Loads..... 10

1. Types of Dynamic Loadings
2. Analytical Methods
3. Test Results

III. TEST FACILITIES, EQUIPMENT AND MODEL PILES.. 20

A. Quicksand Tank..... 20

1. Tank Construction
   a. Tank
   b. Water Supply System
   c. Filter System
2. Sand
3. Working Platform
4. Hoist System
5. Reaction Beam

B. Sand Density Control..... 35

1. Spud Vibrator
2. Dutch Cone Penetrometer

C. Loading Systems..... 36

1. Static Test
   a. Screw-jack
   b. Gilmore Acutator
   c. Plucking Test
2. Dynamic Tests
   a. Lazan Oscillator
   b. Gilmore Actuator

D. Instrumentation..... 41

1. Transducers
   a. Load Cell
   b. LVDT
   c. Velocity Transducer
2. Recorders
   a. Dual Channel Recorder
   b. Four Channel Recorder
   c. Oscilloscope
3. Resonant Column Device
4. Data Trak
5. Miscellaneous
   a. Dynamometer
   b. Proving Ring
   c. Dial Gauges

E. Piles..... 45

IV. TEST PROCEDURES..... 49

A. Preparation of Sand..... 49

1. Quicksand Operation
2. Densification of Sand
3. Density Control Test
   a. In-situ Density Test
   b. Dutch Cone Test

B. Installation of Pile..... 52
C. Dynamic Properties of Sand..... 53

1. Cross-Hole Test
2. Resonant Column Test

D. Plucking Tests..... 55
E. Static Tests..... 58
F. Dynamic Tests..... 59

1. Load-Controlled Tests
2. Displacement-Controlled Tests

G. Pull-Out Capacity Tests..... 64

V. PROPERTIES OF SAND..... 65

A. Density Control..... 65

1. In-situ Density Test
2. Dutch Cone Penetrometer Test

B. Shear Modulus of the Sand..... 66

1. Cross-Hole Tests
2. Resonant-Column Tests
3. Empirical Equation
4. Comparison of Modulus by Three Methods
5. Curved Path Theory

VI. RESISTANCE OF PILES TO STATIC HORIZONTAL LOADS..... 75

A. Theoretical Analysis..... 75

1. Kubo's Method
   a. Determination of Conversion Factors
   b. Standard Curves
   c. Procedures for the Application
2. Kuhlemeyer's Method

B. Comparison of Experimental Data with Theoretical Analyses..... 86

VII. RESPONSE OF PILES TO DYNAMIC LOADS..... 96

A. Theoretical Analysis..... 96

1. Inverse Non-linear Problem
2. Pure Rotational Solution of a Short Rigid Pile
3. Finite Element Method

B. Results of Dynamic Tests..... 125

1. Displacement-Controlled Dynamic Tests
2. Load-Controlled Dynamic Tests
3. Plucking Tests

C. Parametric Study..... 144

1. Baranov's Solution
2. Kuhlemeyer's Solution

D. Comparisons and Discussions..... 162

1. Comparison of Results
2. Selection of the Shear Modulus and the Modulus of Elasticity of Soil

VIII. PULL-OUT CAPACITY OF PILES..... 168

A. Review of Previous Work..... 168
B. Experimental Results..... 170

IX. SUMMARY AND CONCLUSIONS..... 175

APPENDICES..... 179

REFERENCES..... 198

LIST OF TABLES

Table		Page
3.1.	List of equipment	23
3.2.	Structural characteristics of model piles	48
6.1.	Standard curves for free-head pile	85
7.1.	Polynomial expansion coefficients for I_{ij} and J_{ij}	122
7.2.	Result of Lazan oscillator tests embedded in uniform submerged dense sand	138
7.3.	Results of the plucking tests	142
7.4.	Effect of the change of Poisson's ratio of soil	152
7.5.	Effect of the change of dynamic shear modulus in Baranov's solution	152
7.6.	Average values of E_s for cohesionless soils	156
7.7.	Effect of the change of modulus of elasticity of soil in Kuhlemeyer's solution	162
7.8.	Comparison of test results with theoretical analysis	164
7.9.	Values of E_s for analytical solutions	167
8.1.	Pull-out capacity	174
9.1.	List of tests performed	176

LIST OF FIGURES

Figure		Page
2.1.	Water wave force acting on a cylindrical pile	10
2.2.	Jump phenomena at constant amplitude of force	16
3.1.	General layout of the test facilities	21
3.2.	Picture of the test facilities	22
3.3.	Grainsize distribution of Muskegon sand and filter sand	30
3.4.	Details of filter layers and water distribution system	31
3.5.	Schematic diagram of Dutch cone penetrometer and its support frame on top of the quicksand tank	36
3.6.	Cross-sectional view of the screw-jack static loading system	37
3.7.	Interior of the Lazan oscillator showing rotating eccentric masses	40
3.8.	Attachment of the Gilmore hydraulic actuator to the pile	42
3.9.	Shapes of model piles	46
4.1.	Pattern and order of the vibrator insertions for the densification of sand	51
4.2.	Schematic diagram of cross-hole test	53
4.3.	Schematic diagram of equipment used for the resonant column test	55
4.4.	Analysis of transient response of a viscously damped single-degree-of-freedom system	56

Figure		Page
4.5.	Schematic diagram of equipment used for plucking test.....	57
4.6.	Schematic diagram of equipment used for the high frequency dynamic test using Lazan eccentric rotating mass type oscillator.....	60
4.7.	Picture of the actual setup of equipment for Lazan test.....	61
4.8.	Schematic diagram of equipment used for the displacement-controlled low frequency dynamic test using Gilmore hydraulic actuator.....	62
5.1.	Results of Dutch cone penetrometer tests....	67
5.2.	Variation of shear modulus with depth obtained from the cross-hole test, the resonant column test and the empirical equation.....	69
5.3.	Diagram of curved wave path theory.....	73
5.4.	Variation of shear modulus with depth obtained from the cross-hole test, the resonant column test, the empirical equation and the curved wave path theory....	74
6.1.	Standard curve for free-head pile, deflection at the ground surface.....	82
6.2.	Standard curve for free-head pile, inclination at the ground surface.....	83
6.3.	Relationship between $\bar{N}$ and k_s for the uniform sand.....	84
6.4.	The rectangular ring element for Kuhlemeyer solution.....	86
6.5.	Static test results, displacement vs. horizontal load.....	92
6.6.	Static test results, displacement vs. horizontal load.....	93
6.7.	Static test results, horizontal displacement vs. horizontal load per unit width.....	96

Figure		Page
7.1.	Determination of undamped natural frequency curve.....	100
7.2.	Calculation of damping from non-linear response curves.....	101
7.3.	Diagram of soil-pile system subjected to lateral dynamic excitation and assumption of Baranov's thin elastic layers.....	103
7.4.	Graphical presentation of vector Aexp(iα) in complex plane.....	112
7.5.	Coefficients of side layer reaction for horizontal displacement.....	117
7.6.	Coefficients of side layer reaction for rotation for all Poisson's ratios.....	118
7.7.	Load-displacement curves from displacement-controlled dynamic test.....	126
7.8.	Load-displacement curves from displacement-controlled dynamic test.....	126
7.9.	Load-displacement curves from displacement-controlled dynamic test.....	127
7.10.	Load-displacement curves from displacement-controlled dynamic test.....	127
7.11.	Load-displacement curves from displacement-controlled dynamic test.....	128
7.12.	Load-displacement curves from displacement-controlled dynamic test.....	128
7.13.	Load-displacement curves from displacement-controlled dynamic test.....	129
7.14.	Load-displacement curves from displacement-controlled dynamic test.....	129
7.15.	Load-displacement curves from displacement-controlled dynamic test.....	130
7.16.	Load-displacement curves from displacement-controlled dynamic test.....	130

Figure		Page
7.17.	Load-displacement curves from displacement-controlled dynamic test.....	131
7.18.	Load-displacement curves from displacement-controlled dynamic test.....	131
7.19.	The exciting force generated by the Lazan oscillator with different angles of eccentricity of the unbalanced masses.....	133
7.20.	Dynamic response curves of load-controlled Lazan test.....	135
7.21.	Dynamic response curves of load-controlled Lazan test.....	136
7.22.	Dynamic response curves of load-controlled Lazan test.....	137
7.23.	Transient decay curve of plucking test.....	140
7.24.	Transient decay curve of plucking test.....	141
7.25.	Comparison of the transient decay curves of plucking tests in submerged and in drained dense sand.....	143
7.26.	Effects of increase of the exciting force, and pile size.....	147
7.27.	Damping ratio curves calculated from Baranov's solution for 3½ in. and 4½ in. OD round steel pipe piles.....	148
7.28.	Effect of the height of the excitation from the ground surface.....	149
7.29.	Effect of the mass located on top of the pile.....	151
7.30.	Effect of increase of the exciting force, and pile size.....	156
7.31.	Damping ratio curves calculated from Kuhlemeyer's solution for 3½ in. and 4½ in. OD round steel pipe piles.....	157
7.32.	Effect of the mass located on top of the pile.....	158

Figure		Page
7.33.	Effect of the height of the excitation from the ground surface.....	160
7.34.	Effect of the height of the excitation from the ground surface.....	161
A.3.1.	Dynamic response curves of load-controlled Lazan test.....	192
A.3.2.	Dynamic response curves of load-controlled Lazan test.....	193
A.3.3.	Dynamic response curves of load-controlled Lazan test.....	194
A.3.4.	Dynamic response curves of load-controlled Lazan test.....	195
A.3.5.	Dynamic response curves of load-controlled Lazan test.....	196
A.3.6.	Dynamic response curves of load-controlled Lazan test.....	197

LIST OF APPENDICES

Appendix		Page
I.	Computer program for Baranov's solution...	179
II.	Computer program for Kuhlemeyer's solution.....	184
III.	Additional dynamic response curves from Lazan tests.....	191

NOMENCLATURE

A	vibration amplitude, inch
a_o	dimensionless frequency
a_{ij}	dimensionless flexibility coefficients
A_s	coefficient of shear modulus which depends on void ratio and the confining pressure
A_ψ	dimensionless rotational amplitude
A_T	horizontal displacement amplitude at which a straight line from the origin becomes tangent to the response curve
A_u	dimensionless displacement amplitude
B	width of the pile, inch
c	damping coefficient, lb-sec/in.
c_c	critical damping coefficient, lb-sec/in.
C_D	drag coefficient
c_e	the equivalent linear damping coefficient
c_ψ	the rotational damping coefficient, in.-lb-sec/rad
C_M	coefficient of mass
D	damping ratio, percent
d	diameter of pile, inch
e	void ratio
$\bar{e}$	eccentricity of the unbalanced masses in the Lazan oscillator

E_p	modulus of elasticity of the pile material, psi
E_s	modulus of elasticity of the soil, psi
f_d	damped natural frequency, Hz
f_n	undamped natural frequency, Hz
F_{ij}	flexibility coefficient
G	shear modulus, psi
G_s	shear modulus at the tip of the pile, psi
g_{ij}	stiffness terms of the function H_{ij}
h_{ij}	damping terms of the function H_{ij}
h_Q	distance from the rotation center to the excitation point, ft.
i	$= (-1)^{\frac{1}{2}}$
i	= dy/dz (Kubo's solution)
I_ψ	mass moment of inertia of the pile and weight located on top of the pile about the center of rotation, in-lb-sec^2
I_p	moment of inertia of the pile cross-section, in^4
I_{US}	displacement influence factor for horizontal load only
I_{UM}	displacement influence factor for moment only
$I_{\theta S}$	rotation influence factor for horizontal load only
$I_{\theta M}$	rotation influence factor for moment only
k, k_h	coefficient of horizontal subgrade reaction, ton/cu. ft.
k_s	coefficient of horizontal subgrade reaction, Kubo's solution, g-cm$^{-3.5}$
k_e	the equivalent linear spring constant

k_ψ	rotational spring constant, in-lb/rad
K_o	coefficient of the earth pressure at rest
k_x	lateral translation spring constant, lb/in.
L	embedded length of the pile, ft.
L_c	distance between two boreholes in cross-hole test, ft.
ℓ_Q	height of the excitation from the ground surface, ft.
m	mass located on top of the pile, slug
m_e	the rotating unbalanced masses, slug
N	standard penetration number, blow
$\bar{N}$	standard penetration number at 1 meter depth, blow
n_h	constant of horizontal subgrade reaction, ton/cu. ft.
N_ψ	side reactive moment from the soil surrounding the pile
p	lateral earth pressure, psi
p_h	horizontal pressure on a vertical face of the pile, psi
P_h	horizontal load, lbs
Q	shearing force acting on the pile, lbs
Q(t)	dynamic horizontal exciting force, lbs
q_c	bearing capacity obtained from Dutch cone test, kg/cm^2
r_o	radius of the pile, in.
R_{EI}	ratio of the pile flexibilities
R_i	ratio of the slope of the pile deflections
R_Q	ratio of the shear force occurred in the piles

R_M	ratio of the moment occurred in the piles
R_y	ratio of the horizontal displacement of the piles
R_z	ratio of the depth of the piles
S	horizontal load acting at the ground surface, lbs
S_p	horizontal load for prototype pile
S_s	horizontal load for standard pile
S_ψ	rigidity parameter for rotation
S_u	rigidity parameter for displacement
t	time, sec.
T_d	undamped period of the vibration, sec.
T(t)	torque caused by the excitation of the lateral load Q(t), in-lb
T_o	overturning torque for a rotating mass type excitation, in-lb
u	horizontal displacement, inch
u	horizontal component of the water velocity, (Morison, 1950)
U	horizontal displacement function
v_s	shear wave velocity in soil, ft/sec
w	water content of the soil, percent
y	horizontal displacement, inch
y_o	horizontal displacement at ground surface, inch
z	depth, ft
z_o	depth to the source of the body wave in cross-hole test, ft.

$\alpha = \omega_o D$	damping coefficient
$\alpha_e = c_e(A)/2m$	coefficient of equivalent linear damping
γ_D	dry unit weight of the soil, pcf
$\gamma_{sub.}$	submerged unit weight of the soil, pcf
θ	angle of eccentricity of the unbalanced masses in the Lazan oscillator, degree
λ	depth to the rotation center from the ground surface, ft.
ν	Poisson's ratio
ξ	distance from the rotation center, ft.
π	3.14159.....
ρ	mass density of fluid, slug/ft^3
$\rho_m = m_e\bar{e}/m$	reduced eccentricity
ρ_s	mass density of soil, slug/ft^3
$\bar{\sigma}_o$	confining pressure, psi
ϕ	phase angle, rad
ψ	rotational amplitude of the pile, rad
ω	frequency of excitation, rad/sec
ω_o	natural frequency of linear vibration, rad/sec
ω_{on}	arbitrary natural frequency on the backgone curve of the non-linear vibration, rad/sec
ω_T	frequency corresponding to the amplitude, A_T, rad/sec
$\omega_{I,\ II}$	frequencies of points of interaction with straight line passing through origin, rad/sec

CHAPTER I

INTRODUCTION

A. Background

Foundations for large machines, buildings and other structures generally fall into either of two major categories: shallow foundations or deep foundations. Both categories of foundations are easily analyzed and designed for static loads and shallow foundations are now routinely analyzed and designed for dynamic loads, but deep foundations (piles, piers, caissons) cannot, with confidence, be analyzed or designed for dynamic loads.

For many sites and many kinds of structures, piles are the only possible foundation, and when, either because of the seismicity of the site or because of machine generated forces, the piles will be subject to dynamic loads, dynamic analysis and design are necessary. Recently, there have been several methods proposed for dynamic analysis and design for both vertical and horizontal (lateral) pile loads, but none of these have been widely accepted.

B. Objective

This study has been performed in an attempt to establish the influence of several "soil-pile interaction"

parameters on the dynamic and static response of single friction piles to lateral loads. The lateral response was studied because lateral pile displacement dramatically influences the vertical pile capacity by changing the pile-soil interface conditions.

By performing model pile tests and comparing the results with analyses suggested by others, the influence of pile, soil, and loading parameters were investigated.

C. Approach

Both dynamic and static model pile tests were performed in a specially constructed facility which was designed to operate as a "quicksand" tank. The quicksand operation provided for rapid and easy reconstitution of the sand to preselected conditions before each test.

The static lateral pile test results were compared with a non-linear elastic theory and a finite element method solution. The dynamic lateral pile test results were compared with an elastic side layer reaction theory (closed form solution) and a finite element method solution.

Because of the dependency of vertical pile capacity on horizontal pile displacement, pull-out capacity tests were also performed on all piles after they had undergone static or dynamic lateral testing. Those results were compared with vertical pull-out control test for which no lateral displacement had occurred.

CHAPTER II

REVIEW OF PREVIOUS WORK

A. Resistance of Piles to Static Horizontal Loads

Pile foundations are designed to transfer load from the superstructure to the soil whenever the soil or loading conditions do not allow selection of shallow foundations. Pile foundations for structures such as bridge abutments, piers, dolphins and tall buildings may receive eccentric or horizontal static loadings. These loadings depend on the location and use of the structures, and may be developed by ship impacts, wave forces, wind loads, machine vibrations, or earthquake motions.

To analyze the complex phenomena which occur in pile-soil systems, the following factors should be considered; dimensions and elastic characteristics of the pile (width, length, material, moment of inertia, flexural rigidity, ultimate strength), depth of embedment of pile, displacement of pile, stress-strain relations of the soil, effective unit weight of soil, creep or consolidation of soil, magnitude of horizontal load, height of the loading point, loading rate, load duration, and load history. It is often difficult to consider all these factors in actual

design, but some of them have been simplified or omitted at times.

Many experimental and/or theoretical investigations on the resistance and behavior of laterally loaded piles have been reported through the years. No attempt will be made herein to summarize the voluminous literature treating the static behavior of a pile subjected to horizontal loads. However, two recent summaries should be noted. Broms (1972) presented a state-of-the-art report summarizing the work up to 1972. Nishida (1975) published another state-of-the-art review for lateral resistance of pile foundations for the Japanese Association for Steel Pipe Piles. He included not only studies on a single pile but also studies on groups of connected piles. He also added a lengthy bibliography of more than 500 articles, most of which were from the United States of America and Japan, on lateral resistance of pile foundations and related subjects.

Theoretical procedures which have been adopted for the study of laterally loaded piles generally use methods based on (a) ultimate soil strength, (b) elastic subgrade reaction, (c) theory of elasticity, (d) theories for beam on visco-elastic foundation, or (e) elasto-plastic layered soil. These analytical studies may involve exact mathematical solutions or approximate solutions obtained from the finite difference method or the finite element method.

Studies of laterally loaded piles in sand have usually been evaluated by considering a coefficient of horizontal subgrade reaction k_h (see Terzaghi, 1955) which relates the horizontal pressure on a vertical pile face p_h to the horizontal displacement of the pile y, or

$$p_h = k_h\, y \tag{2.1.1}$$

The terms on the right hand side of Eq. (2.1.1) represent the increase in horizontal stress because of pile motion. As noted from previous studies, k_h may be a function of a number of variables including some function of depth and horizontal displacement. Terzaghi (1955) indicated that it was often sufficient to consider k_h as a linear function of z, expressed as:

$$k_h = n_h\, (z/B) \tag{2.1.2}$$

in which B is the pile width, and n_h is a constant of horizontal subgrade reaction. Terzaghi suggested typical values for n_h. With the above assumptions, it is possible to develop dimensionless coefficients for the displacement, slope, shear, and moment along the pile through the application of the theory of subgrade reaction. Diagrams of these coefficients have been prepared by Reese and Matlock (1956), Richart (1957) (developed for sheet-pile walls, but these diagrams apply directly to single piles also), Davisson (1960), and others.

Model tests on single piles and pile groups in sand (for example, Mitchell, 1957; Prakash, 1961; Davisson and Salley, 1970) have shown that the concept of subgrade reaction described by Eq. (2.1.2) permits reasonably good correlation with test results. That is, the theoretical solutions can be adjusted to agree with test results by a suitable choice of n_h. Mitchell (1957) tested a flexible steel pile in medium dense sand under relatively small deformations to illustrate this concept. Tests (for example, Richart, 1959) which have developed larger lateral displacements under single loads have demonstrated that n_h decreases as the displacement increases. Pile behavior based upon Eqs. (2.1.1) and (2.1.2) represent linear elastic solutions for which superposition is valid.

Kubo (1961, 1962a, 1962b, 1964) and Kubo et al. (1967) have suggested a non-linear relationship between lateral earth pressure and horizontal displacement

$$p = k_s \, z \, y^{\frac{1}{2}} \qquad (2.1.3)$$

for soils where the coefficient of subgrade reaction increased with depth as with uniform sand and normally consolidated clay. He established the above relation through many lateral load tests on single free-head model piles embedded in layered, saturated uniform sand. Kubo determined from the test data "Standard Curves" for displacement at ground level, displacement at the top of the

pile, maximum bending moment and effective length of embedment. The actual behavior of piles can be predicted by applying similarity rules between the standard pile and prototype pile. However, similarity rules result in non-linear differential equations which are difficult to solve analytically. Kubo made many diagrams to facilitate the application of the theory to practical design. Kubo's method is also known as the "Port and Harbor Research Institute method" in Japan. Yamashita et al. (1971) calculated new standard curves following Kubo's theory by adopting a new standard pile and through numerical integration by the Runge-Kutta-Gill method of the dimensionless equation

$$\frac{d^4y}{dz^4} + Z^m Y^{\frac{1}{2}} = 0 \qquad (2.1.4)$$

in which

$$Z = z/C_z,$$

and

$$Y = y/C_y$$

are dimensionless. C_z and C_y are any arbitrary non-zero numbers which have the relationship of

$$C_y = \left(\frac{Bk}{EI}\right)^2 C_z^{2m+8} \qquad (2.1.5)$$

in which k = coefficient of subgrade reaction of soil, and m = dimensionless constant which is 1 for uniform sand. Results based on the new standard pile show extremely good agreement with Kubo's results for displacement at the top of pile, displacement at ground level, and maximum moment. However, for the effective length it shows slightly higher values.

Tadashi (1974) suggested a complex subgrade reaction theory which assumed that the soil near the surface, where displacement was large, showed plastic behavior and the soil below the plastic zone followed elastic behavior. The resistance of soil in the plastic zone was assumed to increase in proportion to the nth power of the depth along pile. The results were compared with the test data and concluded that n = 2 could be used for dry sand, and n = 1 applied for clay. Many diagrams were presented for the application of the solution.

Spillers and Stoll (1964) calculated lateral pile deflections from Mindlin's equations, based on the theory of elasticity, which assumed that the soil could be replaced by an ideal, elastic and isotropic material with a constant modulus of elasticity, E_s, and a constant Poisson's ratio, ν . The behavior of the pile was analyzed by replacing the normal force distribution on the pile by a series of concentrated forces along the pile. As a

result, they indicated the presence of plastic and elastic zones in the soil.

Poulos (1971a, 1971b) and Oteo (1972) have used a similar approach to investigate the behavior of single piles and pile groups. The finite difference method was used to calculate the lateral distribution of pressure and the lateral deflections. The major variables Poulos (1971a) mentioned were the influence of the length-to-diameter ratio, L/d and pile flexibility factor K_R, defined as

$$K_R = E_p I_p / E_s L^4 \qquad (2.1.6)$$

Displacements and rotations increased as either K_R decreased, (i.e., as the pile became more flexible) or as L/d increased. Poulos also compared the results from the subgrade reaction solutions obtained by evaluating the Hetenyi (1946) solutions. The subgrade reaction theory always indicated greater displacements than did the elastic theory. Poulos' solution has some limitations in solving pile problems in sand because it may be unrealistic to assume that the soil modulus E_s remains constant over the entire soil layer.

Kuhlemeyer (1976) suggested an improved solution similar to Poulos' by applying the finite element method for a single pile embedded in a single layer of elastic soil overlying an infinite elastic half-space with a

different modulus of elasticity. The solution readily provides an estimate of pile deflection and rotation. A critical assumption for valid application of Kuhlemeyer's solution is that the pile-soil interaction relationship is linear within the working load range.

B. Response of Piles to Dynamic Loads

The analysis of response of a soil-pile system to various dynamic horizontal loads is a very complicated problem. Nair (1969) has presented a comprehensive state-of-the-art review of dynamic and earthquake forces acting on deep foundations. He gave definitions of the dynamic loads and showed presently used methods for describing them, and several methods of analysis were also reviewed. Dynamic loads that have to be considered frequently in deep foundation design require additional discussion.

1. Types of Dynamic Loadings

Machine vibrations are primarily low amplitude steady-state vibrations which are developed by machines having rotating or reciprocating parts, and these vibrations are applied directly to the foundation. The loads are generally well defined and can be calculated from the manufacturer's data in most cases. Knowledge of the operating frequency of the machine and soil-pile response at its resonant frequency is especially important.

Earthquake and other vibratory motions of the soil may be transferred to structures through the piles and pile caps. Most earthquakes result from rock movement along existing faults, but foundations are not designed to withstand surface faulting which, in general, produces large vertical and/or horizontal displacements. In general, the horizontal displacement predominates in seismic vibrations due to a large amplitude, low frequency shear wave in the horizontal plane.

In addition, seismic vibriations can generate liquefaction in a saturated, cohesionless soil. Liquefaction affects the performance of piles adversely by decreasing the resistance of the surrounding soil which causes loss of end bearing and friction support from the soil.

Water wave forces acting on piles have been studied extensively in recent years as the number of offshore structures increased. Morison et al. (1950), for example, suggested a method of calculating the forces exerted by the surface water wave based on particle motion and empirically determined coefficients, see Fig. 2.1. The horizontal force exerted on a differential section dz for a cylindrical pile is

$$dF = (C_M \rho V \frac{\partial u}{\partial t} + \tfrac{1}{2} C_D \rho A |u| u)\, dz \qquad (2.2.1)$$

in which, V = volume of fluid displaced by the pile, ρ = mass density of fluid, C_M = coefficient of mass,

C_D = coefficient of drag, A = projected area perpendicular to the stream velocity u, t = time, u = horizontal component of water velocity based on linear theory. The horizontal component of water velocity, u, can be computed from

$$u = \frac{gHT}{2L} \frac{\cosh 2\pi (z + d)L}{\cosh 2\pi d/L} \cos 2\pi \left(\frac{X}{L} - \frac{t}{T}\right) \quad (2.2.2)$$

in which H = wave height, L = wave length, T = wave period, d = depth. The coefficients C_M and C_D are determined experimentally. The total force exerted on a pile at any time can be obtained by integration of Eq. (2.2.1).

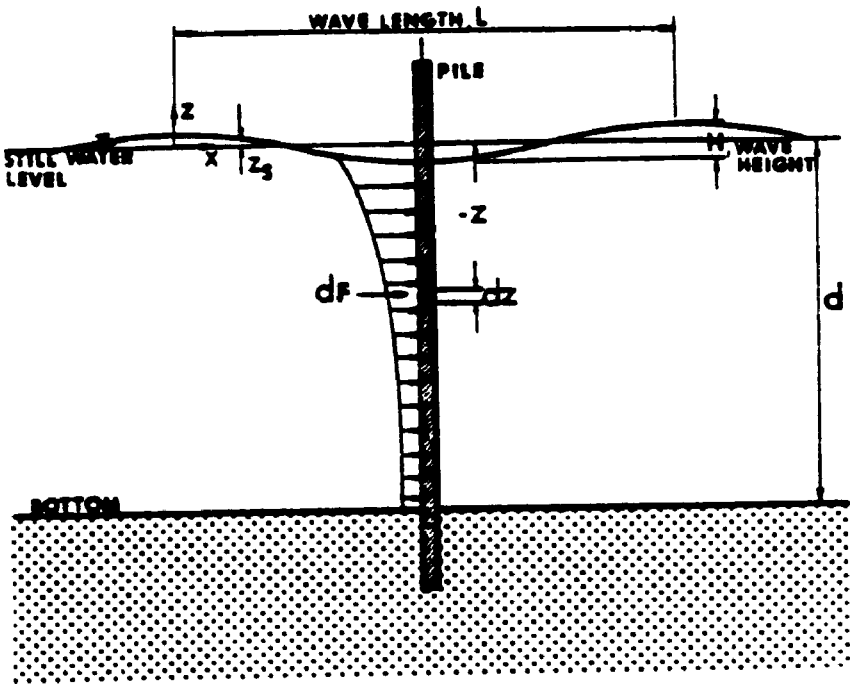

Figure 2.1 Water wave force acting on a cylindrical pile (Morison, 1950)

2. Analytical Methods

The analysis of piles embedded in soil and subjected to dynamic loading is in most cases based on either the theory of a beam on an elastic foundation, or the elastic half-space theory. Parmelee et al. (1964) combined the use of the elastic half-space theory and the Winkler assumption and presented a general method of determining the dynamic response to seismic disturbances of structures when supported on long piles extending through deep sensitive clays. Using the idealized lumped mass, soil-pile-structure system, they computed the effective soil modulus for each pile and soil mass location by using the Mindlin equation. The Winkler assumption uncoupled the springs. The viscous damping ratio was found as approximately 9.4 percent of critical damping at all depths and the creep rate was assumed constant over the first 10 seconds. Use of the elastic theory was considered satisfactory if the shear wave length was long compared to pile spacing in a particular bridge-pile-clay system which they studied. The analysis concluded that when the exciting earthquake frequency was near the fundamental shear mode frequency of the soil layer, ground level amplitudes of horizontal motion increased. Piles did not cut through the soil, but the soil movement forced the pile curvature. Thus smaller diameter piles would develop lower peak stresses than larger piles.

For bridge piers and similar structures located on long slender piles, the method outlined by Penzien (1970) may be used for analysis. He used the Mindlin theory and uncoupled Winkler model to determine the dynamic response of the clay medium alone when excited through its lower boundary by a prescribed horizontal seismic motion, and to determine the interaction of the entire system including the piles with the moving clay medium. This approach also has been applied by Yamamoto and Seki (1970) to study the earthquake response of buildings on piles.

In studying the effect of embedment on the vibration response of rigid block-type foundations, Beredugo and Novak (1971, 1972, 1973) presented an approximate analytical approach. It was based on Baranov's (1967) side layer reaction theory of linear elasticity and established the dimensionless parameters for the dynamic response of footings. They found that embedment decreased the resonant amplitude and increased the resonant frequency of the foundation. Novak (1974) also applied this theory to pile supported structures. He obtained closed-form formulas for dynamic stiffness and damping. He found that the dynamic stiffness and geometric damping of piles depended on soil-pile interaction and were governed by the following dimensionless parameters: ratio of specific mass of the soil to specific mass of the pile, ratio of shear wave velocity in the soil to longitudinal wave

velocity in the pile, ratio of length of the pile to pile radius, ratio of pile static load to Euler's buckling load, and the dimensionless frequency. The most important parameters were the wave velocity ratio and the slenderness ratio. Both pile stiffness and damping increased with increasing wave velocity ratio and with horizontal excitation. These were very sensitive to the pile length for a slenderness ratio smaller than about 25 and practically independent of pile length above this limit. A high value of slenderness ratio caused the influence of end conditions at pile tip to vanish.

Prakash and Chandrasekaran (1971) suggested a solution based on the linear elastic single-degree-of-freedom system with a spring and dashpot. They used the lumped mass idealization with the linear springs attached to analyze the pile system dynamically up to four modes of vibration. They used the Reese and Matlock (1965) solution to get the static response of the pile.

Singh, Donovan and Jobsis (1975) presented a simple and practical method of designing pile-supported foundations subjected to machine vibrating loads. They used a single-degree-of-freedom mass-spring-dashpot model and concept of an equivalent cantilever. They assumed an equivalent damping coefficient using the damping ratio in the range between 10 and 15 percent from the observation of other studies.

Nonlinear response was discussed by Muga and Wilson (1970) and this results when the natural frequency of the system depends on the amplitude of the forcing function. At one value of frequency both of a large and small magnification may occur which leads to a jump phenomena (see Fig. 2.2).

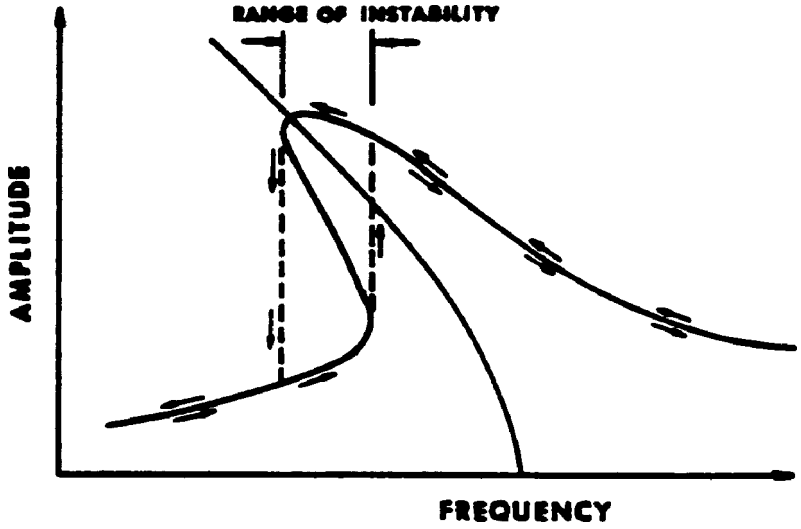

Figure 2.2 Jump phenomena at constant amplitude of force

Kuhlemeyer (1976) suggested a dynamic fundamental solution for a pile embedded in a homogeneous, isotropic elastic half-space in terms of the static solution multiplied by the associated complex frequency-dependent factors. These factors were based on a finite element solution of a beam of circular cross-section restrained by an elastic material. He found that the dynamic solution is solely dependent on the ratio of modulus of elasticity of pile

and soil and the geometric damping is proportional to dynamic stiffness.

3. Test Results

A series of model tests were analyzed using the subgrade reaction theory by Gaul (1958). Model piles of 2.375 in. OD and 96 in. long were embedded in a bentonite clay and subjected to a sinusoidally varying horizontal load at 1 cycle per second. The dynamic bending moments closely corresponded to the moments found when the load was applied statically. In these tests, there was little phase difference between the maximum dynamic load and the maximum moment, which implied low damping of the system. In the dynamic analysis it was found that the soil inertia acted as an added mass equivalent to the volume of soil displaced by the deflected pile.

Hayashi et al. (1965) used the theory of subgrade reaction for dynamic response of piles, and from model pile tests they found that the coefficient of subgrade reaction for dynamic loads was 1.1 times that for the static case. The total soil response might be treated as a nonlinear spring attached to the top pile and the pile might be treated as an inverse pendulum with a hinge at the depth where the first zero deflection was calculated. Experiments showed the following results: 1) a decrease in the amplitude of vibration leads to an increased value

of natural frequency, 2) as the number of blows of the standard penetration test increased at different sites, the resonant frequency of a given size of pile increased, and 3) the area and shape of the hysteresis curve was an exponential function of displacement, y^a where $\underline{a}$ varied between 1.0 and 1.7. It was noted that for purely viscous damping the area was proportional to y^2, and for solid friction damping it was proportional to y; thus, two forms of damping were apparently active. Further studies showed that the damping ratio of a steel pile was less than 7 percent and that the resonant amplitude decreased as $\underline{a}$ increased. The damping ratio decreased with an increased free length of the pile.

The type of response for embedded footings predicted by the theory of Beredugo and Novak was also observed in model and field experiments by Stokoe (1972). However, the condition of the backfill was found to be very important. Loose backfill reduced the effect of embedment. Experiments showed that the elastic theory was not conservative because by assuming constant soil stiffness throughout the side layer, the effect of backfill was overestimated. In shake table tests, Mononobe and Matso (1932) found that tamping the backfill reduced maximum soil pressures against vertical surfaces during vibration compared to the results found with a loose backfill.

Petrovski and Jurukovski (1975) performed fullscale single pile tests that showed a significant change in resonant frequency with a change in dynamic horizontal load. They also implied that there was a strain-softening effect of the soil-pile system. Larger amplitudes of vibration showed a decrease of the resonant frequency and damping coefficient.

Novak and Grigg (1976) conducted several dynamic experiments with model pile foundations in the field and compared the experimental results with theoretical predictions made on the basis of the Baranov theory. It was found that theory predicted the resonant amplitudes and natural frequencies reasonably well if the shear modulus of the soil was established from static pile tests.

CHAPTER III

TEST FACILITIES, EQUIPMENT, AND MODEL PILES

The scheduled tests were performed with facilities constructed in G. G. Brown Laboratory. This chapter will describe the details of those facilities and individual equipment employed at various steps of this study. Figures 3.1 and 3.2 show the general layout of the test facilities and Table 3.1 lists the major equipment used. The equipment and the procedures will be described in detail in the next chapter.

A. Quicksand Tank

A test bin was constructed as a large quicksand tank to facilitate reconstitution of the sand after each test. The test piles were located at the center of this bin, penetrating a specially prepared sand bed.

1. Tank Construction

a. Tank -- A section of corrugated, galvanized steel culvert, 7½ ft. diameter and 10 ft. long, was erected vertically to form the soil bin. The culvert was manufactured by Armco Steel Corp. at Ashland, Kentucky and was donated through Armco's Metal Production Division at

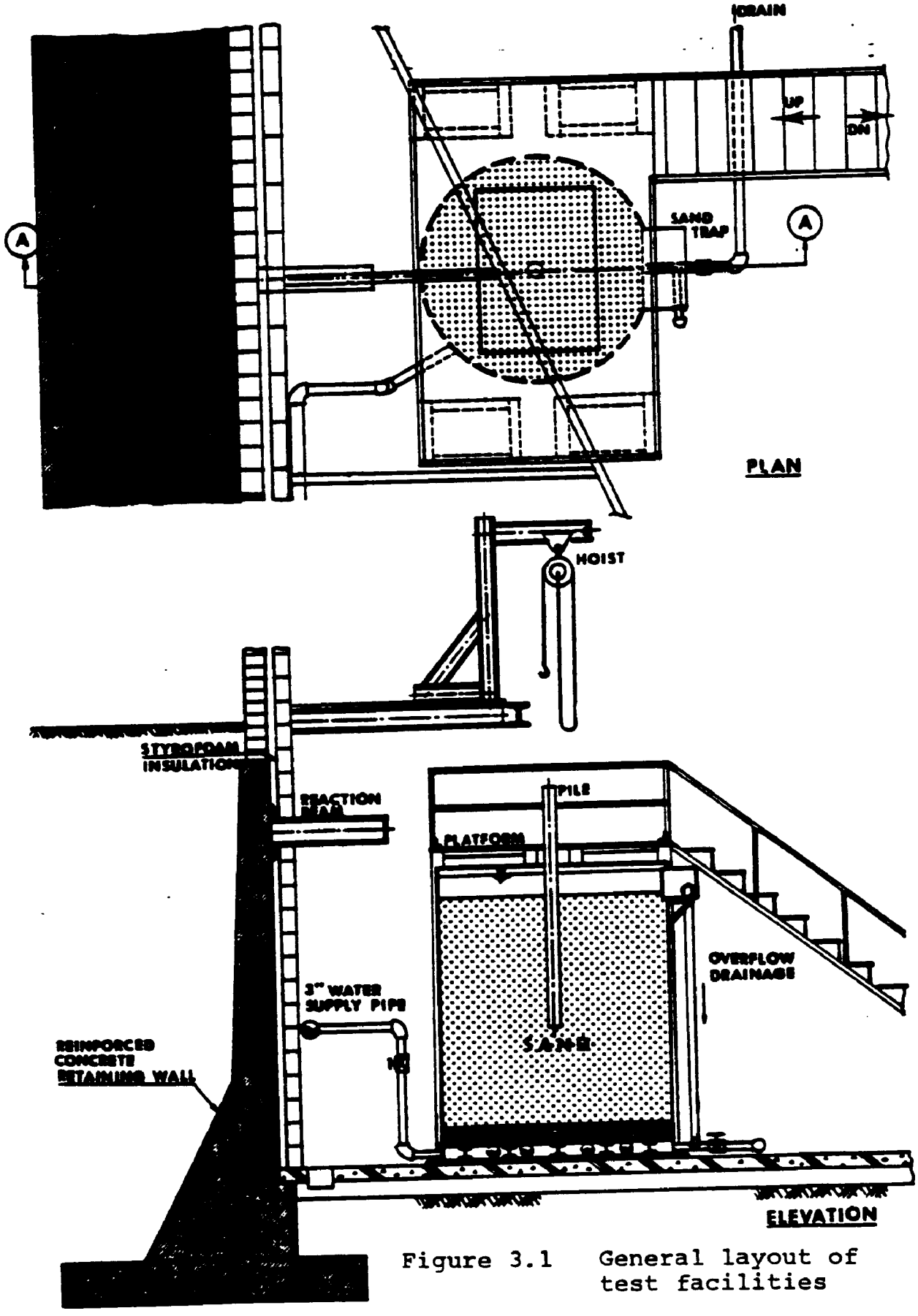

Figure 3.1 General layout of test facilities

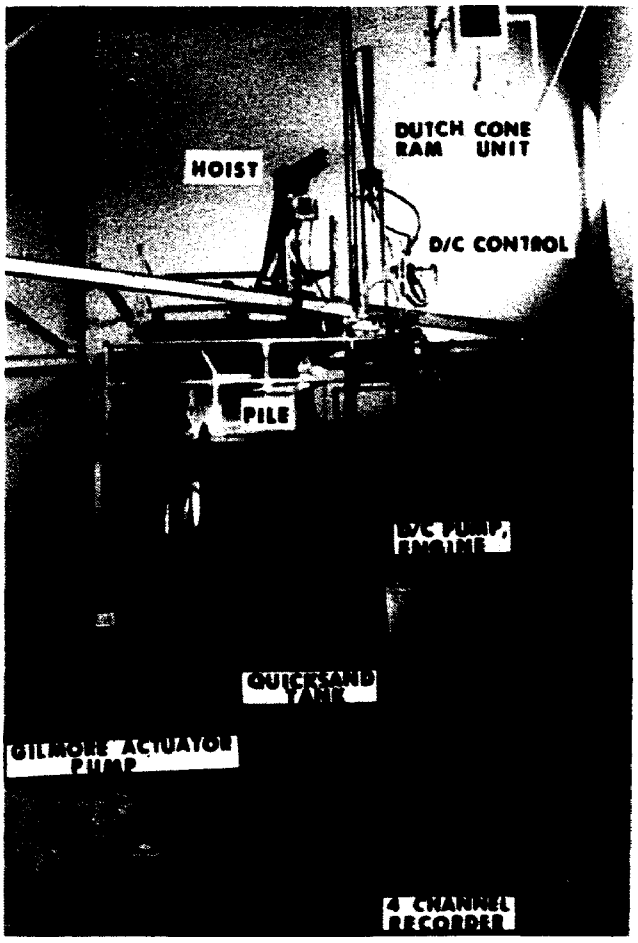

Figure 3.2 Picture of the test facilities

Table 3.1. List of Equipment

Equipment	Trade Name	Manufacturer	Model	Remarks
Spud Vibrator	Concrete Vibrator	Thor Power Tool Co. 175 North State St. Aurora, Ill.	CV3-10	Densification of Sand
Dutch Cone	Static Friction Cone Penetrometer	N. V. Goudsche Machinefabrik Gouda, Holland		Sounding for Bearing Cap. 10 ton Driving 8 ton Pulling
Actuator	Gilmore Fatigue Actuator	Gilmore Ind., Inc. Cleveland, Ohio	433-20	Electro-hydraulic Actuator 20 kips, 6 in. stroke
Oscillator	Lazan Mechanical Oscillator	Wiedemann Machine Co. King of Prussia, Penn.	LA-1	Rotating mass type Oscillator
Hoist	Electric Hoist	Manning, Maxwell & Moore, Inc. Muskegon, Mi		1 ton capacity
Load Cell	Lebow Load Cell	Lebow Assoc., Inc. 1728 Maplelawn Rd. Troy, Mi 48084	3132-500	Compression & Tension Measurement
Transducer	LVDT, Sanborn	Hewlett Packard, Inc.* P.O. Box 301 Loveland, Colo 80537	585DT-500	Linear Displacement Measurement $\pm$0.500 inch
Transducer	LVDT, Schaevitz	Schaevitz Eng. P.O. Box 505 Camden, N.J. 08101	HR-500	Linear Displacement Measurement $\pm$0.500 inch

Table 3.1. (Continued)

Equipment	Trade Name	Manufacturer	Model	Remarks
Velocity Transducer	Electro-Tech Geophone	Mandrel Ind., Inc. 5134 Glenmont Houston, Texas	EVS-4BH	Velocity of Vibration, Horizontal comp.
Recorder	Dual Channel Hot Pen Recorder	H/P, Inc.*	Sanborn 7702B	Record Output from LVDTs
Recorder	Dual Channel Hot Pen Recorder	H/P, Inc.	H/P 320	Record Output from Geophones
Recorder	Four Channel Hot Pen Recorder	H/P, Inc.	H/P 7704B	Record Output from Load Cell & LVDTs for Gilmore Tests
Oscilloscope	Dual Trace, Storage Oscilloscope	H/P, Inc.	141A	Cross-Hole Test
Curve Follower	Data Trak Programmable Curve Follower	Research Inc. P.O. Box 24064 Minneapolis, Minn	FGE5110	Displacement Control for Gilmore Tests
D. C. Power Supply	Regulated D. C. Power Supply	Power Designs, Inc. 1700 Shames Dr. Westbury, L.I. New York, N.Y.	3650S	Power Supply for DATA TRAK
D. C. Power Supply	D. C. Power Supply	Harrison Lab.	6204A	Power Supply for Load Cell

Table 3.1. (Continued)

Equipment	Trade Name	Manufacturer	Model	Remarks
Dynamometer	Dillon Dynamometer	W. C. Dillon & Co., Inc. Chicago, Ill		Pull-out, Tests
Proving Ring	Karol-Warner Proving Ring	Karol-Warner, Inc. 261 S. Adelaide Ave. P.O. Box 1255 Highland Park, N.J.		Load Measurement for Static Tests
Dial Gauge		Federal Prod. Corp. Providence, R.I.	E81S	Linear Displacement Measurement 1.000 inchs
Dial Gauge		B. C. Ames Co. Waltham, Mass.	AMES4826	Linear Displacement Measurement 6.000 inches

*H/P is Hewlett Packard, Inc., Loveland, Colo.

17360 West Eight Mile Road, Southfield, Michigan. It was 90 in. in diameter with 2-2/3 in. x ½ in. helical corrugation, 0.168 in. thick, and the estimated average handling weight was 186 pounds per linear foot.

A ¼ in. thick steel plate was welded to the bottom to form a watertight container which was subsequently filled with sand. The joint at the base of the tank was made watertight by applying Colma-Dur Gel extensively. This gel was manufactured by Sika Chem. Corp., Lyndhurst, New Jersey. Colma-Dur Gel is a general purpose gap filling epoxy resin system used to bond irregular, non-mating dry surfaces of concrete, steel, wood, glass, stone and brick. It developed a compressive strength of 4,000 psi in 4 hours and over 10,000 psi in 24 hours when cured at an ambient temperature of 75 degrees F.

Water under pressure was introduced at the bottom of sand, through a filter system, and the upward flow of this water developed a "quick" condition in the sand. This procedure left the sand in a loose condition when the flow was discontinued, and the soil could be reconstituted to any desired density by vibration.

b. Water Supply System -- A 3 in. diameter galvanized water supply line was introduced at the bottom of the bin. This was connected to a high pressure (75 psi) process cold water line which served the entire G. G. Brown

Lab. Inside the tank, the water supply line branched into a manifold consisting of four parallel lines of different length. Each pipe was perforated at the bottom and plugged at the end to avoid localized upward flow and to distribute flow uniformly across the whole section. A drainage pipe with a valve was provided at the opposite side of the tank.

At the top of the tank a sand trap was provided to prevent the floating sand from entering the drainage system of the building. This box was 3 ft. 4 in. x 1 ft. 10 in. x 1 ft. 6 in., and was equipped with a 90 degree V-notch sharp-crested weir to measure and control the flow of water. The V-notch weir was calibrated for discharges up to 16 cubic feet per minute. A drainage pipe was connected between the sand trap and the bottom tank drainage pipe which was extended to the building drainage system.

c. Filter System -- A high pressure water supply chamber was formed by building a filter layer on top of the manifold to diffuse the upward flow of water and to retain the soil in its place above the manifold. The filter was designed as an inverted filter to prevent loss of soil during downward water flow.

The inverted filter was constructed in three layers using different grain sizes which became finer toward the top. The lower layer was of pea-gravel size ranging between ¼ in. and ½ in.; the second layer was of sandy

gravel mixed with the coarse sand and fine gravel; and the third and top layer had coarse sand with most of the fines washed out. Curve "a" in Fig. 3.3 shows the grain size distributions for the third layer.

All the aggregates were provided by Holloway Sand and Gravel Co., Inc. at 2170 S. Zeeb Road, Ann Arbor, Michigan and already were classified by commercial standards such as "pea-gravel" and "ice-controlled" sand. The aggregates were screened again in G. G. Brown Lab. to meet the design specification, then washed throoughly with fresh water, and air dried for a week at room temperature.

The aggregate for each layer was measured and mixed with Prairie Film epoxy at a 4 percent by weight mixture. This mixture when cast in a 4 in. thick slab could support approximately 5,000 pounds with a 12 in. span. The "Prairie Film" is manufactured and distributed by the Prairie Company at 510 East Main St., Urbana, Illinois. It is a resin and catalyst (3 parts resin, 1 part catalyst) type epoxy which is soluble in water when liquid, but after 7 days of complete curing at the ambient temperature of 85 degree F., it becomes water resistant. The mixture of aggregate and epoxy were precast into 1 foot square by 1 in. thick blocks. When the blocks were cured completely, the first layer was installed on a sheet

of ½ in. flattened, expanded steel mesh supported by 4 in. I-beam sections placed between the water pipes.

The mixture of Ottawa 20-30 sand and Prairie Film epoxy was used as the bonding material between blocks. After the first layer was installed, No. 3 reinforcing steel deformed bars were placed between each layer (see Fig.3.4) and welded to each other and to the tank 12 in. center to center to reinforce the load bearing capacity of each layer. Another batch of the same size aggregate and epoxy were mixed and cast-in-place ½ in. thick on top of the first layer to cover the reinforcing bars and to provide level surface to the next layer. The second and third layer were also built on top of each layer in same manner. After the cast-in-place mixture was cured completely, the periphery of the top filter layer was bonded again to the steel tank with Colma-Dur gel.

2. Sand

Muskegon Dune Sand was used as the soil medium for all tests and was purchased from the Nugent Sand Co. at Box 506, Muskegon, Michigan. It was designated as controlled Muskegon Nugent Sand 390, which has also an American Foundry Society Fineness Number 39. Curve (b) in Fig. 3.3 shows the grain size distribution of the sand. It is a poorly graded, fine, light brownish sand with some organic inclusions and fines like clay. However, the

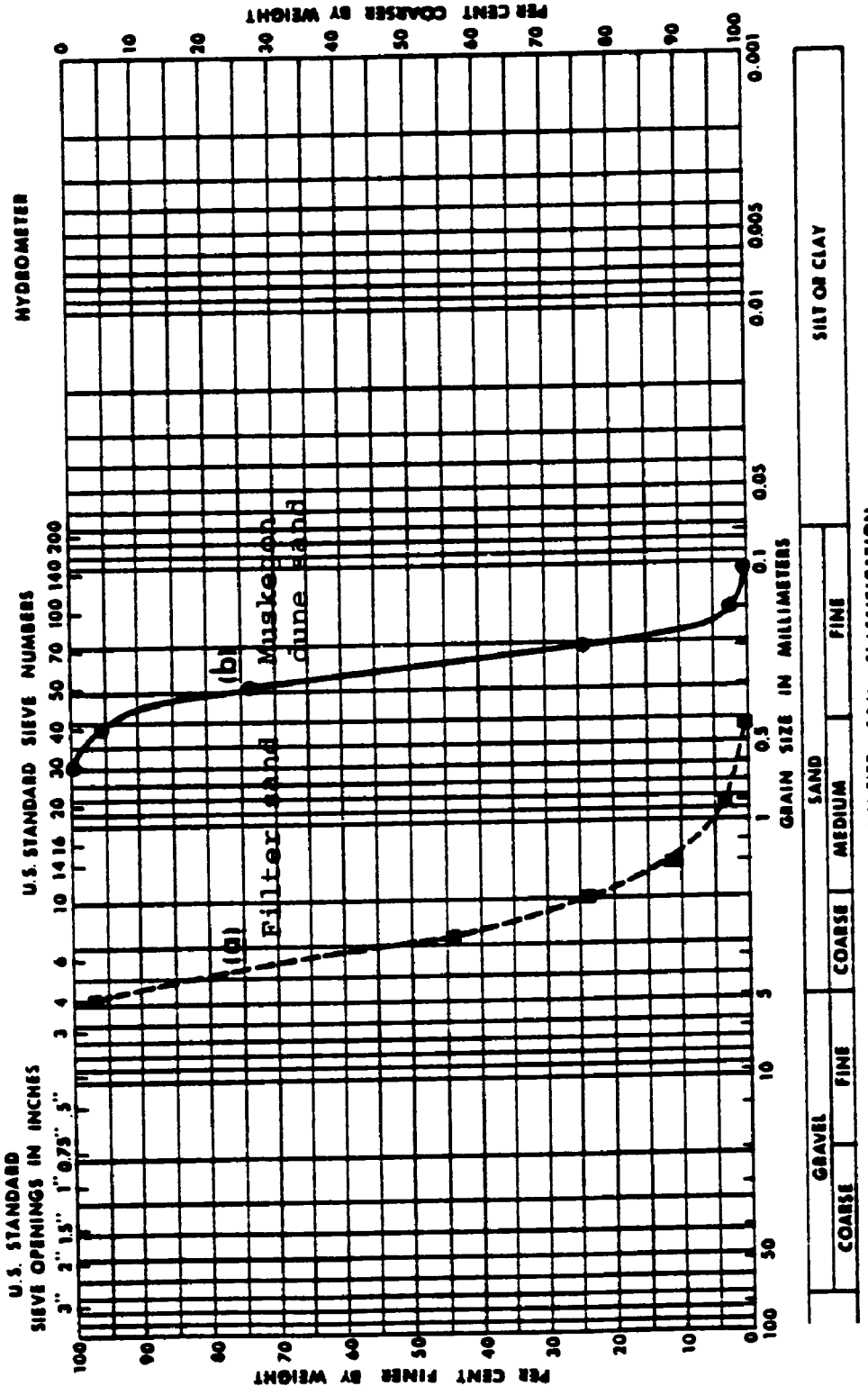

Figure 3.3 Grainsize distribution of Muskegon dune sand, and filter sand.

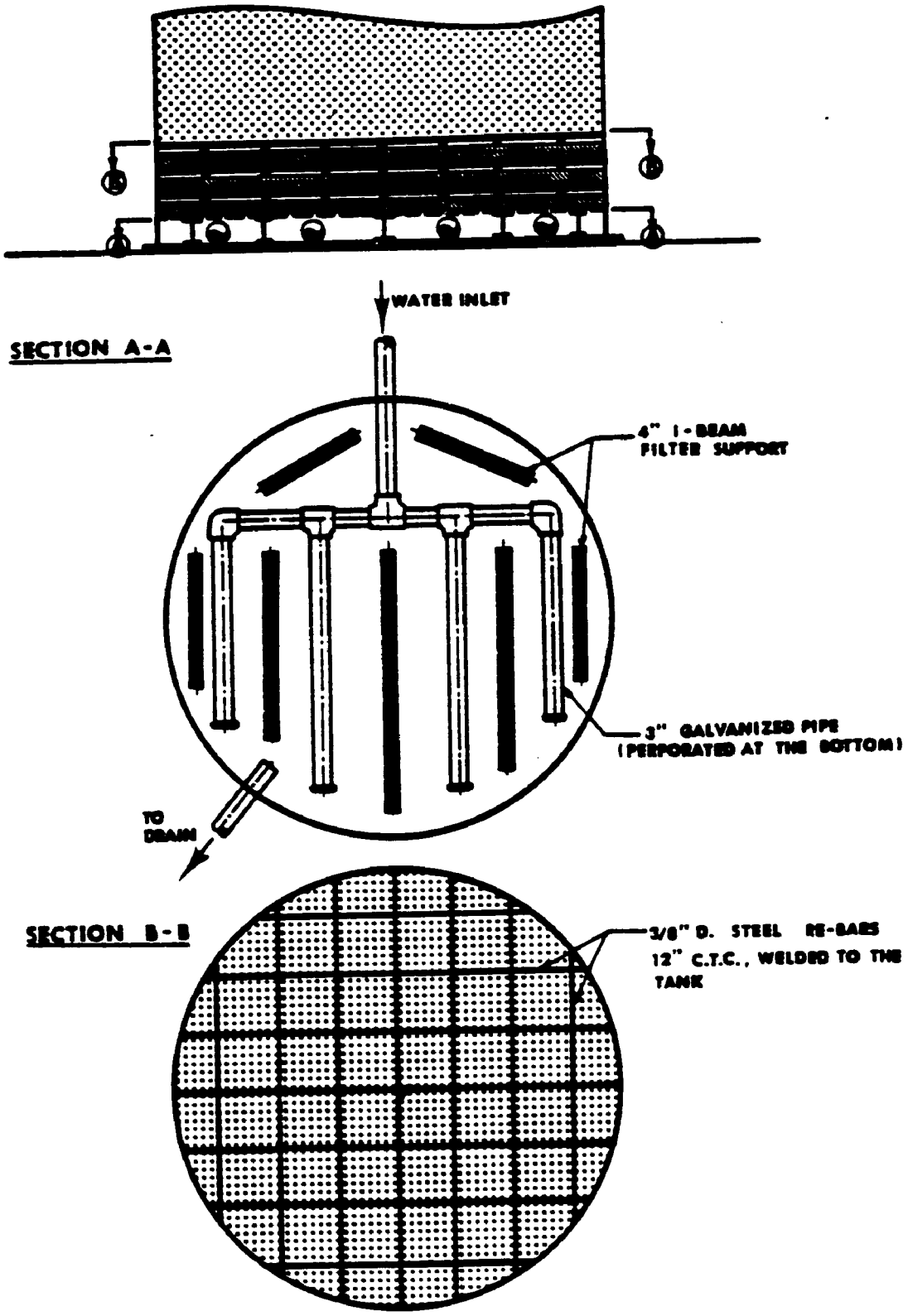

Figure 3.4 Details of filter layers and water distribution system

organic substance and fines were almost completely eliminated by preliminary washing operations during check-out of the development of the quick conditions. The sand had the characteristics as follows: maximum void ratio (lab.) = 0.78, minimum void ratio (lab.) = 0.55, uniformity coefficient = 1.5, coefficient of curvature = 1.2, range of relative density obtainable in the tank = 15 to 85 percent, and a specific gravity of 2.63. The weight of the sand in the tank was approximately 38,000 pounds when dry, thus the tank transferred approximately 870 pound per square foot of veritcal load to the building floor.

Before the tank was filled with sand, it took 15 to 20 minutes to fill the tank with water. However, after the sand was installed the time to fill the voids with water was extended to more than 30 minutes to avoid abrupt upheaval (boiling) of the sand due to the high water pressure built near the bottom. The details of quicksand tank operation will be described in the section on the test procedures.

3. Working Platform

Steel frames and a stairway were constructed around the tank to support a working platform which provided an 8 ft. by 13 ft. working space on the top of the tank. An opening in the center of working platform 5 ft. by 4 ft. permitted access to the tank.

Another steel frame, separated from the platform structures, was required (Fig. 3.5) to support the steel truss for part of the Dutch cone penetrometer. The Dutch cone penetrometer was used in the experimental phase of this work to control sand density in the tank. (see Section III. B.2.) The original mobile Dutch cone equipment was disassembled and modified to fit the truss prepared on the working platform.

4. Hoist System

A hoist system was added to the existing over-hanging steel frame to handle the piles and other heavy equipment. A one ton capacity overhead electrical hoist provided a controlled lifting force at a speed of 17 ft. per minute. This hoist was used in pull-out capacity tests of the piles, as well as for lifting equipment.

5. Reaction Beam

To provide horizontal reaction to lateral forces applied to the piles, a steel WF 10 in. X 5-3/4 in. beam section was attached to the building wall. The beam section, 5 ft. 8-3/4 in. long, was attached at 10 ft. 6½ in. above the floor to the outside reinforced concrete wall of the building. This wall was a cantilever type retaining wall 16 ft. 9½ in. high having a thickness of 1 foot at the top and 4 ft. 6 in. at the bottom. The

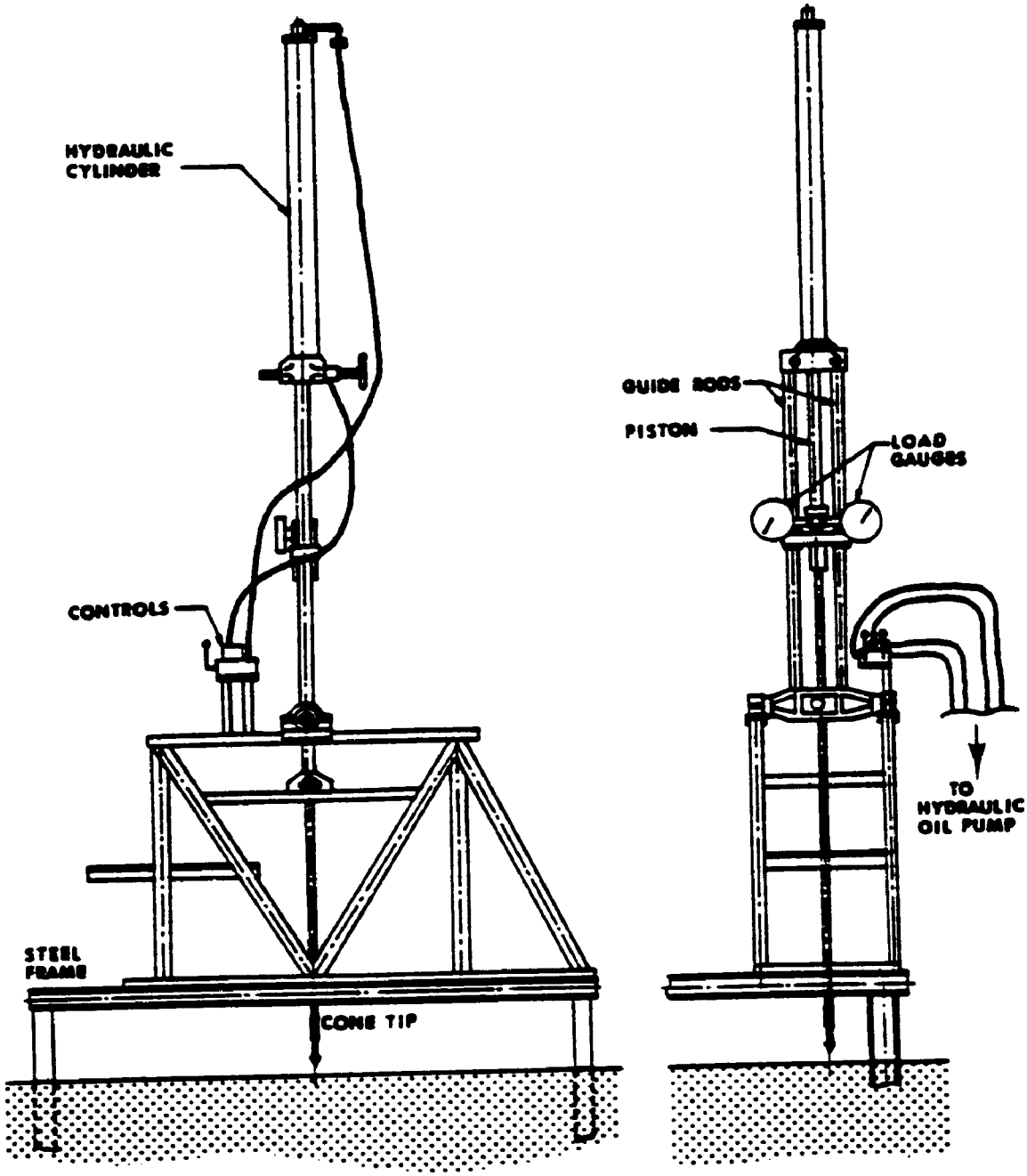

Figure 3.5 Schematic diagram of Dutch Cone Penetrometer and its support frame on top of the quicksand tank

wall rested on a 10 ft. wide base pad, 1 ft. 6 in. thick. A part of the building block wall, 6 in. thick, and 4 in. of styrofoam insulation were chipped away and removed to reach the surface of the retaining wall (see Fig. 3.1 for wall section).

The reaction beam was fixed to the retaining wall with four 3/4 in. diameter 7 in. long, "Red Head" ww-3470, stainless steel wedge anchor bolts manufactured by Philips Drill Company. Each bolt had 9,825 pound pull-out resistance and 17,000 pound shear resistance capacities. After four 3/4 in. diameter and 4 in. deep holes were drilled horizontally into the retaining wall, the wedge anchor bolts were securely placed and grouted. The I-beam was installed after the grout was cured for 72 hours, and the insulation and the blocks were re-sealed around the beam as before.

B. Sand Density Control

1. Spud Vibrator

An electric spud concrete vibrator, Thor Power Tool Model CV3-10, was used for the densification of sand in the quicksand tank. It was a high torque, motor-in-head electric vibrator which could deliver 15,000 revolutions per minute. The size of the head was 2-5/8 in. in diameter and 16½ in. long, and attached to a 10 ft. long, 1-3/4 in. in diameter, 4-ply neoprene flexible hose.

2. Dutch Cone Penetrometer

The Dutch cone penetrometer was an engine-driven, hydraulic, sounding apparatus. It had a maximum driving capacity of 10,000 kg force and a pulling capacity of 8,000 kg force. The device was composed of a gasoline engine, hydraulic pump, hydraulic cylinder, control valves, measuring head, and sounding gear. The hydraulic cylinder, control valves, and measuring head were detached from the original portable frame and rearranged on a truss frame at the top of the quick-sand tank as shown in Fig. 3.5. Detail of Dutch Cone Operation and application can be found in Sanglerat (1972).

C. Loading Systems

1. Static Test

a. Screw Jack -- The screw jack shown in Fig. 3.6 was a manually operated horizontal loading system used for the static tests. It was attached to the reaction beam on one end, and to the pile clamp on the other end with a proving ring in between the jack and the pile clamp. The jack was capable of pushing the pile 5-3/4 in. horizontally at the loading point.

b. Gilmore Actuator -- This device was used at a slow speed of 1 cycle per minute to establish

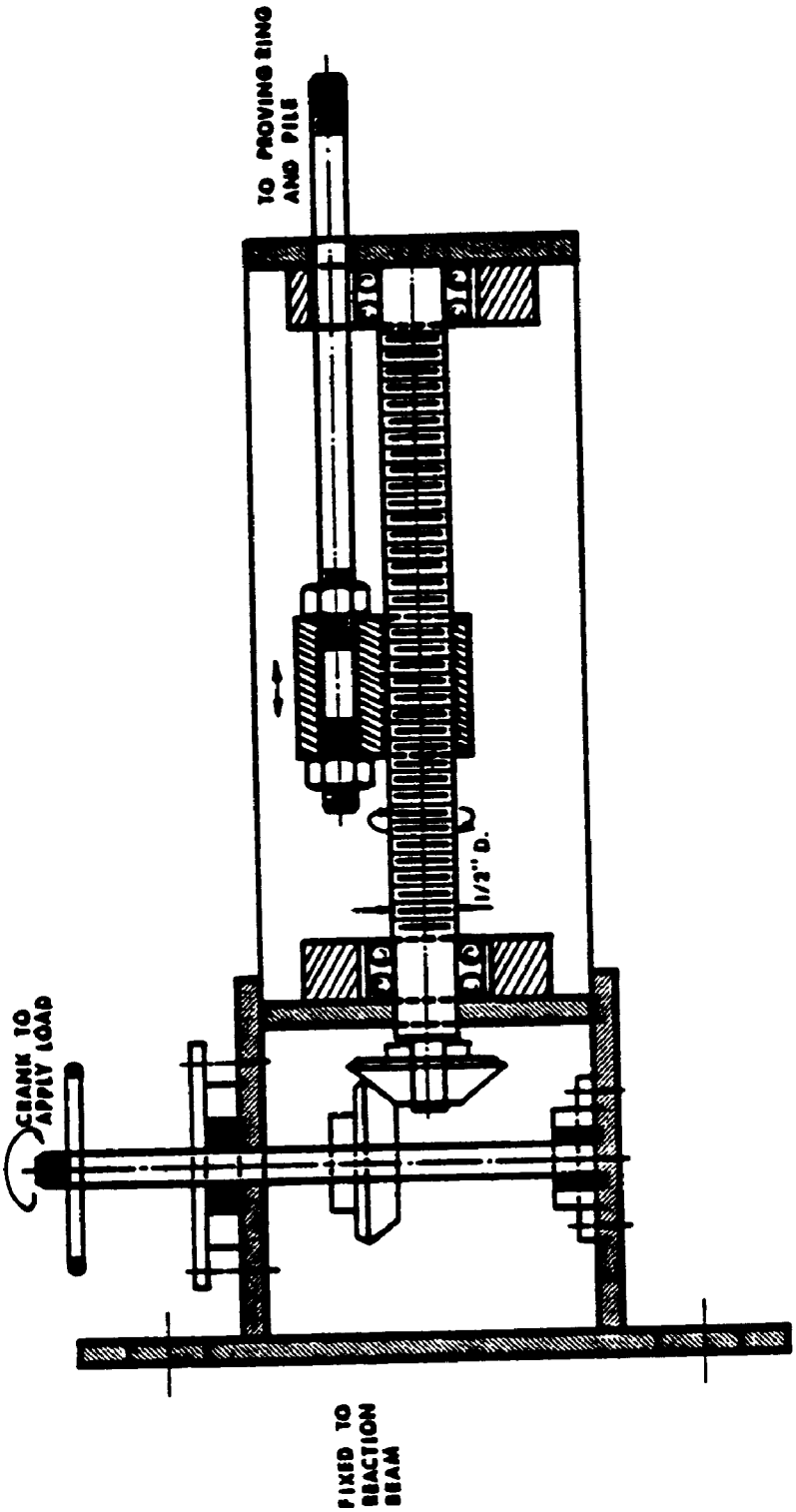

Figure 3.6 Cross-sectional view of screw-jack static loading system

a quasi-static load deformation behavior of the pile. The Gilmore actuator will be described in detail in the following section for the dynamic loading system.

c. Plucking Tests -- The "plucking" test consisted of statically displacing the pile and quickly releasing it to generate a transient vibration of the pile-soil system. The load for the plucking tests was provided by placing selected weights manually on a weight pan which was connected to the loading point of the pile through a pulley. Steel weights of 36 pounds each were used. As shown in Fig. 4.5, the weights dropped onto the weight catching platform when the loading cable was cut.

2. Dynamic Tests

a. Lazan Oscillator -- The steady-state horizontal sinusoidal load for load-controlled dynamic tests was provided by a Lazan mechanical oscillator, Model LA-1. The oscillator utilized the centrifugal force of unbalanced masses mounted on two shafts rotating in opposite directions to generate a variable alternating force in a horizontal plane. The magnitude of the force depended upon the phase angle between two small masses and one large mass which were arranged on each shaft such that the weight of the two masses equal to the single large mass. Figure 3.7 shows the

arrangement of the masses inside the oscillator. The force adjuster was located on one shaft, and consisted of a screw, key and a helical slotted sleeve. The axial position of the key in the shaft determined the angular position of the large eccentric mass with respect to the shaft and the smaller eccentrics. The force could be changed while the machine was running by allowing the key to turn freely while the screw, which moved the key axially and closely positioned, remain stationary. One set of gears transmitted this motion to another sleeve and its eccentric masses so the timing between the shafts remained a constant and changed the phase angle between the eccentrics on each shaft together. The oscillator was powered by a DC motor which delivered 1½ HP through a flexible shaft, and was controlled by the Reliance Style CE electronic motor drive. The motor control was a functional unit which provided a wide-range control of motor speed.

The alternating force output of the oscillator at various settings of the counter unbalance within the oscillator resulting from the use of brass eccentrics was given by the following equation:

$$F = 2\ N^2 \sin(\Theta/2) \qquad (3.3.1)$$

in which, Θ = angle between eccentric weights, F = double amplitude force output of oscillator in pounds,

N = speed of rotation of oscillator in cycles per second.

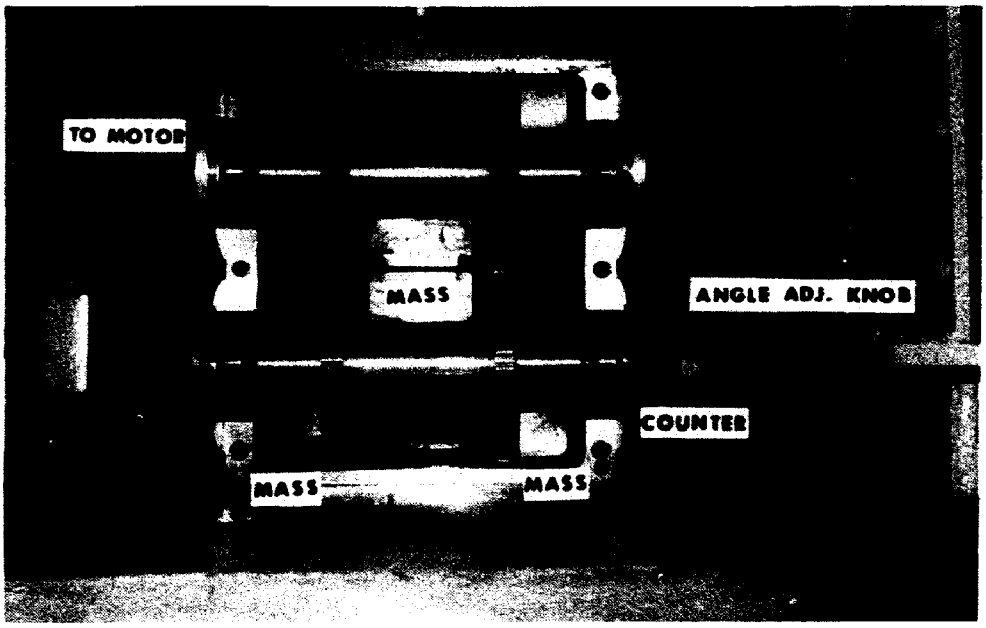

Figure 3.7 Interior of the Lazan oscillator showing rotating eccentric masses

b. Gilmore Actuator -- The Gilmore loading system consist of three principal sections: 1) control console, which houses the servo amplifier, signal conditioners, rate programmer and control pushbuttons, 2) the hydraulic pumping unit, which contains the hydraulic oil reservoir, pump, starter and safety devices, and 3) actuator, which includes a position transducer, a velocity feedback transducer, a load cell and a power

cylinder. The control mode selector and the command selector allowed the programmed displacement to be transferred to the cylinder of the actuator. The hydraulic pump could deliver 15 gallons per minute rated flow of hydraulic oil at the operating pressure of 3,000psi and this flow was regulated by a servo valve, which is also connected to the velocity limiter.

The actuator assembly, Model 433-20 Fatigue Actuator, consisted of a hydraulic cylinder, load cell, linear variable differential transformer (LVDT) position transducer, and velocity transducer. It could deliver 20,000 pound axial tension or compression load with a 6 in. stroke. One end of the actuator was mounted to the reaction beam, and the other to the clamp attached to the pile. (see Fig. 3.8.)

D. Instrumentation

1. Transducers

a. Load Cell -- The Gilmore actuator had a built in 20,000 pound capacity load cell, however this load cell did not have the required accuracy at the low loads expected for these tests (approximately 300 pounds). Therefore a separate load cell, a Lebow Model 3132-500, with a capacity of 500 pounds was used to measure both tension and compression. The load cell and recording system were calibrated and adjusted to record 100 pounds per 5 mm of chart record on the four

channel recorder. The 18 volts DC required for the load cell excitation was provided by a Harrison Lab. Model 6204A DC power supply.

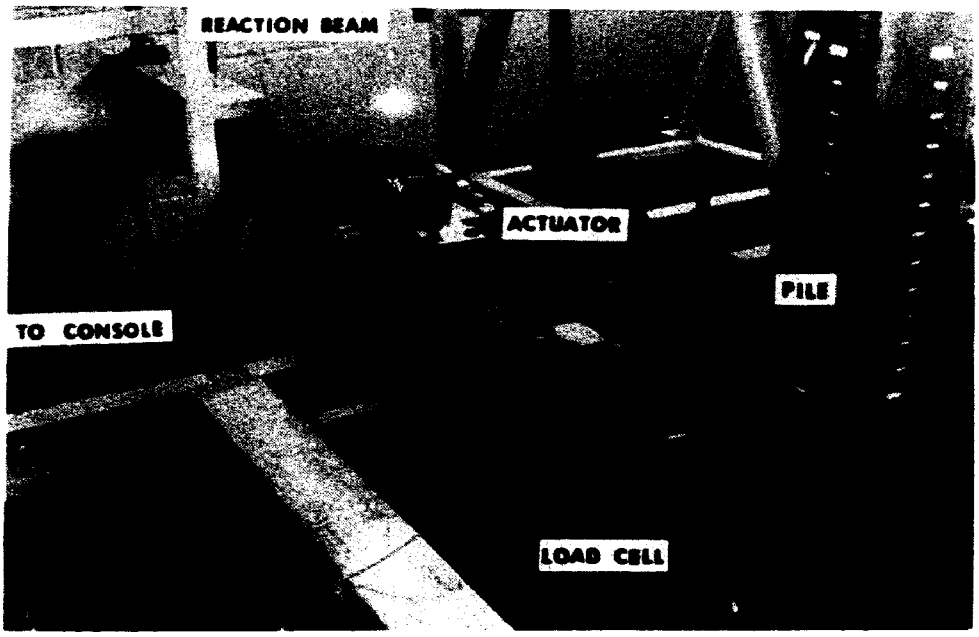

Figure 3.8 Attachment of the Gilmore hydraulic actuator to the pile

b. LVDT -- Two linear variable differential transformers were used to measure pile displacement. One was a Sanborn LVDT and one was a Schaevitz LVDT.

c. Velocity Transducer -- Two Electro-tech Model EVS-4BH horizontal velocity transducers were used to measure pile motion in the plucking tests. These transducers were calibrated using an optical displacement follower Optron (see Chapter 9, Vibrations of

Soils and Foundations, Richart et al., 1970). One transducer had an average calibration factor of 0.7 volts/in./sec. with a cutoff frequency of 20 cps and the other had an average calibration factor of 0.5 volts/in./sec. with a cutoff frequency of 17 cps.

2. Recorders

a. Dual Channel Recorder -- An H/P Model 7702B oscillographic recording system was used to record the output signals from the two LVDTs. The displacement of core of the LVDT was calibrated to the desired scale on the recording chart by varying attenuation and gain control. The LVDTs were calibrated against a 0.001 in. per division dial gage.

The output signals from the two velocity transducers were recorded on a H/P Model 320 dual channel recorder.

b. Four Channel Recorder -- The H/P Model 7704B, a four channel recorder, was used to record the three output signals from the displacement-controlled dynamic tests. One signal was from the load cell, and the other two were from the LVDTs.

The load cell was calibrated to record 20 pounds per mm on the chart record. The LVDTs, L1 and L2, were calibrated to record 0.02 in. per mm on the chart record.

c. Oscilloscope -- A H/P Model 141A storage oscilloscope was used for the cross-hole tests. The storage feature could be used to store single-shot wave forms and to later view or photograph the phenomena. Comparison of wave forms could be accomplished by storing several displays separately and then viewing them simultaneously.

3. Resonant Column Device

The Hall resonant column test was employed to evaluate the dynamic shear modulus of the sand used in the bin. The details of the Hall device can be found in Afifi (1970), Anderson (1974), and Richart et al., (1970).

4. Data Trak

A Data Trak Model FGE5110 Programmable Curve Follower was used to provide the sinusoidal signal to drive the Gilmore actuator at frequencies of 2, 3, and 5 cycles per second. It also provided a 1 cycle per minute signal to drive the actuator for the static horizontal load tests.

The Data Trak had a maximum follow rate of 7 in. per second, which limited the use of the system for the higher frequencies. It was necessary to reduce the amplitude considerably as the frequency was increased.

5. Miscellaneous

a. Dynamometer -- The Dillon dynamometer which had a 3,500 pound tensile load capacity was used to measure the pull-out resistance of the test piles before and after each static or dynamic test.

b. Proving Ring -- The axial horizontal load for the static test which used the screw jack loading system was measured by a Karol Warner proving ring. The proving ring was calibrated to measure 6.57 pound per division.

c. Dial Gauge -- Two dial gauges were used to measure the horizontal displacement of the pile in static and plucking tests. Federal Product Model E81S dial gauge had a 1 in. range, and an Ames Model 4826 had the range of 6 in.

E. Piles

The model piles used in this experimental study were all hollow steel sections to provide rigidity and minimize weight. The piles were designed to behave as rigid piles. Figure 3.9 and Table 3.2 show the shape and structural characteristics of the piles.

Model pile RP3* was a 3.5 in. outside diameter and 0.25 in. thick circular steel pipe pile. RP4 was a 4.5 in. outside diameter combined circular steel pipe pile with a 3 in. diameter grooved aluminum casing for slope indicator inserted concentrically into the pipe. The gap between two pipes was filled with 1:3 cement-sand grout.

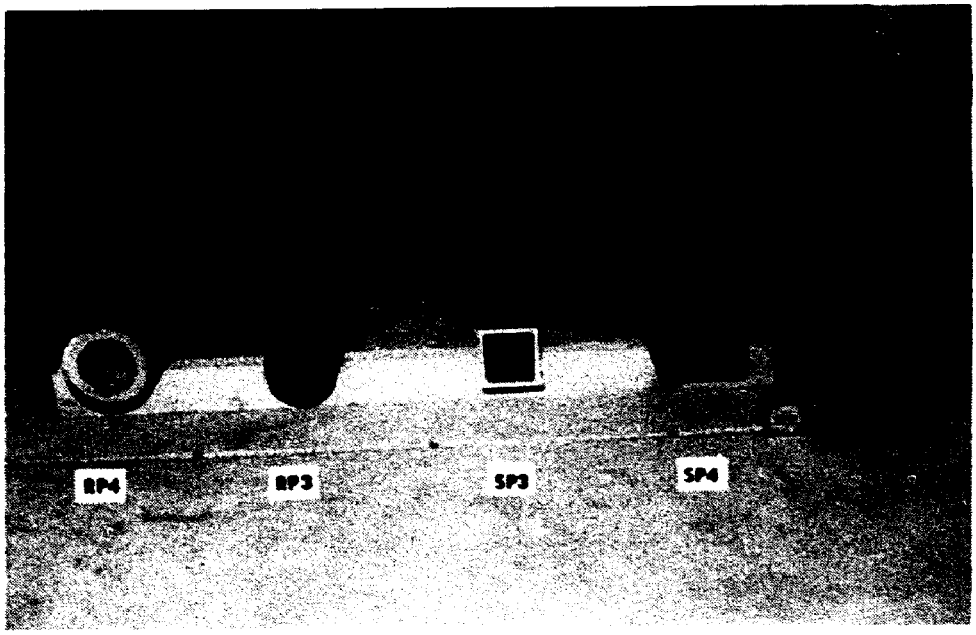

Figure 3.9 Shapes of the model piles

*RP denotes the round piles and SP denotes the square piles. The number after the shape code is the nominal pile size.

SP3 and SP4 were fabricated from 3" X 3" X ¼" and 4" X 4" x ¼" steel angles by welding to form the square piles which have the cross-section of 3" X 3¼" and 4" X 4¼" respectively.

All model piles were plugged at the bottom end with a porous filter block made of coarse sand epoxy to prevent the sand from clogging the inside of the pile. However, the water was allowed to seep through the plug to eliminate the uplift of pile due to buoyancy.

For load-controlled dynamic tests, all the model piles were cut, as shallower embedments were tested, to locate the Lazan oscillator at a constant position of 27 inches above the sand. For example RP3 was originally 9 ft. long but when tested at 5 ft. embedment it was cut to 6.74 ft.

Table 3.2. Structural Characteristics of Model Piles

Pile Design	Size (in)	Length (ft)	EI ($x10^6$ lb-in^2)	Weight (lb)
RP3	OD = 3.5 ID = 3.0	9.0	101.61	65.73(48.70)
RP4	OD = 4.5 ID = 4.0	8.5	261.50	117.22(108.92)
SP3	3.0 X 3.25 B = 3.25	8.0	111.90	79.99(64.50)
SP4	4.0 X 4.25 B = 4.25	7.7	278.10	102.97(89.61)

Note: Weights in parenthesis are the weight of the piles corresponding to the length of 6.74 ft.

CHAPTER IV

TEST PROCEDURES

A. Preparation of Sand

1. Quicksand Operation

The sand in the test bin was brought into the quick condition during the placement of the pile for each test. The water supply valve was opened to fill the water chamber at the bottom of the tank first, and then, with the drainage valve opened, the water was flushed through the chamber for about 20 minutes to wash out the rust. The drainage valve was then closed and the tank was filled with the water very slowly until water started to overflow through the weir of the sand trap. The flow of the water was increased until a quick condition prevailed throughout the tank. The sand was maintained in the quick condition for at least 10 minutes to assure that each sand particle moved to its loosest condition. The flow rate of intake water was carefully controlled to avoid abrupt upheaval or boiling of the sand due to the high water pressure built up near the bottom of the sand bed. Then the water supply valve was closed and bottom drainage valve was opened allowing

the water level to drop to the sand surface. The elevations of the sand surface at six different places were measured.

2. Densification of Sand

After the sand was expanded into its loosest condition by the quicksand operation and the pile was installed, a concrete spud vibrator was inserted in the sand in a predetermined pattern for a pre-established time to achieve the desired relative density. Figure 4.1 illustrated the pattern and order of the vibrator insertions. The vibrator head was lowered to 6 ft. below the sand surface for 1 minute, raised to 4 ft. for 30 seconds, and then again raised to 2 ft. for 30 seconds. The procedure was repeated at all 8 points in the sequence shown. If the vibrator head could not penetrate to the required depth, it was allowed to remain at its next shallower depth for the total time for 2 positions. This whole operation usually took 20 to 25 minutes. The water which was displaced during the densification was drained to the sand surface. The elevations of the sand surface were measured again to determine the average settlement. In this manner a relative density of about 75 percent could be achieved repeatedly.

For the drained tests the water was drained from the tank for at least 24 hours while for the submerged tests the water was raised to an elevation of 1 in. above

the sand surface after the densification and instrumentation was completed.

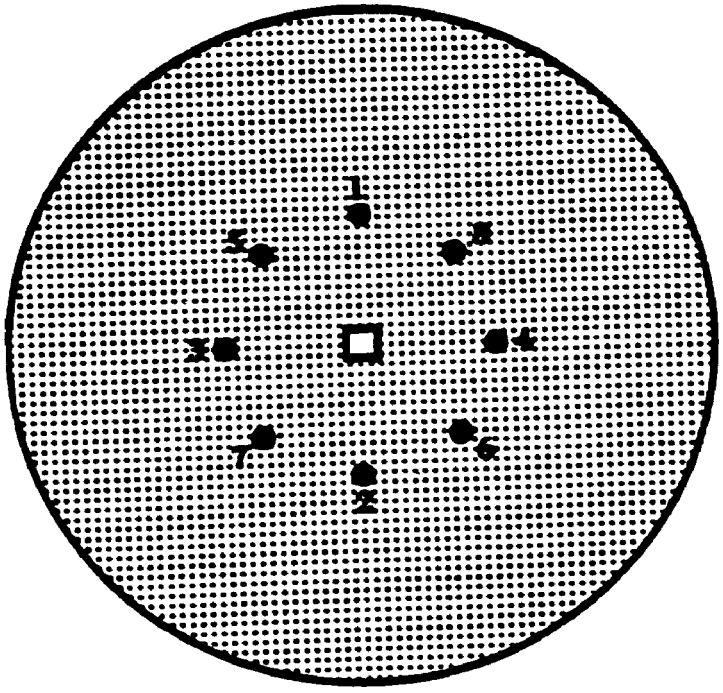

Figure 4.1 Pattern and order of the vibrator insertions for the densification of sand

3. Density Control Test

a. In-situ Density Test -- A series of drive tube type in-situ density test (ASTM Standard D 2937) were performed after the water was drained to determine the void ratio of the densified sand. The tube was driven at random places other than at the vibrator application points after removing about 1 ft. of surface sand.

b. Dutch Cone Test -- Dutch friction cone penetrometer tests were performed to check the uniformity of the densified sand after each quicksand and densification operation. The Dutch cone tests were discontinued after the operator could produce a quite consistent result after 73 tests.

B. Installation of Pile

The piles were equipped with brackets to facilitate the installation using an overhead hoist. The pile was hoisted into its vertical position over a selected location within the tank and lowered slowly while maintaining it vertical. The sand was in the quick condition when the pile was lowered to its selected embedment depth. Then the water flow was stopped, and the pile was checked again for its verticality and any minor adjustments were made. After the pile was installed in its vertical position, the water was drained down to the sand surface and the densification was started. It was necessary to check the pile for verticality during the densification operation. Slight deviations from vertical could be corrected by pushing on the piles by hand and using a spirit level to recheck verticality. After the sand around the pile was densified , the water drained and the embedment depth adjusted, the instrumentation was attached to the pile.

C. Dynamic Properties of Sand

1. Cross-Hole Test

Cross-hole seismic tests were performed in-situ to determine the shear wave velocities of the sand. Stokoe and Woods (1972) and Anderson (1974) described the cross-hole method in detail. Figure 4.2 shows a schematic of the cross-hole test and associated equipment. The primary equipment included a storage oscilloscope, an oscilloscope camera, a velocity transducer, and a triggering system.

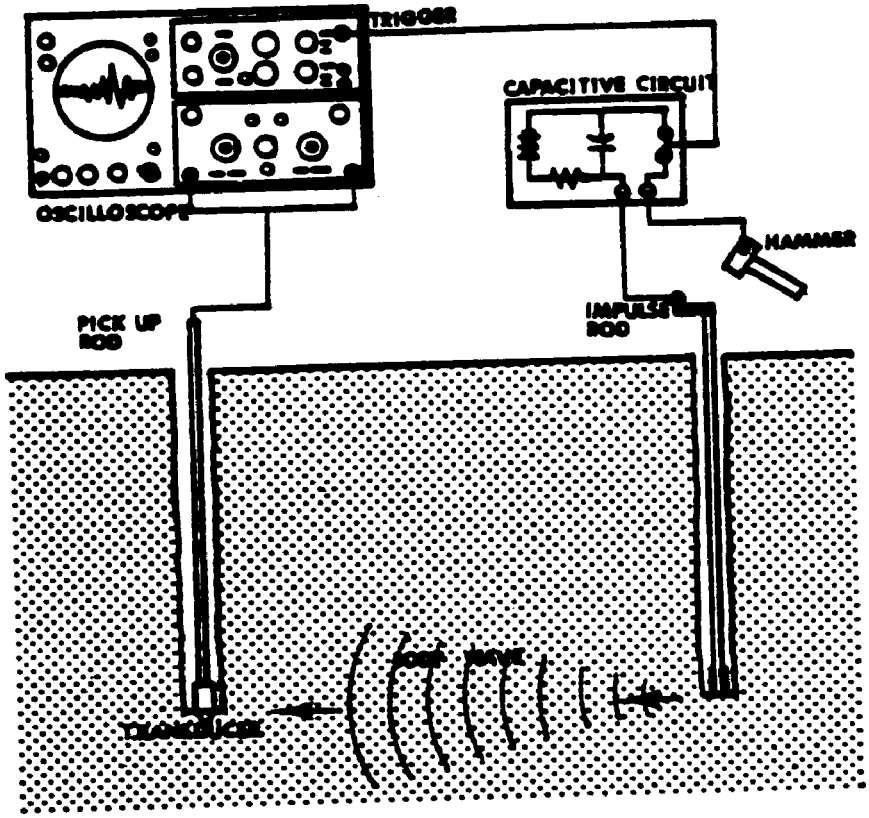

Figure 4.2 Schematic diagram of cross-hole test

Two holes, 2 in. diameter and 4 ft. apart, were bored with a hand auger to a preselected depth. An impulse rod was placed on the bottom of one hole and a pickup transducer was positioned on the bottom of the other. By striking the head of the impluse rod, compression and shear wave were generated in the soil. The output from the transducer was displayed on the same trace that was triggered by short circuiting a capacitive circuit when the hammer hit the impulse rod. The time required for the wave to travel from the trigger location through the impulse rod and the soil was measured from the oscilloscope trace. Time for the wave travel through the rod was deducted from the total time. To facilitate the identification of the arrival of the shear wave, another shear wave was generated by reversing the impact direction. Once the satisfactory traces were obtained, the record was preserved by taking a polaroid picture. The two holes were then extended to the next depth, and the process was repeated.

2. Resonant Column Test

Figure 4.3 is a schematic diagram of the equipment used for the Hall resonant column test. The details of the test procedures can be found in Richart et al (1970), Afifi (1970), and Anderson (1974).

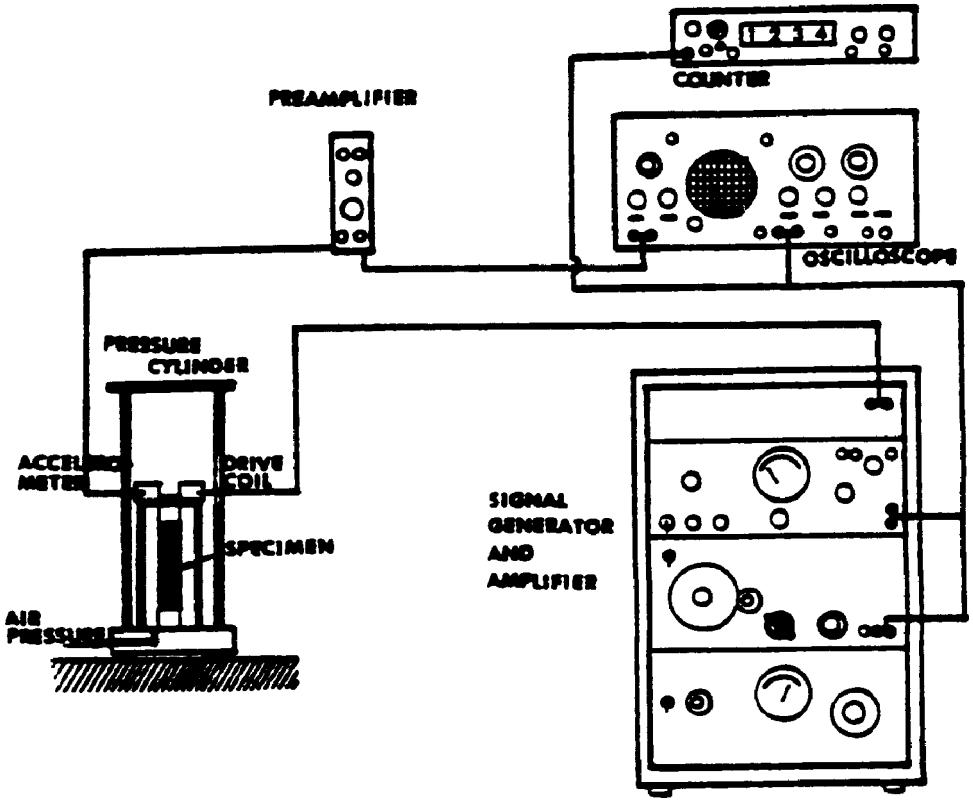

Figure 4.3 Schematic diagram of equipment used for the resonant column test

Coarse sand particles were epoxied on the top of the bottom pedestal to assure adequate coupling by increasing friction between the pedestal and the sample.

D. Plucking Test

Plucking is an operation of introducing a static deflection to the pile and then releasing the load quickly to give the pile a free vibration. By "plucking" an embedded pile horizontally, an impulse was applied to a

pile-soil system to excite transient vibrations in a horizontal mode. The dynamic response of the pile was recorded. Figure 4.4 illustrates the behavior of a viscously damped single-degree-of-freedom system in response to a transient excitation. By applying the simple theory based on a mass-spring-dashpot system, the transient response of the pile-soil system could be analyzed to determine the damped natural frequency, f_d, and damping ratio, D.

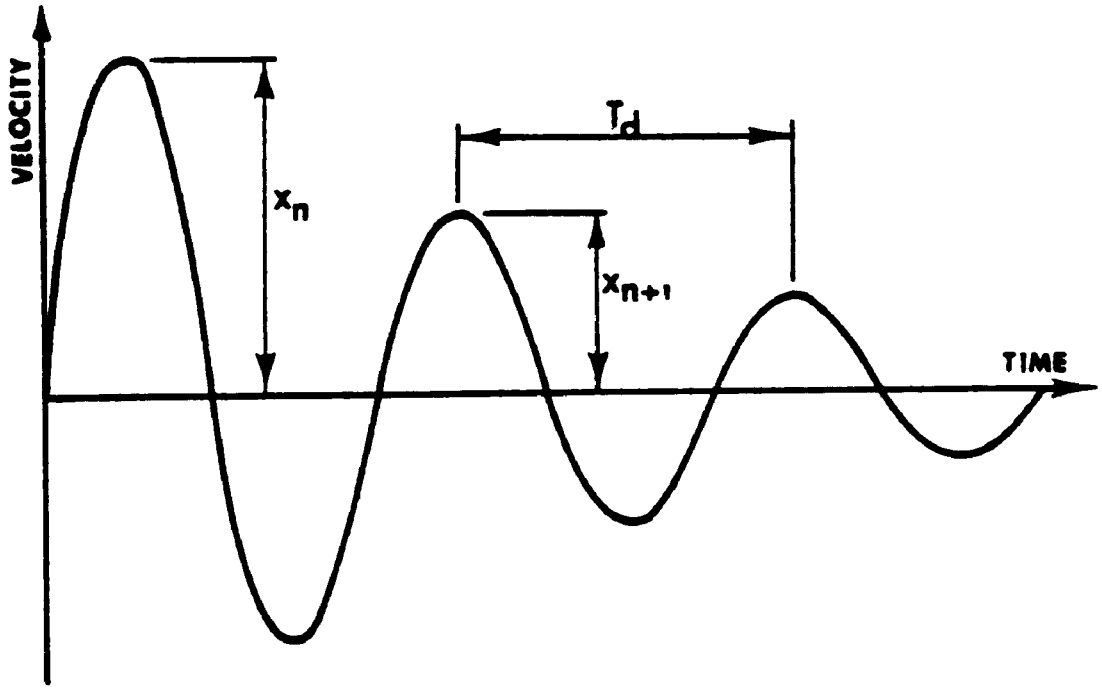

$$f_d = 1/T_d$$

$$\frac{D}{(1 - D^2)^{\frac{1}{2}}} = \frac{1}{2\pi} \ln \left(\frac{X_n}{X_{n+1}}\right)$$

Figure 4.4 Analysis of transient response of a viscously damped single-degree-of-freedom system

Figure 4.5 illustrates schematically the test setup for the plucking test. Two dial gauges were attached at 6 in. and 12 in. from the sand surface to measure the initial static displacement and slope of the pile. Two electro-tech B24H type horizontal velocity transducers were installed at ground level and 30 in. from the sand surface. The output of the transducers were recorded on a dual channel recorder.

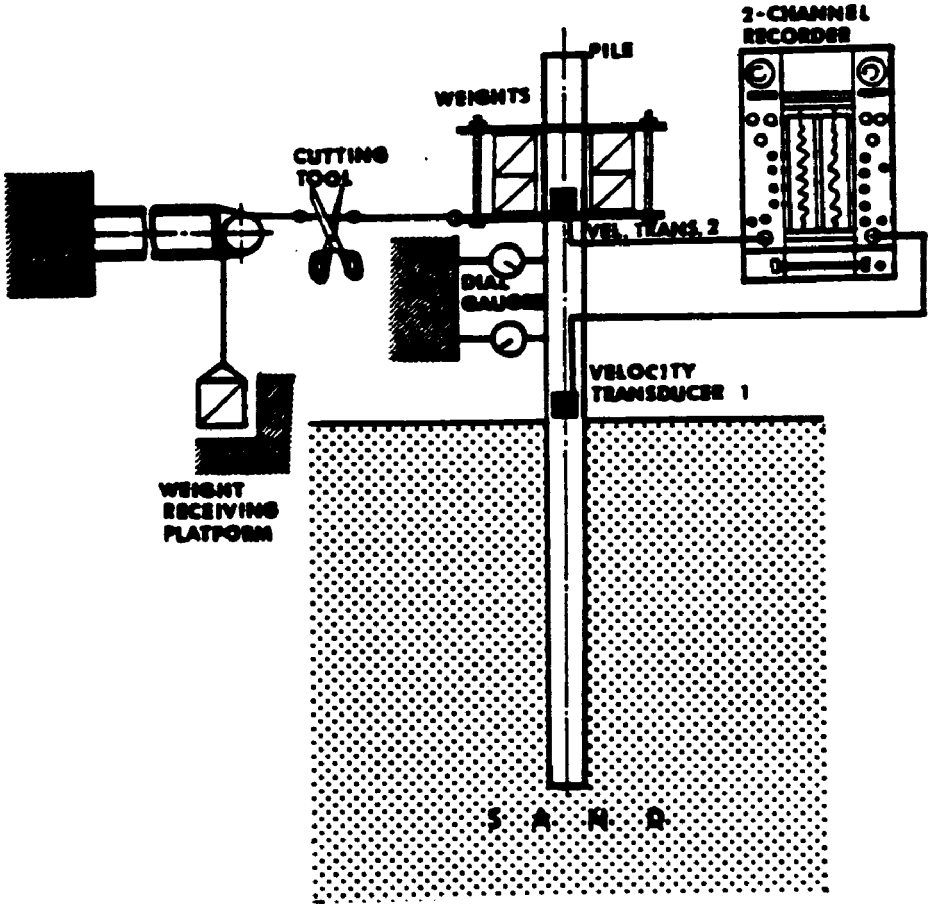

Figure 4.5 Schematic diagram of equipment used for plucking test

After the sand was densified with the pile installed vertically, a weight of 145 pounds was attached to the pile at 30 in. from the sand surface. A 1/8 in. diameter steel cable was connected to the bottom of the weight and to the loading weight through a pulley that was attached to the reaction beam. The pile was loaded horizontally and the static displacement was measured. The loading cable was then cut instantaneously with side cutting pliers to "pluck" the pile.

E. Static Tests

The static laterally loaded pile tests were performed with the sand in the drained loose and dense condition, and in the submerged dense condition. The jack screw loading system with the dial gauge displacement measuring system was used for the drained tests, and the Gilmore actuator, programmed for 1 cycle per minute (quasi-static loading), and LVDT system was used for the submerged tests. A proving ring was used to measure the force applied to the piles in the drained tests, and a 500 pound capacity load cell was used to measure the load transferred to the pile in the submerged tests. The tests were performed for one or more cases of the following conditions for each pile with different embedment lengths; a) single loading in one-direction only, b) single loading in two-directions,

c) repeated one-directional loading, and d) repeated two-directional loading.

The screw jack and the proving ring were attached to the pile after the sand was prepared for the test. Then a dial gauge was attached to the pile to establish a pre-test location of the pile.

Two dial gauges attached at different elevations along the pile were used to determine the horizontal displacement and the slope for each specific horizontal loading.

F. Dynamic Tests

1. Load-Controlled Tests

The Lazan mechanical oscillator was used as a vibration source for the steady-state sinusoidal dynamic test. Figures 4.6 and 4.7 illustrate a schematic diagram and actual setup of equipment for the tests. The Lazan oscillator was originally designed to deliver vertical and torsional vibrations, however, it was adapted for the horizontal oscillation. All the piles were cut to 6 ft. 8-7/8 in. to allow the oscillator to be installed on top of the pile. Two LVDTs attached to the pile at 3 and 9 in. from the sand were used to determine the displacement and rotation of the pile.

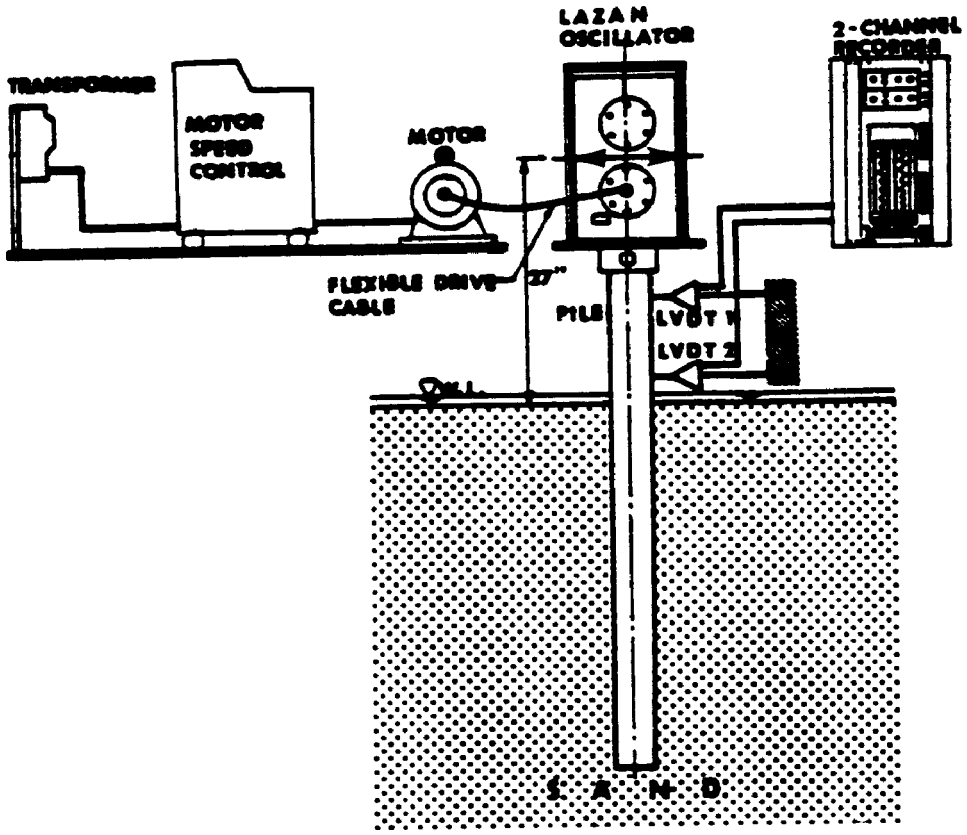

Figure 4.6 Schematic diagram of equipment used for the high frequency dynamic test using Lazan eccentric rotating mass type oscillator

The angle between eccentric weights in the Lazan oscillator was adjusted to produce 4 eccentricities or force levels. The motor speed was controlled to increase the oscillator speed gradually until the resonant frequency of the pile system was reached.



Figure 4.7 Picture of the actual setup of equipment for Lazan test

2. Displacement-Controlled Tests

Figure 4.8 illustrates a schematic diagram of equipment used for the displacement-controlled sinusoidal dynamic tests. The tests were performed at the frequencies of 2, 3, and 5 cycles per second with the sand in the

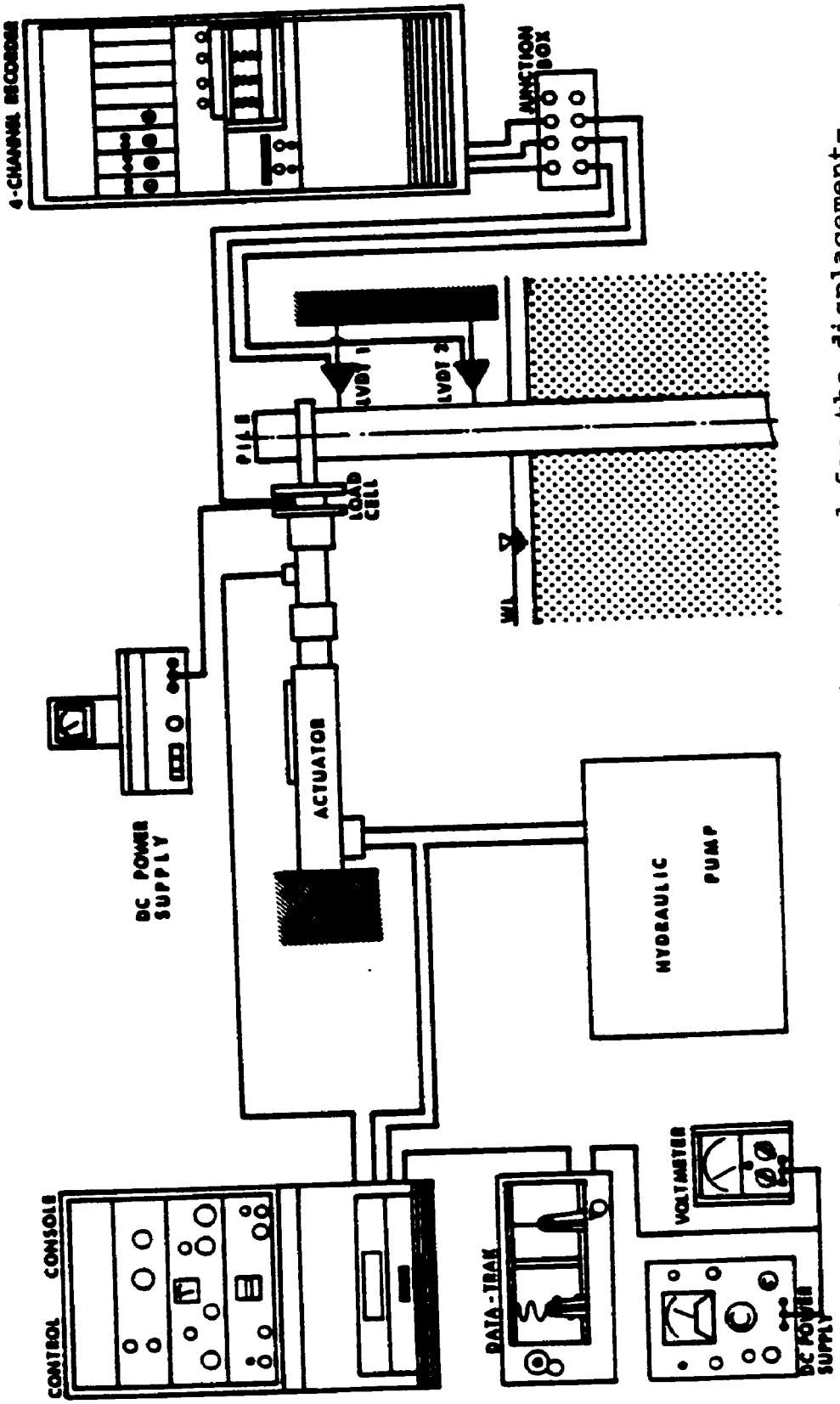

Figure 4.8 Schematic diagram of equipment used for the displacement-controlled low frequency dynamic test using Gilmore hydraulic actuator

submerged dense condition. The Gilmore actuator movement was controlled by using a Data Trak programmer. The Data Trak programmer controlled not only the frequency of lateral vibration of the pile but also the amplitude of vibration.

After the pile was installed and the sand was densified, the water was drained to the sand surface. The elevation of the sand surface was checked to ensure the proper embedment depth. If the pile was embedded too deep, the sand was removed from around the pile until the right elevation was established. If the pile was too shallow, it was reinstalled beginning with the sand in the "quick" condition. The LVDTs were attached to the pile at elevations of 3 and 9 in. from the sand surface. The load cell was attached to the actuator in between the end of actuator and the pile clamp at an elevation of 27 in. from the surface and zeroed on the chart. The water level was again brought up to 1 in. above the surface to ensure the submerged condition.

The actuator had an internal vibration of 70 to 100 cycles per second when the velocity limit dial was turned to its maximum for the dynamic test. This high frequency noise in the load cell output signal was subdued by connecting three parallel capacitors in series between the load cell output lead and the recording system.

G. Pull-Out Tests

The pull-out test was performed to observe the effect of the horizontal pile motion on the pull-out resistance of the pile. It was performed before and after each test except for the load-controlled dynamic test. The pre-test pull-out resistance was determined without any further disturbance after the pile installation and soil preparation. The test after the vibration was performed as soon as instrumentation was removed. A dynamometer was hooked to the overhead electric hoist and the pile head, and the pile was pulled up until the dynamometer showed the maximum value. For some limited tests, a calibrated strain gauge type load cell was also used in series with the dynamometer to compare the accuracy.

CHAPTER V

PROPERTIES OF SAND

A. Density Control

One of the most important factors in this research was to provide approximately the same initial soil condition for each test in order to assure comparable test results. The uniformity of void ratios obtained after the quicksand operations was checked using the Dutch Cone penetrometer.

1. In-situ Density Test

The drive tube in-situ density tests were performed after drainage of water from the tank following the quicksand and densification operations. Settlement of the sand surface during densification was measured and recorded, and drive tube samples for evaluation of in-situ void ratio were taken about 1 ft. below the sand surface. As note in Section III. A. 2, the Muskegon Dune Sand had a maximum void ratio of 0.78, and minimum void ratio of 0.55. The range of void ratios obtained for dense condition within the tank was between 0.58 and 0.61, with an average void ratio of 0.60 which

corresponded to a relative density of 76 percent. The density obtained within the tank depended on the length of time water flowed through the sand while it was in "quick" condition and the densification energy (vibrating time and pattern).

2. Dutch Cone Penetrometer Test

The static Dutch friction cone penetrometer tests were performed in drained sand. Although the equipment could measure both bearing capacity and shear resistance of soil, the comparisons were made with bearing capacity alone. Figure 5.1 shows the range of result of the end bearing capacity tests performed and illustrates the typical curve for shallow layer of dense granular soil. A series of 73 penetrometer tests were performed throughout the period of establishing a procedure for reproducing the same density within the tank.

B. Shear Modulus of The Sand

The dynamic shear modulus is an important factor in the analysis of dynamic soil behavior and of soil-supported structures. Shear modulus can be evaluated by static laboratory torsion tests but unless special equipment is available, only the modulus corresponding to large shearing strains may be obtained. Resonant column tests can also be used to measure the shear modulus, G, over a range of shearing strain from small

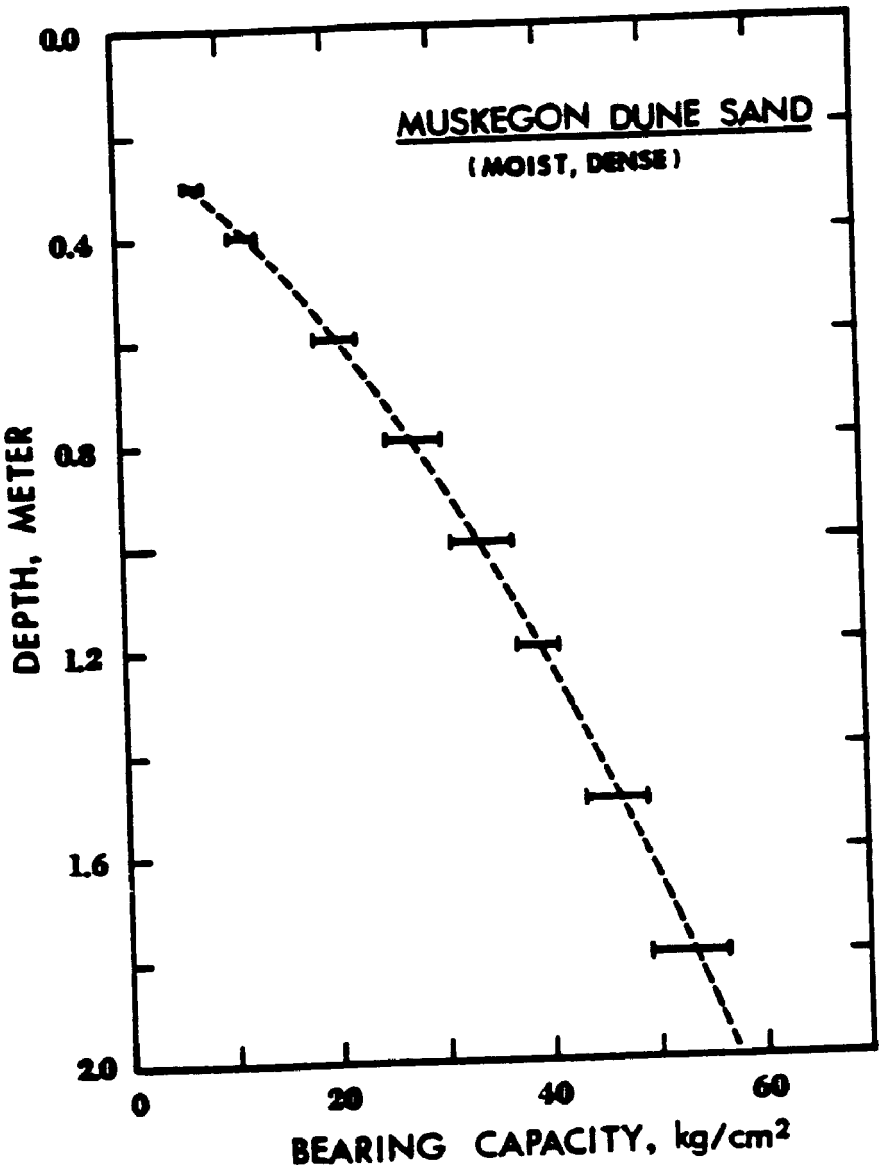

Figure 5.1 Results of Dutch Cone Penetrometer tests

to large amplitude by measuring the shear wave velocity, v_s, developed in the soil and by using the equation

$$G = \rho v_s^2 \qquad (5.2.1)$$

in which, ρ = the mass density of soil.

Both in-situ cross-hole tests and the resonant column tests were performed to determine the shear wave velocity and thus the shear modulus of the sand.

1. Cross-hole Tests

The "cross-hole method" of establishing the shear wave velocity was described in Section IV. C. 1, and has proved to be effective and relatively inexpensive. Since the quicksand tank had a limited soil surface boundary of 7½ ft. in diameter, the two augered holes were spaced 4 ft. apart. The impulse rod was placed in one hole and the transducer pickup was placed in the other, and tests were run at depths of 2, 3, 4 and 5 ft. into the dense moist sand. The time needed for the wave to travel the known distance was obtained from a trace on the oscilloscope representing the shear wave arrival time. Curve (a) of Fig. 5.2 shows the shear modulus vs depth from the cross-hole test. The improvement of the triggering system as described by Stokoe and Woods (1973), and the application of reversed impact signal technique by Schwarz and Musser (1972) made the cross-hole test more reliable and easier to analyze.

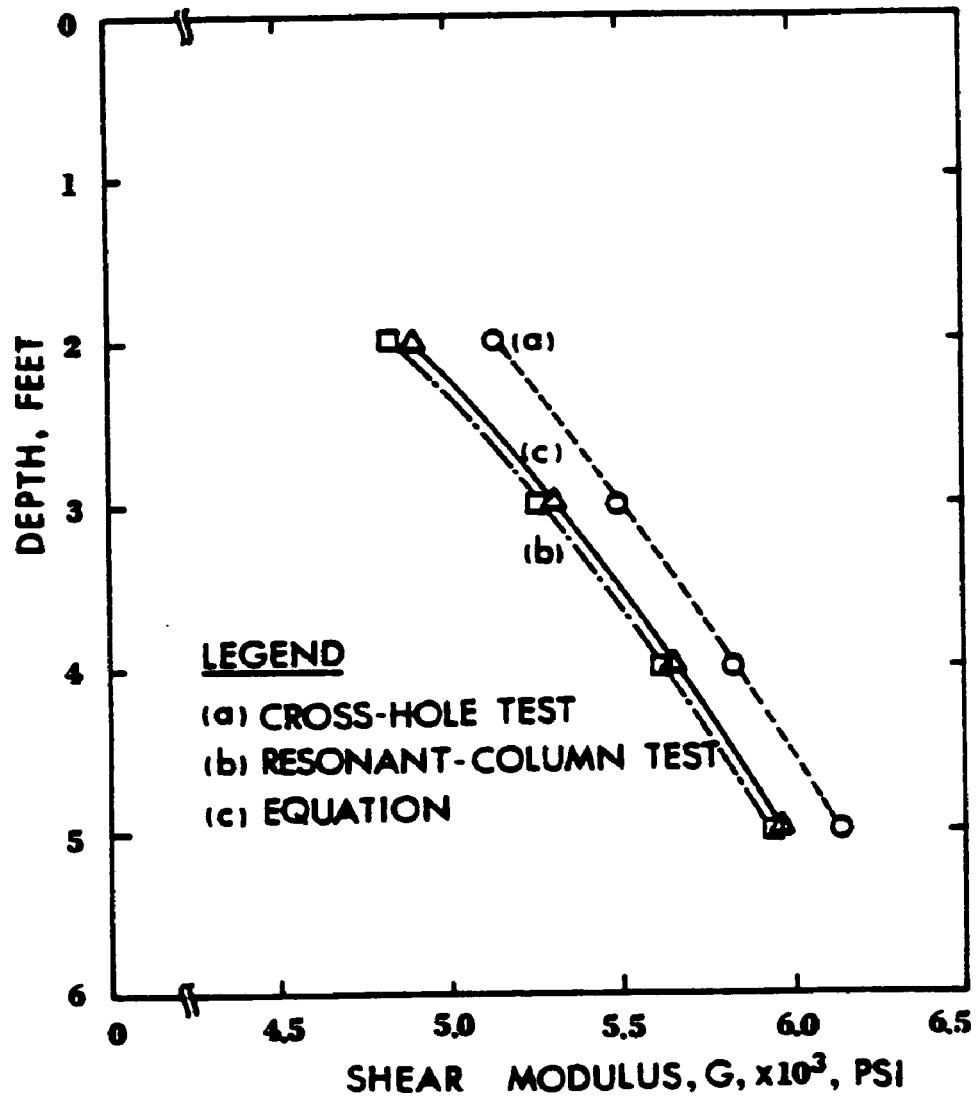

Figure 5.2 Variation of shear modulus with depth obtained from the cross-hole test, the resonant column test and the empirical equation

2. Resonant Column Tests

The resonant column test is a well established laboratory method of determining wave propagation velocities in soil samples.

Curve (b) of Fig. 5.2 shows test results from resonant column test for the Muskegon sand at a void ratio of 0.60, and at the confining pressures developed within the tank.

3. Empirical Equations

The shear modulus of soil is influenced by a number of quantities such as average effective confining pressure, void ratio, ambient stress history and vibration history, degree of saturation, octahedral shearing stress, grain characteristics, amplitude strain, frequency of vibration, secondary effects that are function of time and magnitude of stress increment, soil structure and temperature (Hardin and Black, 1968, Richart et al., 1970). Richart (1975) explained the effects of each factor clearly and in detail. However, it was demonstrated that for clean sands the shear modulus at low shearing strain amplitudes (less than 10^{-5}) is primarily a function of void ratio, e, and the confining pressure, $\bar{\sigma}_o$. Hardin and Richart (1963) showed this relationship by an empirical equation for round grained sand as:

$$G_{(psi)} = \frac{2630(2.17 - e)^2}{1 + e} (\bar{\sigma}_o)^{\frac{1}{2}}_{(psi)} \qquad (5.2.2)$$

The shear modulus for the Muskegon sand was also computed from the above equations for the purpose of comparisons with the results of the Cross-hole test and the resonant column test. Curve (c) of the Fig. 5.2 shows the results from the computation assuming K_o = 0.40, e = 0.60 and γ_d = 102.6 pcf. If K_o increases, the empirical values of the shear modulus shift to the right in Fig. 5.2., but at the same time the resonant column test curve shifts upward.

4. Comparison of Modulus by Three Methods

Figure 5.2 illustrates that the maximum difference in shear modulus between the three methods is approximately 14 percent at 2 ft. depth and 6 percent at 5 ft. The Cross-hole in-situ shear modulus shows higher numbers compared to that of the resonant column test results. The values again showed the better agreement at the relatively large depth when compared with the Cross-hole test results. Stokoe and Woods (1972) believed this phenomena to be due to bending of the waves downwards to higher velocity material.

5. Curved Path Theory

Haupt (1973) expressed the above concept in a mathematical form using curved wave path theory and

the equation established by Hardin and Richart (1963). Figure 5.3 illustrates Haupt's theoretical assumption. He suggested that there is some depth z_m which is greater than z_o, where the velocity has such a value, that the travel time of a wave along a horizontal straight path at this depth would be exactly same as on the curved path started at z_o. Then, the equivalent depth z_m, is found while source and sensor are still at depth z_o. The equivalent depth, z_{m1} can be calculated from

$$\frac{L_c}{C_s z_m^{0.25}} = T = 2 \int_{z_o}^{z_1} \frac{\sqrt{1 + (\frac{dx}{dz})^2}}{C_s z^{0.25}} \qquad (5.2.3)$$

in which, $C_s = (170 - 78.2\ e)\ (\frac{1 + 2K_o}{3}\ \gamma)^{\frac{1}{4}}$, L_c = distance between two boreholes, and T = travel time on the curved path.

By calculating the equivalent depth, z_m, for each data point, and then calculating the shear modulus again using Eq. (5.2.2) and substituting the equivalent depth instead of z_o, the curve (d) shown in Fig. 5.4 was obtained. This curve showed excellent agreement with the resonant column test results.

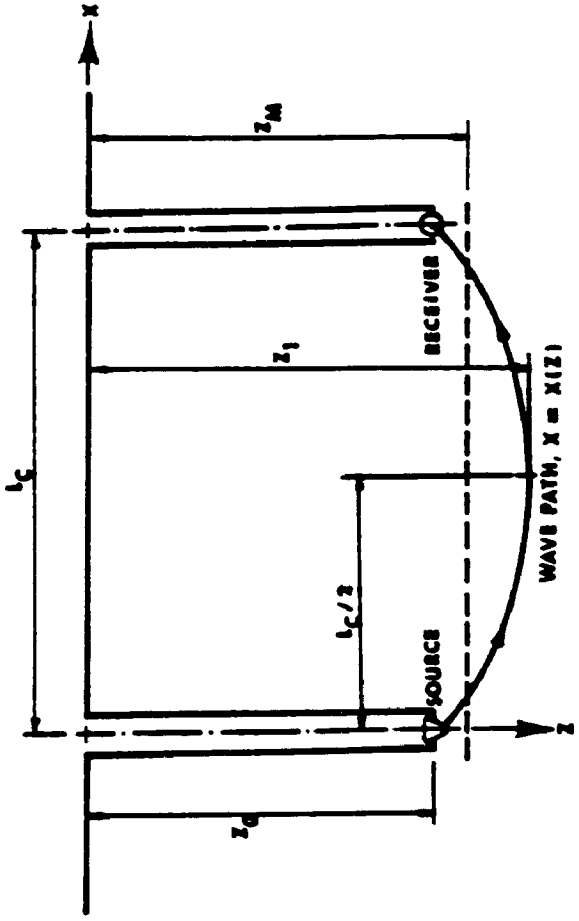

Figure 5.3 Diagram of curved wave path theory (Haupt, 1973)

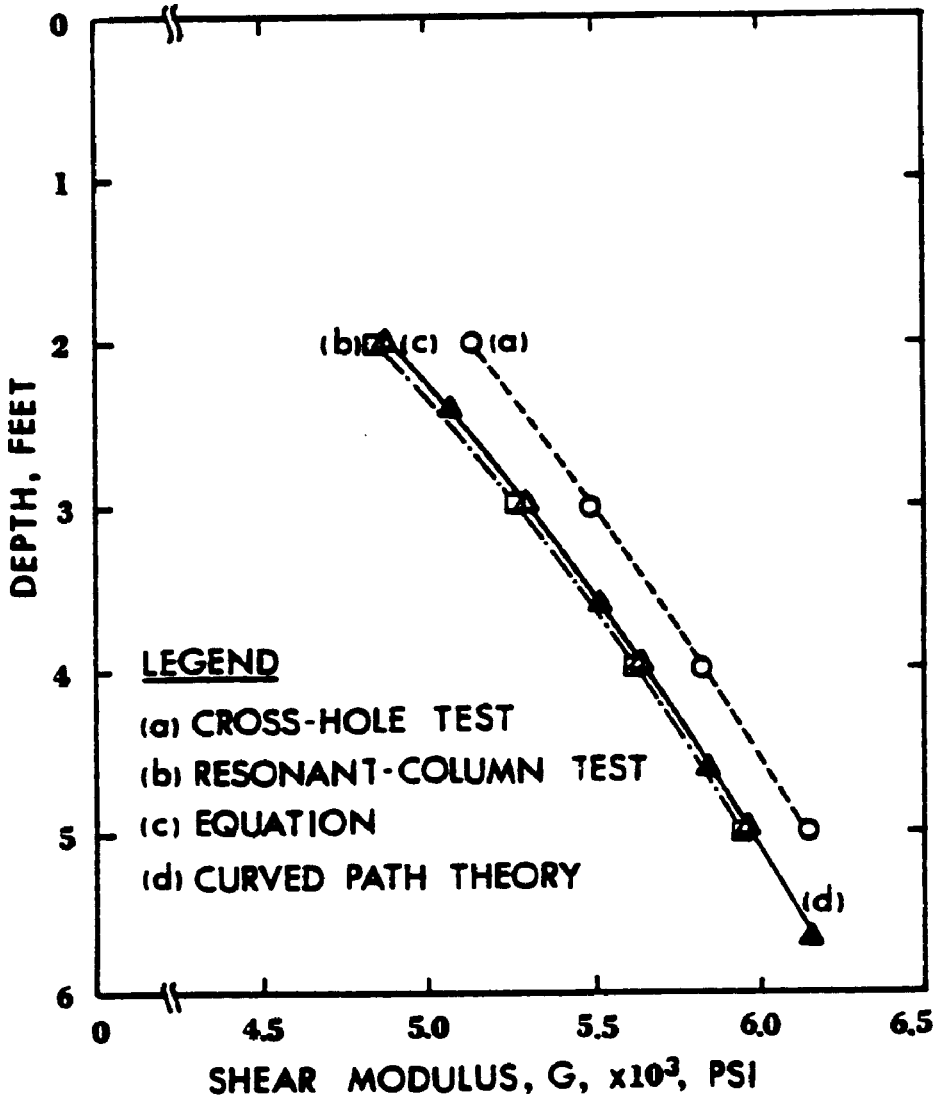

Figure 5.4 Variation of shear modulus with depth obtained from the cross-hole test, the resonant column test, the empirical equation and the curved wave path theory

CHAPTER VI

RESISTANCE OF PILES TO STATIC HORIZONTAL LOADS

A. Theoretical Analysis

1. Kubo's Method

In general, the following differential equation for beam deflection has been used to solve the pile problem by treating the system as a beam on elastic foundation

$$EI \frac{d^4y}{dz^4} = -P = -pB \qquad (6.1.1)$$

in which EI = flexural rigidity of pile, z = depth from the surface, y = displacement of pile at depth z, P = subgrade reaction per unit length of pile which occurs at depth z, p = subgrade reaction per unit area of pile which occurs at depth z (= -P/B), B = width of pile.

Shinohara and Kubo (1961), and Hayashi et al. (1963) have found from many model tests that the relationship between horizontal subgrade reaction and displacement can be expressed by the equation

$$p = k\, z^m\, y^n \qquad (6.1.2)$$

in which k = coefficient of horizontal subgrade reaction, $m \geq 0$, $1 \geq n \geq 0$. Kubo suggested the following relationship

$$p = k_s z y^{\frac{1}{2}} \tag{2.1.3}$$

for sand. Equation (6.1.1) can be rewritten as

$$EI \frac{d^4y}{dz^4} = -k_s z y^{\frac{1}{2}} B \tag{6.1.3}$$

The solution of Eq. (6.1.3) represents the response of a laterally loaded pile. However, it is almost impractical to solve this nonlinear differential equation for each varying condition. Kubo et al. (1967) showed an approximate solution using similarity rules to predict the behavior of laterally loaded piles without directly solving Eq. (6.1.3). The method involved the determination of conversion factors and standard curves.

a. Determination of Conversion Factors -- If it is assumed that the deflection curves of the prototype pile and standard pile are similar to each other, the following relationship should be established at the corresponding depth z,

$$\left.\begin{aligned} R_z &= z_p/z_s = \text{const.} \\ R_y &= y_p/y_s = \text{const.} \end{aligned}\right\} \tag{6.1.4}$$

in which z = depth to the corresponding point, y = horizontal displacement occurring at depth z, R = ratio of the corresponding quantity occurring at prototype pile and standard pile. (Subscript p is for prototype pile and s is for standard pile.) Then we can get the derivatives as follows:

$$\left.\begin{aligned} \frac{dy_p}{dz_p} &= \left(\frac{R_y}{R_z}\right)\frac{dy_s}{dz_s} \\ \frac{d^2y_p}{dz_p^2} &= \left(\frac{R_y}{R_z^2}\right)\frac{d^2y_s}{dz_s^2} \\ \frac{d^3y_p}{dz_p^3} &= \left(\frac{R_y}{R_z^3}\right)\frac{d^3y_s}{dz_s^3} \\ \frac{d^4y_p}{dz_p^4} &= \left(\frac{R_y}{R_z^4}\right)\frac{d^4y_s}{dz_s^4} \end{aligned}\right\} \qquad (6.1.5)$$

From the beam deflection theory

$$\left.\begin{aligned} \frac{d^2y}{dz^2} &= \frac{M}{EI} \\ \frac{d^3y}{dz^3} &= \frac{Q}{EI} \\ \frac{d^4y}{dz^4} &= \frac{P}{EI} \end{aligned}\right\} \qquad (6.1.6)$$

in which M = bending moment, Q = shearing force, P = subgrade reaction per unit length of pile, and EI = flexural rigidity of pile. Substitute Eqs. (6.1.6) into (6.1.5)

$$\left.\begin{aligned} \frac{M_p}{(EI)_p} &= \left(\frac{R_y}{R_z^2}\right) \frac{M_s}{(EI)_s} \\ \frac{S_p}{(EI)_s} &= \left(\frac{R_y}{R_z^3}\right) \frac{S_s}{(EI)_s} \\ \frac{P_p}{(EI)_s} &= \left(\frac{R_y}{R_z^4}\right) \frac{P_s}{(EI)_s} \end{aligned}\right\} \qquad (6.1.7)$$

Let $(EI)_p/(EI)_s = R_{EI}$ = constant. (6.1.8)

Substitute Eq. (6.1.8) into Eq. (6.1.7),

$$\left.\begin{aligned} \frac{M_p}{M_s} &= R_M = \left(\frac{R_y}{R_z^2}\right) R_{EI} \\ \frac{Q_p}{Q_s} &= R_Q = \left(\frac{R_y}{R_z^3}\right) R_{EI} \\ \frac{P_p}{P_s} &= R_P = \left(\frac{R_y}{R_z^4}\right) R_{EI} \end{aligned}\right\} \qquad (6.1.9)$$

Rewrite Eqs. (6.1.9),

$$\left.\begin{aligned} R_{EI} &= R_P\, R_z^{\,4}\, R_y^{-1} \\ R_Q &= R_P\, R_z \\ R_M &= R_P\, R_z^{\,2} \\ R_i &= R_P\, R_z^{-1} \\ R_y &= R_y \end{aligned}\right\} \qquad (6.1.10)$$

in which $R_i = i_p/i_s$, $i = dy/dz$.

From Eq. (6.1.2),

$$P = pB = k\, z^m\, y^n\, B \qquad (6.1.11)$$

we get

$$R_P = R_k\, (R_z)^m\, (R_y)^n\, R_B \qquad (6.1.12)$$

substitute Eq. (6.1.12) into Eq. (6.1.10) and rewrite the conversion factors as follows.

$$\left.\begin{aligned} R_Q &= (R_z)^a\, (R_{EI})^{bn}\, (R_k)^{-b}\, (R_B)^{-b} \\ R_M &= (R_z)^c\, (R_{EI})^{bn}\, (R_k)^{-b}\, (R_B)^{-b} \\ R_i &= (R_z)^d\, (R_{EI})^{bn}\, (R_k)^{-b}\, (R_B)^{-b} \\ R_y &= (R_z)^e\, (R_{EI})^{bn}\, (R_k)^{-b}\, (R_B)^{-b} \end{aligned}\right\} \qquad (6.1.13)$$

in which a = (-m-3n-1)/(n-1), b = 1/(n-1), c = (-m-2n-2)/(n-1), d = (-m-n-3)/(n-1), and e = (-m-4)/(n-1).

To satisfy the similarity rule for the deflection curves, the ratio of height of loading point (R_h) should be equal to the ratio of depth to the corresponding point,

$$R_h = R_z \tag{6.1.14}$$

Substitute m = 1 and n = 0.5 from the model tests into Eqs. (6.1.13) and take logarithm of both sides to get

$$\left.\begin{aligned} \log R_Q &= 7(\log R_z) - (\log R_{EI}) + 2(\log R_k) + 2(\log R_B) \\ \log R_M &= 8(\log R_z) - (\log R_{EI}) + 2(\log R_k) + 2(\log R_B) \\ \log R_i &= 9(\log R_z) - 2(\log R_{EI}) + 2(\log R_k) + 2(\log R_B) \\ \log R_y &= 10(\log R_z) - 2(\log R_{EI}) + 2(\log R_k) + 2(\log R_B) \end{aligned}\right\} \tag{6.1.15}$$

b. Standard Curves -- Kubo et al. (1967) drew standard curves for the standard pile which has the following characteristics.

$EI = 27.54 \times 10^6$ kg-cm^2

h = 15 cm

B = 10 cm

$k_s = 0.05$ kg-cm$^{-3.5}$

Standard curves for the displacement and slope of the pile at ground level are shown as Figs. (6.1) and (6.2), and their values were shown in Table 6.1. The value of k_s for prototype is determined from Fig. (6.3), where $\bar{N}$ is the standard penetration number at one meter depth.

c. Procedures for the Application --

1) Determine the corresponding k_s-value to the $\bar{N}$ value of the soil.

2) Compute ratio of variables: R_h, R_{EI}, R_k, R_B

3) Compute ratio of variables: R_y, R_Q, R_M, R_i

4) Compute S_s from

$$\log S_s = \log S_p - \log R_Q$$

5) Determine the corresponding $(y_o)_s$, $(i_o)_s$, $(M_{max})_s$, to S_s obtained in 4 by "standard curves."

6) Compute $(y_o)_p$, $(i_o)_p$, $(M_{max})_p$ from the following relations.

$$(\log y)_p = (\log y_o)_s + \log R_y$$

$$(\log i_o)_p = (\log i_o)_s + \log R_i$$

$$(\log M_{max})_p = (\log M_{max})_s + \log R_M$$

$$(\log \ell_{ml})_p = (\log \ell_{ml})_s + \log R_h$$

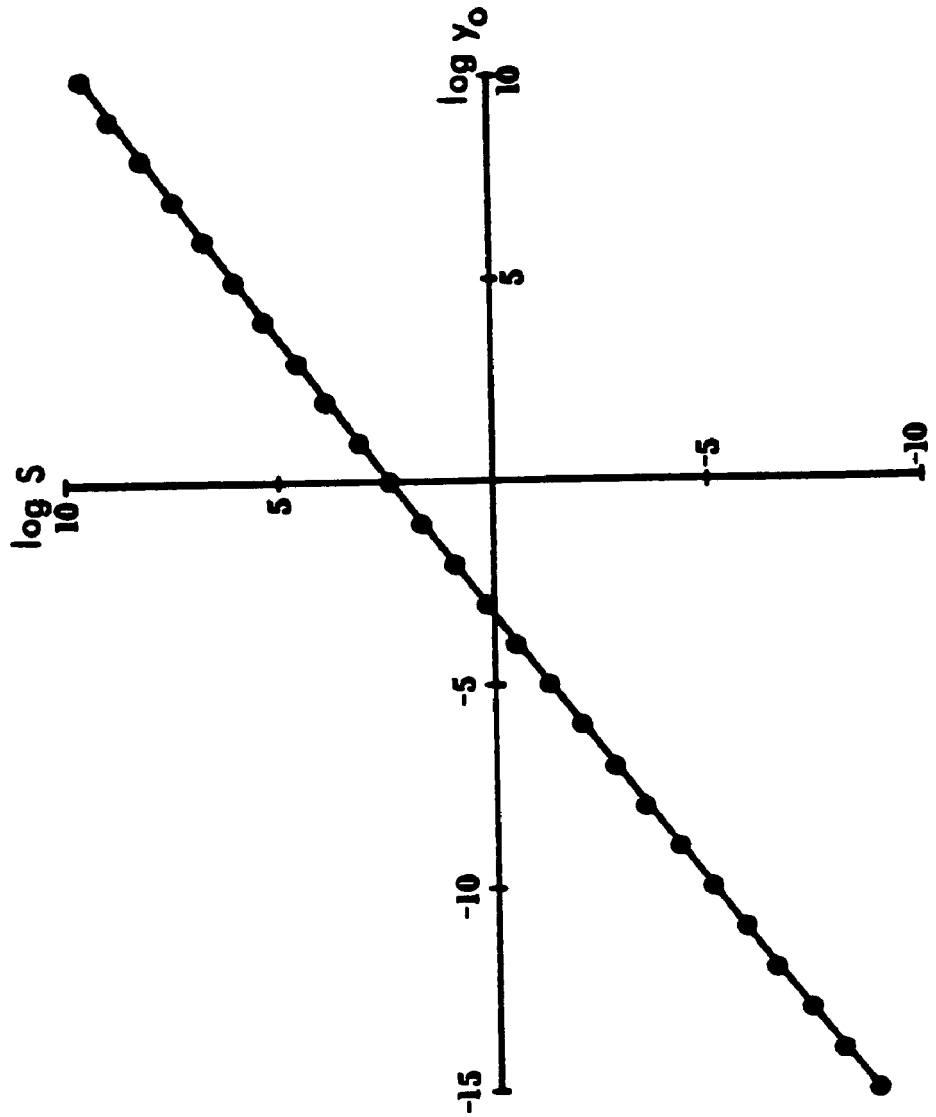

Figure 6.1 Standard curve for free-head pile, deflection at the ground surface (Kubo, 1964)

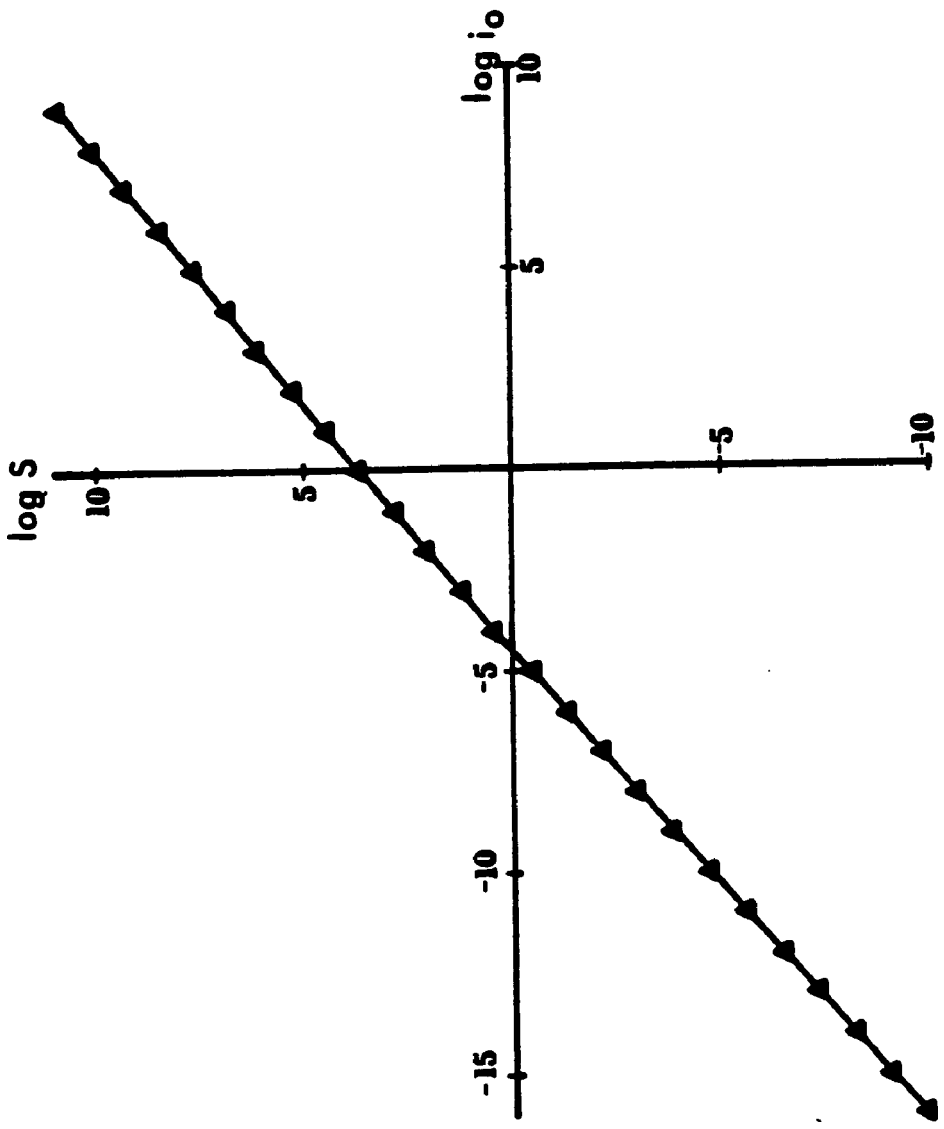

Figure 6.2 Standard curve for free-head pile, inclination at the ground surface (Kubo, 1964)

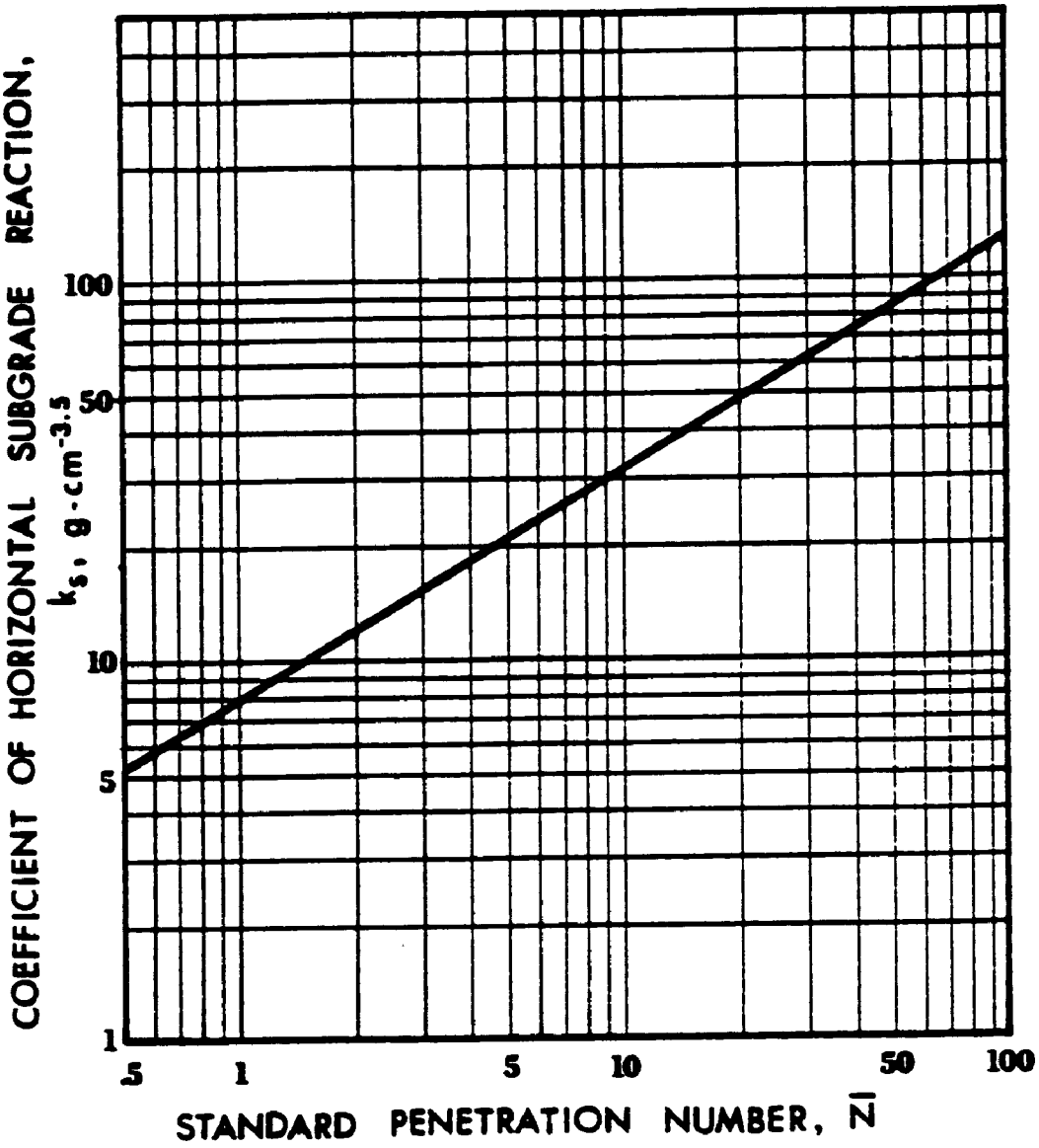

Figure 6.3 Relationship between $\bar{N}$ and k_s for the uniform sand (Kubo, 1964)

Table 6.1. Standard Curves for Free-Head Pile (Kubo, 1964)

Ground Surface Deflection		Maximum Moment		Depth of 1st Zero Moment Point		Inclination at Ground Surface	
$\log y_o$	$\log S$	$\log M_{max}$	$\log S$	$\log \ell_{m1}$	$\log S$	$\log i_o$	$\log S$
-15	-8.906	-10	-11.187	0.0	-12.244	-16	-9.837
-14	-8.131	-9	-10.188	0.1	-11.544	-15	-8.971
-13	-7.360	-8	-9.189	0.2	-10.844	-16	-8.106
-12	-6.591	-7	-8.191	0.3	-10.144	-13	-7.242
-11	-5.826	-6	-7.194	0.4	-9.444	-12	-6.379
-10	-5.065	-5	-6.198	0.5	-8.744	-11	-5.518
-9	-4.306	-4	-5.206	0.6	-8.044	-10	-4.659
-8	-3.551	-3	-4.217	0.7	-7.344	-9	-3.803
-7	-2.799	-2	-3.234	0.8	-6.644	-8	-2.950
-6	-2.050	-1	-2.261	0.9	-5.944	-7	-2.100
-5	-1.304	0	-1.299	1.0	-5.244	-6	-1.254
-4	-0.561	1	-0.352	1.1	-4.544	-5	-0.413
-3	0.179	2	0.580	1.2	-3.844	-4	0.434
-2	0.915	3	1.699	1.3	-3.144	-3	1.255
-1	1.649	4	2.140	1.6	-2.444	-2	2.080
0	2.380	5	3.314	1.5	-1.744	-1	2.900
1	3.108	6	4.213	1.6	-1.044	0	3.714
2	3.833	7	5.108	1.7	-0.344	1	4.523
3	4.555	8	6.001	1.8	0.356	2	5.326
4	5.274	9	6.890	1.9	1.056	3	6.124
5	5.991	10	7.778	2.0	1.756	4	6.918
6	6.705	11	8.664	2.1	2.456	5	7.709
7	7.417	12	9.548	2.2	3.156	6	8.497
8	8.126	13	10.432	2.3	3.856	7	9.283
9	8.834			2.4	4.556	8	10.067
10	9.540			2.5	5.256	9	10.850
				2.6	5.956		
				2.7	6.656		
				2.8	7.356		
				2.9	8.056		
				3.0	8.756		

2. Kuhlemeyer's Method

Kuhlemeyer (1976) suggested an approximate linearly elastic finite element analysis for a laterally loaded pile using modified, four-nodal point, rectangular finite elements (see Fig. 6.4) as in beam bending problems. He assumed that the length of pile embedded into soil exceeded the effective length, which is a minimum length of pile required to resist the lateral load. It is also assumed that all forces are applied at ground level.

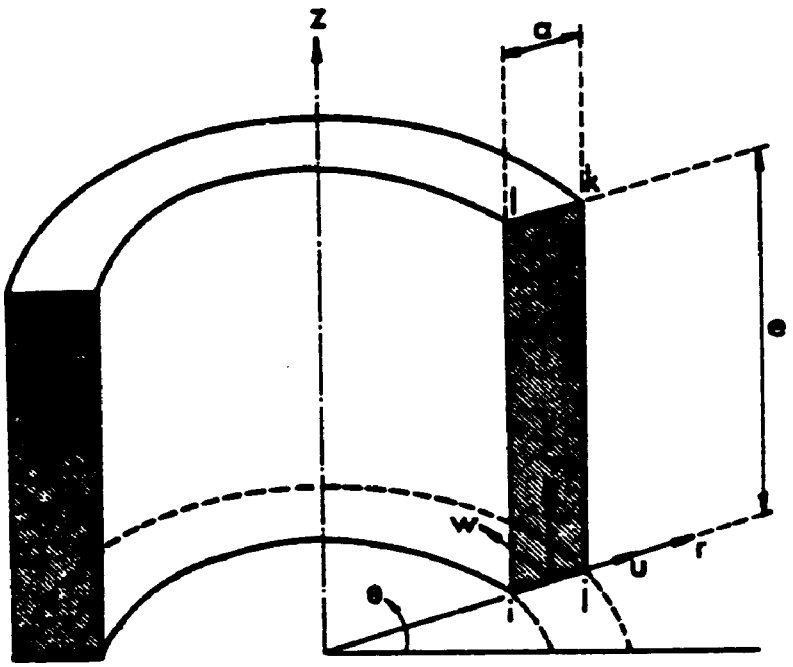

Figure 6.4 The rectangular ring element for Kuhlemeyer solution (kuhlemeyer, 1976)

A reduced integration technique was applied to the non-axisymmetrically loaded axisymmetric element in order

to model the bending behavior of a pile embedded in an elastic layered media.

For the free-headed pile, to which forces and moments are applied, the displacement-force relationship can be expressed as

$$\begin{bmatrix} U \\ \phi r_o \end{bmatrix} = \begin{bmatrix} a_{11} & a_{12} \\ a_{21} & a_{22} \end{bmatrix} \begin{bmatrix} S/k_x \\ Mr_o/k_\psi \end{bmatrix} \qquad (6.2.1)$$

in which a_{ij} are dimensionless flexibility coefficients, r_o is the radius of the pile, k_x = lateral translation spring constant, and k_ψ = rotational spring constant, S = horizontal load acting at the ground surface, M = moment acting at the ground surface, U = horizontal displacement, ϕ = rotation of the pile. It is assumed that the k_x and k_ψ are equal to $E_s r_o$ and $E_s r_o^3$ respectively. The Eqs. (6.2.1) can be rewritten as

$$U = a_{11} \frac{S}{E_s r_o} + a_{12} \frac{M}{E_s r_o^2}$$

$$\phi = a_{21} \frac{S}{E_s r_o^2} + a_{22} \frac{M}{E_s r_o^3} \qquad (6.2.2)$$

Kuhlemeyer compares the above equations with Poulos' (1971) equations which are

$$U = I_{US} \frac{S}{E_s L} + I_{UM} \frac{M}{E_s L^2}$$

$$\phi = I_{\theta S} \frac{S}{E_s L^2} + I_{\theta M} \frac{M}{E_s L^3} \qquad (6.2.3)$$

in which I_{US} and I_{UM} are the displacement influence factors for horizontal load only and for moment only, respectively, acting at the ground surface. $I_{\theta S}$ and $I_{\theta M}$ are the rotation influence factor for horizontal load only and for moment only respectively, acting at the ground surface. These influence factors are functions of L/r_o and a pile flexibility factor, K_R,

$$K_R = \frac{E_p I_p}{E_s L^4} \qquad (6.2.4)$$

Approximate relationship between a_{ij} and E_p/E_s were established as

$$\begin{cases} a_{11} = 0.567 \ (E_p/E_s)^{-0.170} \\ a_{12} = a_{21} = 0.369 \ (E_p/E_s)^{-0.407} \\ a_{22} = 0.585 \ (E_p/E_s)^{-0.663} \end{cases} \qquad (6.2.5)$$

By applying the Eqs. (6.2.2) and (6.2.5), the approximate static behavior of a laterally loaded pile which has a

length longer than the effective length and embedded in an elastic layer overlying an elastic half-space can be computed.

3. Comparison of Experimental Data with Theoretical Analyses.

The static test results shown in Figs. 6.5 and 6.6 were obtained from piles embedded in a submerged, dense sand loaded horizontally by the Gilmore actuator.

The value of $\bar{N}$ for Kubo's method was calculated from the relationship established by Schmertmann (1970) between the bearing capacity, q_c, by static Dutch cone penetrometer test and the standard penetration number N,

$$q_c = 18.3 + 2.9\ N \tag{6.3.1}$$

The value of q_c to determine $\bar{N}$ was taken at depth of 1 meter from the ground surface. The modulus of elasticity of sand was also determined from the relationship established by Schmertmann (1970) between the modulus of elasticity and bearing capactiy by static Dutch cone penetrometer test,

$$E_s = 2\ q_c \tag{6.3.2}$$

The value q_c for the determination of E_s was taken at depth of 1½ ft. from the ground surface. Kubo determined

the effective length of embedment to be 1.5 times the depth to the first zero point of the moment distribution curve. He assumed that the pile has an infinite length of embedment. Kuhlemeyer also assumed that the pile should be longer than the effective length. The effective length of piles tested showed the ranges of between 5.7 ft. and 9.0 ft. for Kubo, and 5.25 ft. and 6.75 ft. for Kuhlemeyer for 4½ in. and 3½ in. round piles, respectively.

Yoshimi et al. (1971) calculated new standard curves computed for the new standard pile with round number dimensions (B = 50 cm, h = 100 cm) by numerically integrating the equilibrium equation of a non-dimensional laterally loaded pile. The new standard pile has more practical dimensions and can be applied to real life problems. However, it was decided to use Kubo's standard pile in comparing with the present test results because of its similarity in dimensions.

Test results for all piles which were embedded 5 ft. into submerged, dense sand showed better agreement with Kubo's method, which specifies non-linear relationships between the lateral resistance and displacement of piles as noted by Eq. (2.1.3), than with Kuhlemeyer's linear elastic theory. Piles of shorter embedment (3 ft. and 4 ft.) showed a great disagreement with both methods and gave larger displacements as the depth of embedment

decreased. It is believed that these piles responded as short piles.

Another observation indicated that the influence of pile width should be considered in determining the coefficient of subgrade reaction, k_s, since the effect of the pile width, B, is quite large for the smaller B. Kubo stated that this effect became negligible as the pile width exceeded approximately 8 in. Terzaghi (1955) on the other hand assumed that the coefficient of subgrade reaction is inversely proportional to pile width.

One advantage in applying Kuhlemeyer's method is its simplicity in calculating the first estimate of the probable static behavior of laterally loaded piles.

Figure 6.7 shows results obtained here from model pile tests with those calculated from Kubo's and Kuhlemeyer's theoretical procedures. Kubo's solutions in Fig. 6.7 were obtained using the standard penetration number at 1 meter depth of 5 blows/ft., which was calculated from the Dutch cone test results by applying Eq. (6.3.1). The corresponding value of the coefficient of subgrade reaction, k_s, was 21.5 kg-cm$^{-3.5}$ from Fig. 6.1. Kuhlemeyer's solutions in Fig. 6.7 were calculated from Eqs. (6.2.3) and (6.2.5) by assuming the lateral load applied was approximately the same as the maximum static load in the experimental work. The modulus of elasticity of the soil was assumed as 300 psi which was

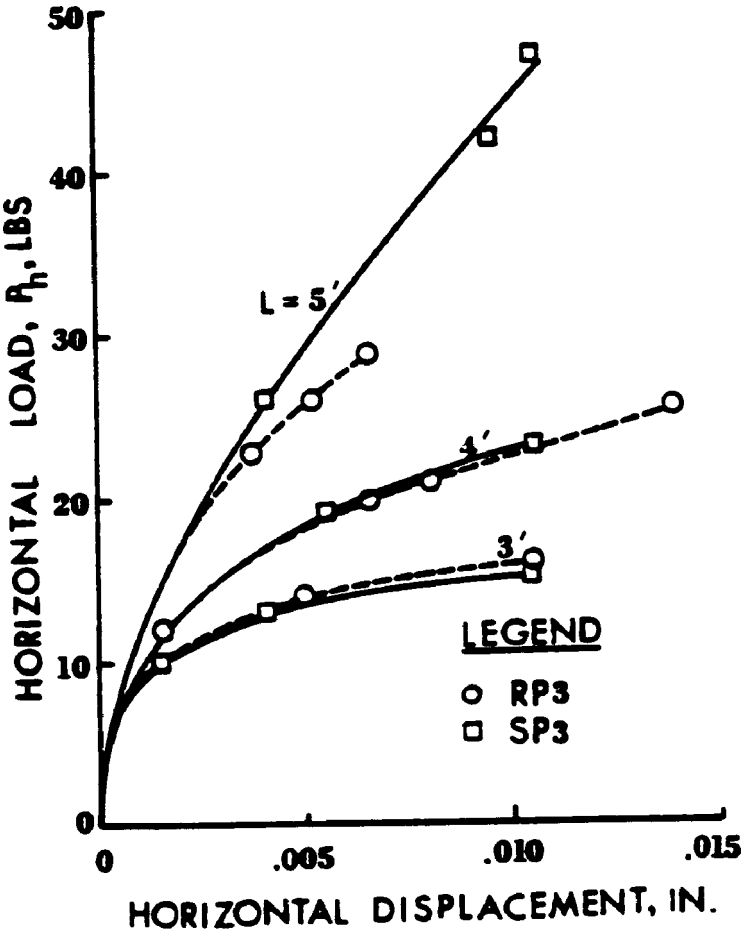

Figure 6.5 Static test results, displacement vs. horizontal load.

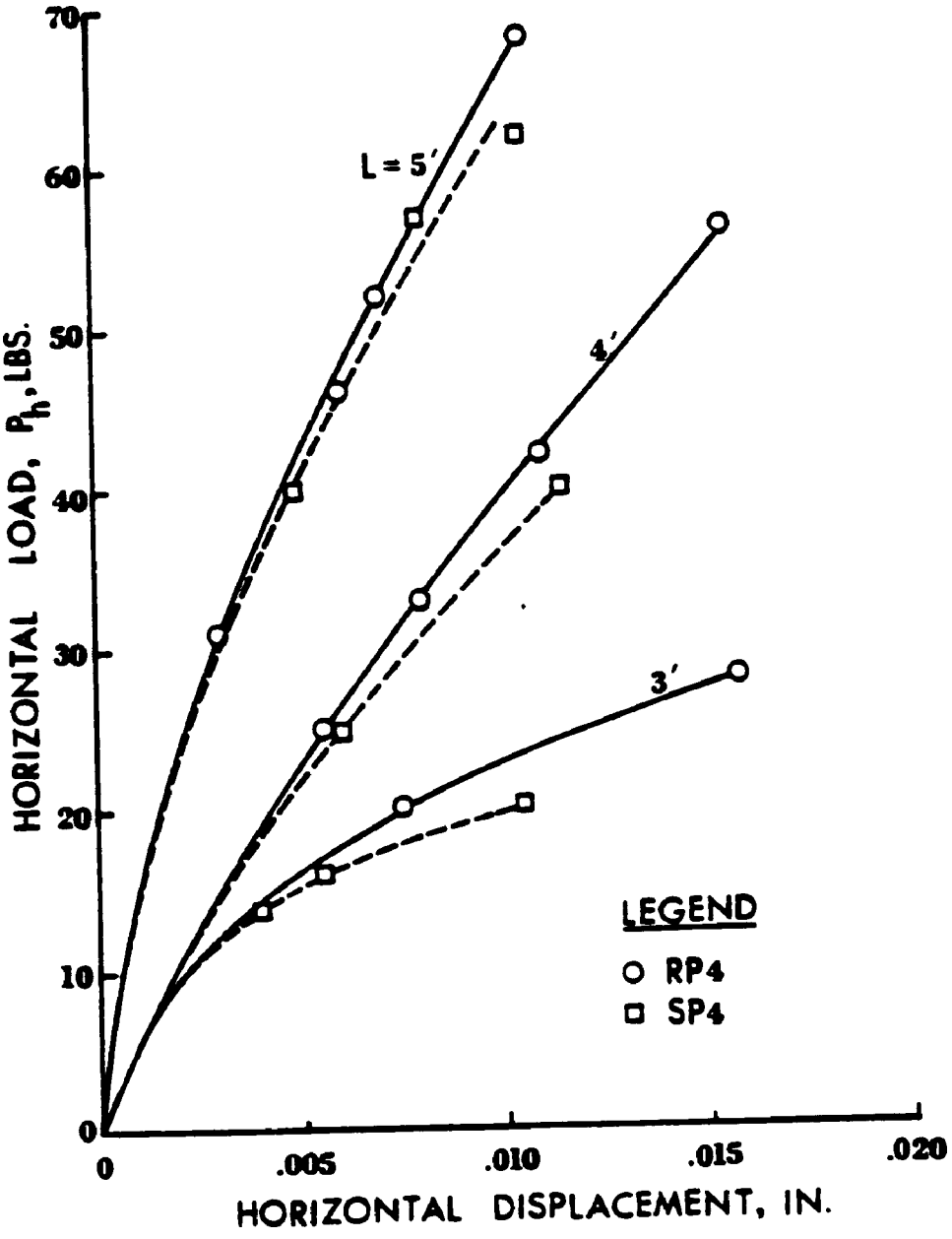

Figure 6.6 Static test results, displacement vs. horizontal load

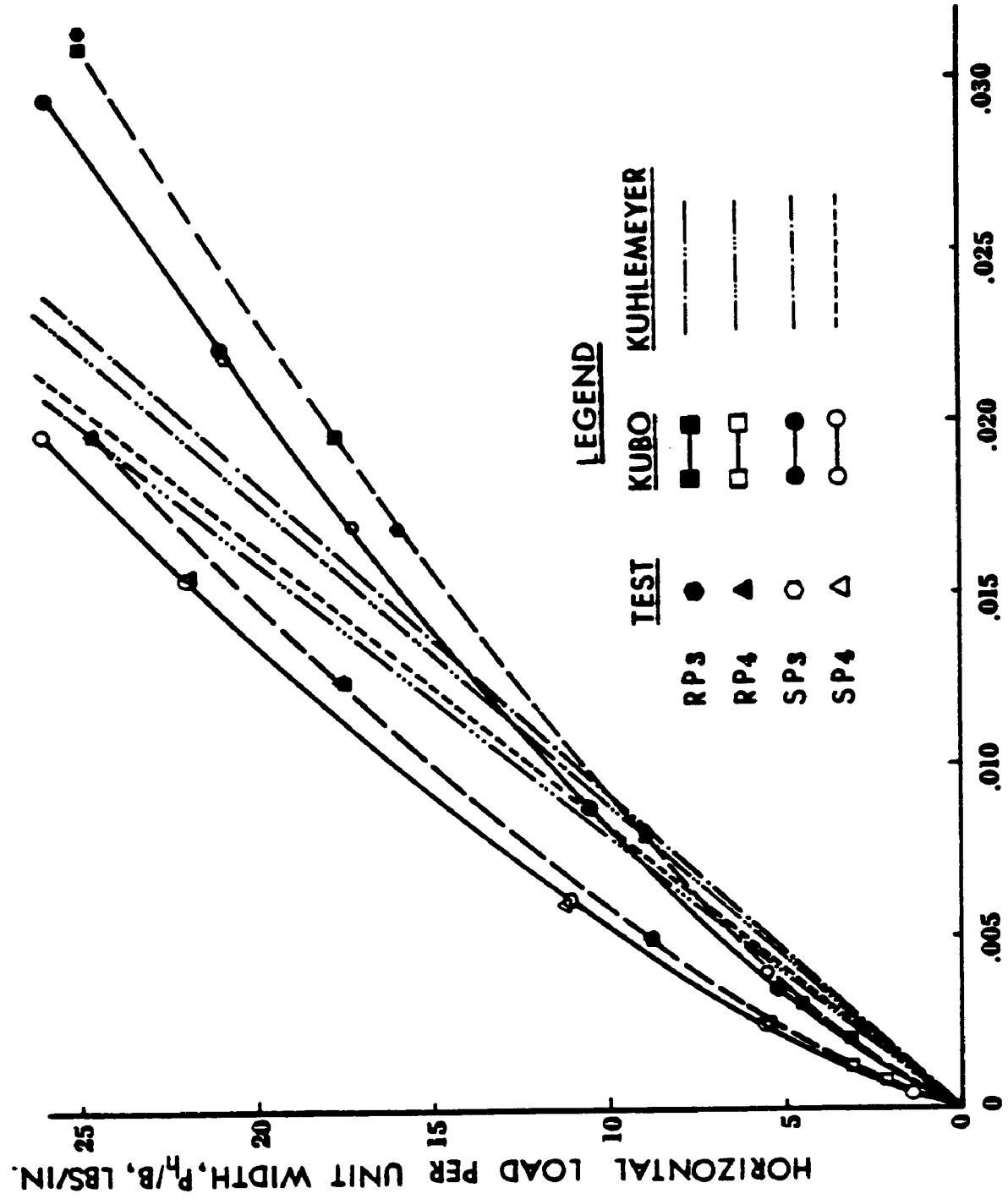

Figure 6.7 Static test results, horizontal displacement vs. horizontal load per unit width.

calculated from the Dutch cone test results, and by applying Eq. (6.3.2) at depth of 1½ ft. from the ground surface.

CHAPTER VII

RESPONSE OF PILES TO DYNAMIC LOADS

A. Theoretical Analysis

1. Inverse Non-linear Problem

A series of rotating eccentric-mass type steady-state dynamic tests were performed with steel piles embedded in a submerged dense sand. The test data obtained through these tests showed a non-linearity in soil-pile interaction which is characterized by changes in resonant frequencies with vibration amplitudes (excitation intensity) and the lack of proportionality between exciting force and response amplitudes. Novak (1971) suggested a procedure to solve the inverse problem of determining the non-linear characteristics of both the resulting force and the damping force from test results. It is valid only for steady-state oscillation excited by a harmonic force whose amplitude increases with the square of the frequency, as is the case in these tests. Only motion with a frequency equal to the excitation frequency is considered and only its first harmonic component is taken into account.

Consider a non-linear system excited by a harmonic force:

$$Q(t) = m_e \bar{e} \omega^2 \sin \omega t \qquad (7.1.1)$$

in which m_e = the rotating unbalanced mass, $\bar{e}$ = eccentricity of unbalanced mass, and ω = frequency of excitation. When the mass of the system is m, the differential equation of motion in one-degree-of-freedom is

$$m\ddot{y} + ky + f(y,\dot{y}) = Q(t) \qquad (7.1.2)$$

in which ky = the linear part of the restoring force, $f(y,\dot{y})$ = a function expressing the nonlinear part of the restoring force and the total nonlinear damping related to the vibration velocity. The exact solution of Eq. (7.1.2) is usually not possible, however, a number of asymptotic approximations are available. The method of equivalent linearization will be used for the first approximation. The equivalent linear equation of motion becomes

$$m\ddot{y} + c_e(A)\dot{y} + k_e(A)y = Q(t) \qquad (7.1.3)$$

in which $c_e(A)$ = the equivalent linear damping and $k_e(A)$ = the equivalent spring constant. Both c_e and k_e are expected to be functions of steady vibration amplitude A.

The particular solution of Eq. (7.1.3) is

$$y = A\sin(\omega t + \phi) \tag{7.1.4}$$

in which ϕ = phase angle. It is required that this particular solution of the linear equation is equal to the first approximation to the solution of non-linear Eq. (7.1.3). This condition yields for the equivalent linear stiffness

$$k_e(A) = k + \frac{1}{\pi A}\int_o^{2\pi} f(A\sin\tau\ ,\ A\omega\cos\tau)\ \sin\tau d\tau \tag{7.1.5}$$

in which $\tau = \omega t + \phi$, and for the equivalent linear damping coefficient

$$c_e(A) = \frac{1}{\pi A\omega}\int_o^{2\pi} f(A\sin\tau\ ,\ A\omega\cos\tau)\ \cos\tau d\tau \tag{7.1.6}$$

With these equivalent values, Eq. (7.1.3) can be handled as a linear equation. The undamped natural frequency ω_{on} is

$$\omega_{on} = (k_e(A)/m)^{\frac{1}{2}} \tag{7.1.7}$$

Substituting the particular solution into Eq. (7.1.3) to obtain the response curve of forced vibration in the implicit form gives

$$\omega^4(1 - \frac{\rho_m^2}{A^2}) - 2\omega^2(\omega_{on}^2 - 2\ \alpha_e^2) + \omega_{on}^4 = 0 \tag{7.1.8}$$

in which $\rho_m = m_e\bar{e}/m$, and $\alpha_e = c_e(A)/2m$. Because both ω_{on} and α_e are functions of amplitude A, this amplitude generally cannot be expressed in an explicit form from Eq. (7.1.8). For the phase shift ϕ

$$\phi = \sin^{-1}\left(\frac{2\alpha_e}{\rho_m}\frac{A}{\omega}\right) \tag{7.1.9}$$

The response curves with nonlinear restoring force and linear damping have several geometric properties which can be used in data reduction. It is necessary to calculate the curve of natural frequencies, ω_{on}, vs. amplitude which represents the backbone or skeleton curve of the response curve. Cut the given response curve by a straight line passing through the origin as in Fig. 7.1. The frequency of the point intersecting with the backbone curve can be calculated from a simple relation as

$$\omega_{on} = (\omega_I\omega_{II})^{\frac{1}{2}} \tag{7.1.10}$$

The only limitation for this equation is that the damping must be linear. When the straight line passing through the origin touches the response curve at point (ω_T, A_T), the equation of the tangent to the response curve is

$$A_T = \frac{\rho_m}{2\alpha}\omega_T \tag{7.1.11}$$

in which $\alpha = \omega_o D$, ω_o = natural frequency for linear vibration, and D = damping ratio. The tangents passing through the origin apply also for all linear systems and determine on vertical lines the resonant amplitudes of linear systems whose amplitudes are proportional to the excitation.

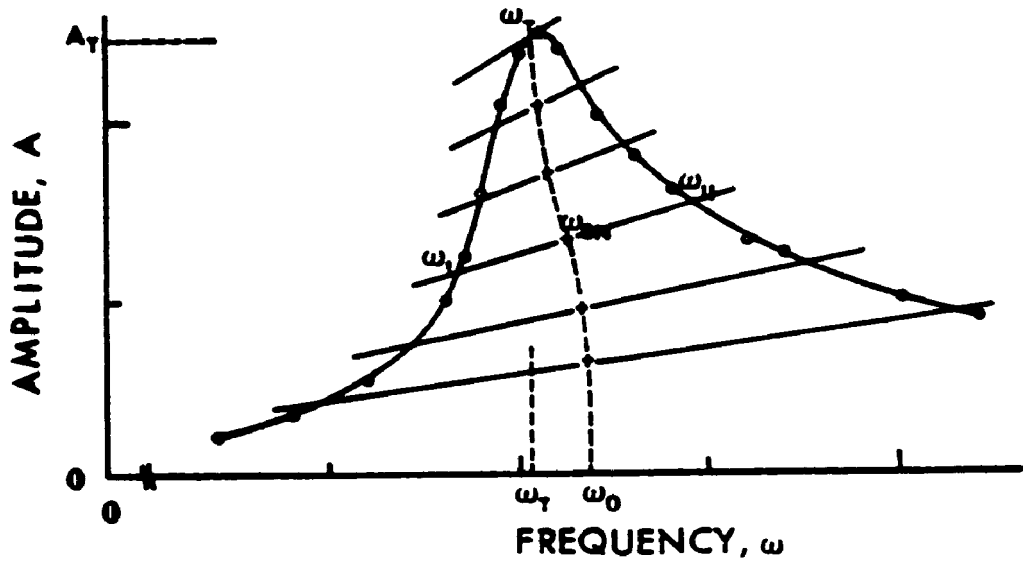

Figure 7.1 Determination of undamped natural frequency curve (Example, Novak, 1971)

The analysis of measured response curves can be complicated by the instability of amplitudes resulting in "amplitude-jumping (see Fig. 2.2). The possibility of jumps usually increases with nonlinearity, force level, and lower damping. Having determined the curve of undamped natural frequency, damping can be established from the general equation of the response curves. Without the use of the resonant peak, damping can be established from two

points on the response curve having any amplitude A and the corresponding point on the curve of natural frequencies with the same amplitude. The amplitude of the two points on the response curve can be expressed.

$$A = \frac{m_e \bar{e} \omega_1^2}{m[(\omega_{on}^2 - \omega_1^2) + 4\alpha^2 \omega_1^2]^{\frac{1}{2}}} = \frac{m_e \bar{e} \omega_2^2}{m[(\omega_{on}^2 - \omega_2^2) + 4\alpha^2 \omega_2^2]^{\frac{1}{2}}} \tag{7.1.12}$$

From the above equation the damping ratio of a nonlinear system is

$$D = \frac{\alpha}{\omega_o} = \frac{1}{2} \frac{\omega_{on}}{\omega_o} \sqrt{2 - \left(\frac{\omega_{on}}{\omega_1}\right)^2 - \left(\frac{\omega_{on}}{\omega_2}\right)^2} \tag{7.1.13}$$

Frequencies at any amplitude can be substituted into the above equation, however, values from the broader middle part of the response curve yields more accurate results.

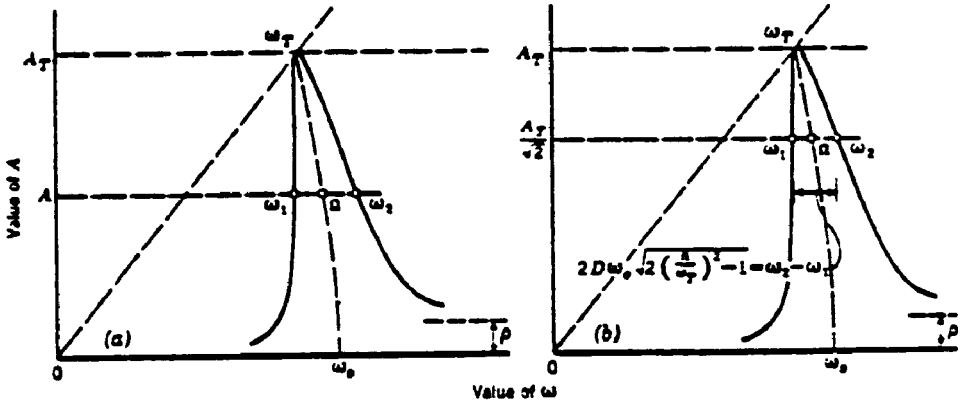

Figure 7.2 Calculation of damping from non-linear response curves (Novak, 1971)

For a very low damping ($D \leq 0.1$) the use of the resonant amplitude can improve the accuracy. Consider two points on the response curve with any arbitrary amplitude A and the corresponding point on the curve of natural frequencies, and also the resonant amplitude A_T. Then

$$D = \frac{\alpha}{\omega_o} = \frac{1}{2} \frac{\omega_2 - \omega_1}{\omega_o} \left[\left(\frac{\omega_{on}}{\omega_T} \frac{A_T}{T} \right) - 1 \right]^{-\frac{1}{2}} \qquad (7.1.14)$$

When the mass is given, a more accurate value of the damping ratio can be found from

$$D = \frac{\alpha}{\omega_o} = \frac{\rho_m}{2A_T} \frac{\omega_T}{\omega_o} \qquad (7.1.15)$$

2. Pure Rotational Solution of a Short Rigid Pile

An approximate solution for the dynamic response of a short rigid pile to lateral harmonic excitation is presented herein, based on the concept of side layer reaction developed by Baranov (1967) for foundations embedded in an elastic half-space. It is assumed that the pile is rigid and the soil surrounding the pile consists of a series of infinitesimally thin elastic layers. The lateral exciting force is in harmonic motion and all of the deformations are assumed small. The mode of motion is pure rocking-rotation about a horizontal axis passing through point O of Fig. 7.3a, however, the effect of

sliding at the pile tip is neglected. The shear modulus of the surrounding soil is assumed to vary with depth according to the square-root distribution.

$$(G)_z = A_s \, z^{\frac{1}{2}} \tag{7.2.1}$$

in which z is the depth at which the dynamic response of the pile is considered, and A_s is a coefficient which depends on the void ratio and density of the soil.

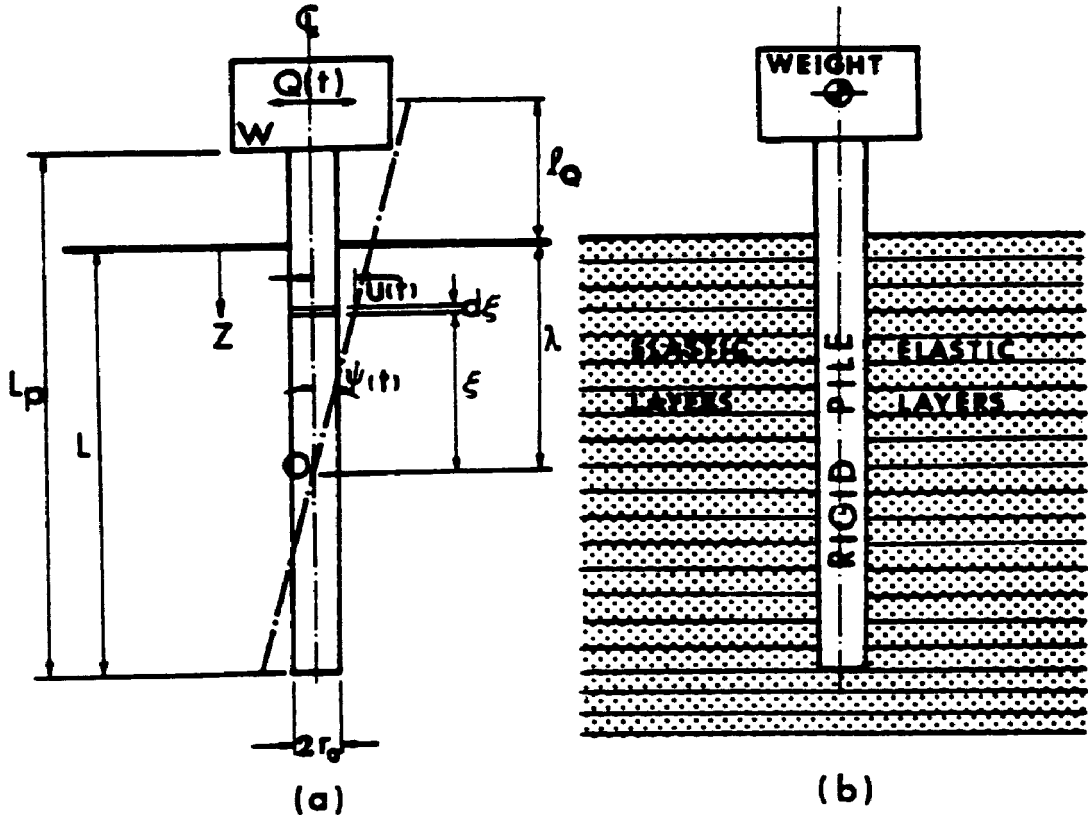

Figure 7.3 Diagram of soil-pile system subjected to lateral dynamic excitation and assumption of Baranov's thin elastic layers

For rotation about a horizontal axis, the basic equation of motion is

$$I_\psi \ddot{\psi}(t) + N_\psi(t) = T(t) \qquad (7.2.2)$$

in which I_ψ = mass moment of inertia of the pile plus the mass located on the top of the pile about a horizontal axis passing through point O of Fig. 7.3, $\ddot{\psi}(t)$ = acceleration of angular rotation, $N_\psi(t)$ = side reactive moment from the soil surrounding the pile, $T(t)$ = torque caused by excitation of the lateral force $Q(t)$, and t = time.

The side reaction $N_\psi(t)$ is, in general, a complex function of the pile geometry, the angular rotation, the shear modulus and Poisson's ratio of the soil, as well as, of the dimensionless frequency, a_o. The dimensionless frequency is defined as

$$a_o = \omega r_o (\rho_s/G_s)^{\frac{1}{2}} \qquad (7.2.3)$$

in which ω = frequency of excitation, rad/sec, r_o = radius of the pile, ft., ρ_s = mass density of the soil, and G_s = shear modulus of the soil at the lower end of the pile. The side layer reaction was defined by Baranov (1967) (see Fig. 7.3b) as

$$N_\psi(t) = \int_o^\ell [S_\psi(\xi,\psi,t) + S_u(\xi,u,t)\xi]d\xi \qquad (7.2.4)$$

in which $S_\psi(\xi,\psi,t)$ = the reactive moment, $S_u(\xi,u,t)$ = the horizontal reaction per unit displacement of a horizontal layer of thickness $d\xi$ at the distance ξ from the center of rotation O, ℓ = depth of embedment, and u = horizontal displacement.

The relation between the complex rotation

$$\psi(t) = \psi_o \exp[i(\omega t+\phi)] \tag{7.2.5}$$

and the reactive moment S_ψ can be expressed as

$$S_\psi(\xi,\psi,t) = S_\psi(a_o,\xi)\psi(t) \tag{7.2.6}$$

Similarly, for horizontal displacement

$$u(t) = u_o \exp[i(\omega t + \phi)] \tag{7.2.7}$$

and for horizontal reaction, the expression is

$$S_u(\xi,u,t) = S_u(a_o,\nu,\xi)u(t) \tag{7.2.8}$$

in which ψ_o = rotational amplitude, u_o = displacement amplitude, $i = (-1)^{\frac{1}{2}}$, ω = frequency of excitation, ϕ = phase angle, and $S_\psi(a_o,\xi)$ = rigidity parameter for rotation. $S_u(a_o,\nu,\xi)$ is a rigidity parameter for displacement, and $S_\psi(a_o,\xi)$ and $S_u(a_o,\nu,\xi)$ are defined as

$$S_{\psi}(a_o,\xi) = \pi r_o^2 \, G(\xi) \left[1 - a_o \frac{H_o^{(2)}(a_o)}{H_1^{(2)}(a_o)} \right] \qquad (7.2.9)$$

$$S_u(a_o,\nu,\xi) = 2\pi a_o G(\xi)$$

$$\left[\frac{(q)^{-\frac{1}{2}} H_2^{(2)}(a_o) H_1^{(2)}(x_o) + H_2^{(2)}(x_o) H_1^{(2)}(a_o)}{H_o^{(2)}(a_o) H_2^{(2)}(x_o) + H_o^{(2)}(x_o) H_2^{(2)}(a_o)} \right] \qquad (7.2.10)$$

in which

$$q = \frac{1 - 2\nu}{2(1 - \nu)} \qquad (7.2.11)$$

$$x_o = a_o (q)^{\frac{1}{2}} \qquad (7.2.12)$$

and $H_n^{(2)}(y) = J_n(y) - iY_n(y)$, in which $H_n^{(2)}(y)$ is Hankel function of the second kind. Series solutions for the Bessel functions J_n and Y_n can be found in the Mathematical Handbook by the Bureau of Standards (1964). It is observed that the distance ξ in Eqs. (7.2.8) and (7.2.9) affects the rigidity parameters and subsequently the side reactions S_{ψ} and S_u only through the shear modulus. If the shear modulus is independent of ξ, then the side reactions are constant along the pile. The rigidity parameters can be expressed in terms of real and imaginary parts as

$$S_{\psi}(a_o,\xi) = r_o^2 G(\xi)\ S_{\psi 1}(a_o) + iS_{\psi 2}(a_o) \qquad (7.2.13)$$

and

$$S_u(a_o,\nu,\xi) = G(\xi)\ S_{u1}(a_o,\nu) + iS_{u2}(a_o,\nu) \qquad (7.2.14)$$

in which $S_{\psi 1}$, S_{u1} are stiffness coefficients and $S_{\psi 2}$, S_{u2} are damping coefficients for the layer. These are not dependent on depth z or distance from the center of rotation, ξ. Expansion of Eq. (7.2.9) in terms of Bessel functions gives

$$S_{\psi}(a_o,\xi) = \pi r_o^2 G(\xi) \left[1 - a_o \left\{ \frac{J_o(a_o) - iY_o(a_o)}{J_1(a_o) - iY_1(a_o)} \right\} \right] . \qquad (7.2.15)$$

The above expression can be divided into the stiffness coefficient

$$S_{\psi 1} = \pi \left[1 - a_o \left\{ \frac{J_o(a_o)J_1(a_o) + Y_o(a_o)Y_1(a_o)}{J_1^2(a_o) + Y_1^2(a_o)} \right\} \right] \qquad (7.2.16)$$

and into the damping coefficient

$$S_{\psi 2} = -\pi a_o \left\{ \frac{J_o(a_o)Y_1(a_o) - J_1(a_o)Y_o(a_o)}{J_1^2(a_o) + Y_1^2(a_o)} \right\}$$

which can be simplified to

$$S_{\psi 2} = \frac{2}{J_1^2(a_o) + Y_1^2(a_o)} \tag{7.2.17}$$

Similarly the expansion of Eq. (7.2.10) gives

$$S_u(a_o,\nu,\xi) = 2\,\pi\,a_o G(\xi) \left\{ \frac{(q)^{-\frac{1}{2}}(a_1 - ib_1) + (a_2 - ib_2)}{c - id} \right\} \tag{7.2.18}$$

in which

$$a_1 = J_1(x_o)J_2(a_o) - Y_1(x_o)Y_2(a_o)$$

$$b_1 = J_1(x_o)Y_2(a_o) + J_2(a_o)Y_1(x_o)$$

$$a_2 = J_1(a_o)J_2(x_o) - Y_1(a_o)Y_2(x_o)$$

$$b_2 = J_2(x_o)Y_1(a_o) + J_1(a_o)Y_2(x_o)$$

$$c = J_o(a_o)J_2(x_o)+J_o(x_o)J_2(a_o)-Y_o(a_o)Y_2(x_o)-Y_o(x_o)Y_2(a_o)$$

$$d = J_2(x_o)Y_o(a_o)+J_o(a_o)Y_2(x_o)+J_2(a_o)Y_o(x_o)+J_o(x_o)Y_2(a_o)$$

From the equations shown above and Eq. (7.2.14), the stiffness coefficient is

$$S_{ul} = 2\,\pi\,a_o \left\{ \frac{((q)^{-\frac{1}{2}}a_1+a_2)c + ((q)^{-\frac{1}{2}}b_1 b_2)d}{c^2 + d^2} \right\} \tag{7.2.19}$$

and the damping coefficient is

$$S_{u2} = 2\pi a_o \left\{ \frac{((q)^{-\frac{1}{2}}a_1+a_2)d - ((q)^{-\frac{1}{2}}b_1+b_2)c}{c^2 + d^2} \right\} \tag{7.2.20}$$

S_{u1}, S_{u2} are coefficients for the side reaction of the layer developed by horizontal displacement. The side reaction of the layer to pile rotation is governed by $S_{\psi 1}$ and $S_{\psi 2}$.

Substituting Eqs. (7.2.6) and (7.2.8) into Eq. (7.2.2) yields the following formula for the side reaction moment:

$$N_\psi(t) = \int \{S_\psi \psi(t) + S_u U(t)\xi\}\, d\xi \tag{7.2.21}$$

This can be further expressed by means of Eqs. (7.2.13), (7.2.14), (7.2.1), and the relation $U(t) = \xi\psi(t)$ to give

$$N_\psi(t) = \int_{\lambda-\ell}^{\lambda} \{r_o{}^2 A(\lambda - \xi)^{\frac{1}{2}}(S_{\psi 1} + iS_{\psi 2}) + A(\lambda - \xi)^{\frac{1}{2}}(S_{u1} + iS_{u2})\ \xi^2\}\ \psi(t)d\xi \tag{7.2.22}$$

Integration of above equation gives

$$N_\psi(t) = \frac{2}{3}G_s r_o^2 \ell (S_{\psi 1}+iS_{\psi 2})\psi(t)$$

$$+ 2G_s\ell\left(\frac{\ell^2}{7} - \frac{2\ell\lambda}{5} + \frac{\lambda^2}{3}\right)(S_{u1}+iS_{u2}) \qquad (7.2.23)$$

$$k_\psi = G_s\ell\{2r_o^2 S_{\psi 1}/3 + \left(\frac{2\ell^2}{7} - \frac{4\ell\lambda}{5} + \frac{2\lambda^2}{3}\right) S_{u1} \qquad (7.2.24)$$

$$c_\psi = (G_s\ell/\omega)\ \frac{2}{3}r_o^2 S_{\psi 2} + \left(\frac{2\ell^2}{7} - \frac{4\ell\lambda}{5} + \frac{2\lambda^2}{3}\right) S_{u2}$$

(7.2.25)

Then the equation of motion can be written as

$$I_\psi\ddot{\psi}(t) + (k_\psi + i\omega c_\psi)\psi(t) = T(t) \qquad (7.2.26)$$

in which k_ψ is the equivalent spring constant and c_ψ is the equivalent damping coefficient. Both k_ψ and c_ψ are frequency dependent.

The equation of motion (Eq. 7.2.26) simulates a single degree of freedom system. For this system, the excitation can be written in complex form as

$$T(t) = T_o \exp(i\omega t) \qquad (7.2.27)$$

in which the amplitude of overturning torque for a rotating mass type excitation is defined as

$$T_o = m_e \bar{e} \omega^2 (\ell_Q + \lambda) \tag{7.2.28}$$

in which m_e = the total eccentric mass of the oscillator, and $\bar{e}$ = eccentricity, the radial distance from center of gravity of m_e to the center of rotation. For the particular solution of Eq. (7.2.26), it is assumed that

$$\psi(t) = \psi_o \exp\, i(\omega t+\phi), \tag{7.2.29}$$

From Eq. (7.2.29),

$$\ddot{\psi}(t) = -\omega^2 \psi_o \exp[i(\omega t+\phi)], \tag{7.2.30}$$

hence the equation of motion can be rewritten as

$$(k_\psi - I_\psi \omega^2 + i\omega c_\psi)\psi_o \exp[i(\omega t+\phi)] = T_o \exp(i\omega t) \ , \tag{7.2.31}$$

The coefficient of $\psi_o \exp[i(\omega t+\phi)]$ has real as well as imaginary terms. As known, multiplication by $\underline{i}$ results in a 90° rotation of a vector in the positive direction. The coefficient may then be plotted in a diagram with the real part along the positive real axis and the imaginary part along the positive imaginary axis in the complex plane as shown in Fig.7.4.

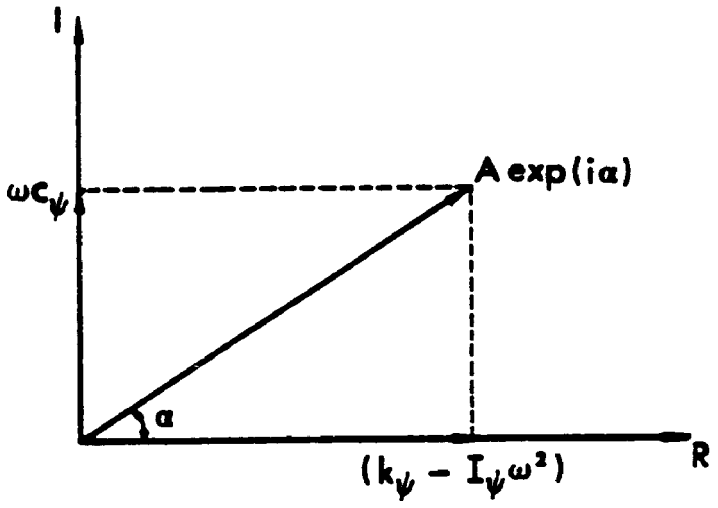

Figure 7.4 Graphical presentation of vector Aexp(iα) in complex plane

The resultant vector is

$$\overline{\text{Rexp}(i\alpha)} = \overline{(k_\psi - I_\psi\omega^2)} + \overline{i\omega c_\psi} \qquad (7.2.32)$$

For this vector the absolute value from the triangle on Fig. 7.4 is found

$$R = [(k_\psi - I_\psi\omega^2)^2 + (\omega c_\psi)^2]^{\frac{1}{2}} \qquad (7.2.33)$$

and the argument of the vector is

$$\alpha = \arctan [\omega c_\psi/(k_\psi - I_\psi\omega^2)] \qquad (7.2.34)$$

Eqs. (7.2.31) and (7.2.32) yield

$$R \exp(i\alpha)\psi_o \exp[i(\omega t+\phi)] = T_o \exp(i\omega t) \qquad (7.2.35)$$

which can be simplified to

$$R\psi_o \exp[i(\alpha+\phi)] = T_o \qquad (7.2.36)$$

Since R, ψ_o and T_o are positive real numbers, it follows that

$$\exp[i(\alpha + \phi)] = 1 \qquad (7.2.37)$$

which gives

$$\phi = -\alpha = -\arctan\left(\frac{\omega c_\psi}{k_\psi - I_\psi \omega^2}\right) \qquad (7.2.38)$$

and

$$\psi_o = \frac{T_o}{R} = \frac{T_o}{\sqrt{(k_\psi - I_\psi \omega^2) + (\omega c_\psi)^2}} \qquad (7.2.39)$$

The solution to Eq. (7.2.26) becomes

$$\psi(t) = \frac{T_o}{\sqrt{(k_\psi - I_\psi \omega^2) + (\omega c_\psi)^2}} \exp[i(\omega t+\phi)] \qquad (7.2.40)$$

and the rotational amplitude for rotating-mass type excitation is given as

$$\psi_o = \frac{M_e \bar{e} \omega^2 (\ell_Q + \lambda)}{\sqrt{(k_\psi - I_\psi \omega^2)^2 + (\omega c_\psi)^2}} \qquad (7.2.41)$$

The natural frequency can be calculated from the following equation.

$$\omega_{on} = \sqrt{k_\psi / I_\psi} \qquad (7.2.42)$$

By relating to the mass-spring-dashpot system, one can define the critical damping coefficient as

$$C_{\psi c} = \sqrt{k_\psi I_\psi} \qquad (7.2.43)$$

and find a "damping ratio," which depends on the frequency of excitation, as

$$D = C_\psi / 2 \sqrt{k_\psi I_\psi} \qquad (7.2.44)$$

This damping is caused by the loss of energy through radiation of elastic waves from the pile throughout the surrounding elastic material, a process which is also called geometric damping.

For piles which do not have any fixed point, i.e., free piles, the unknown λ-parameter may be found from the condition

$$\frac{\partial \psi_d}{\partial \lambda} = 0 \tag{7.2.45}$$

Solution of above equation gives the position of the center of rotation, which establishes the maximum rotational amplitude for each exciting frequency. The exact solution of Eq. (7.2.45) is often too complicated, and the solution by iteration is more desirable. To speed up the iteration procedure, the following initial values of λ_i, which is close to λ, may be used:

$$\lambda_i = \frac{3}{5}L \tag{7.2.46}$$

This relationship has been derived from the condition of minimum side layer reaction, which is

$$\frac{\partial N_\psi}{\partial \lambda} = 0 \tag{7.2.47}$$

In addition to the side layer reaction, the other parameters which are affected by λ (i.e., I_ψ and T_o), are monotonically increasing functions with increasing λ. Therefore, for the initial values λ_i, it can be stated that

$$\lambda_i \leq \lambda \tag{7.2.48}$$

which helps in choosing the next value of λ for the iteration procedure.

A computer program was developed for the Baranov theory to facilitate the computation of dynamic response of a short rigid pile loaded laterally by a rotating-mass type harmonic load (see Appendix I). Figures 7.5 and 7.6 show the coefficients of side layer reaction versus the dimensionless frequency a_o for different Poisson's ratio of soil.

3. Finite Element Method

A finite element dynamic solution was presented by Kuhlemeyer (1976) to analyze the dynamic response of a flexible pile embedded in a linearly elastic half-space and subjected to a steady state lateral force and moment.

The motion of the pile head can be described by the general equation:

$$\begin{Bmatrix} U\, e^{i\omega t} \\ r_o \phi\ \ e^{i\omega t} \end{Bmatrix} = \begin{bmatrix} F_{11} & F_{12} \\ F_{21} & F_{22} \end{bmatrix} \begin{Bmatrix} \frac{S}{k_x}\, e^{i\omega t} \\ \frac{r_o M}{k_\psi}\, e^{i\omega t} \end{Bmatrix} \qquad (7.3.1)$$

in which F_{ij} = flexibility coefficients that are, in general, complex numbers, ω = frequency of excitation, r_o = radius of pile, S = load applied at the ground surface, k_x = lateral translation spring constant, k_ψ = rotational spring constant, M = moment applied at the

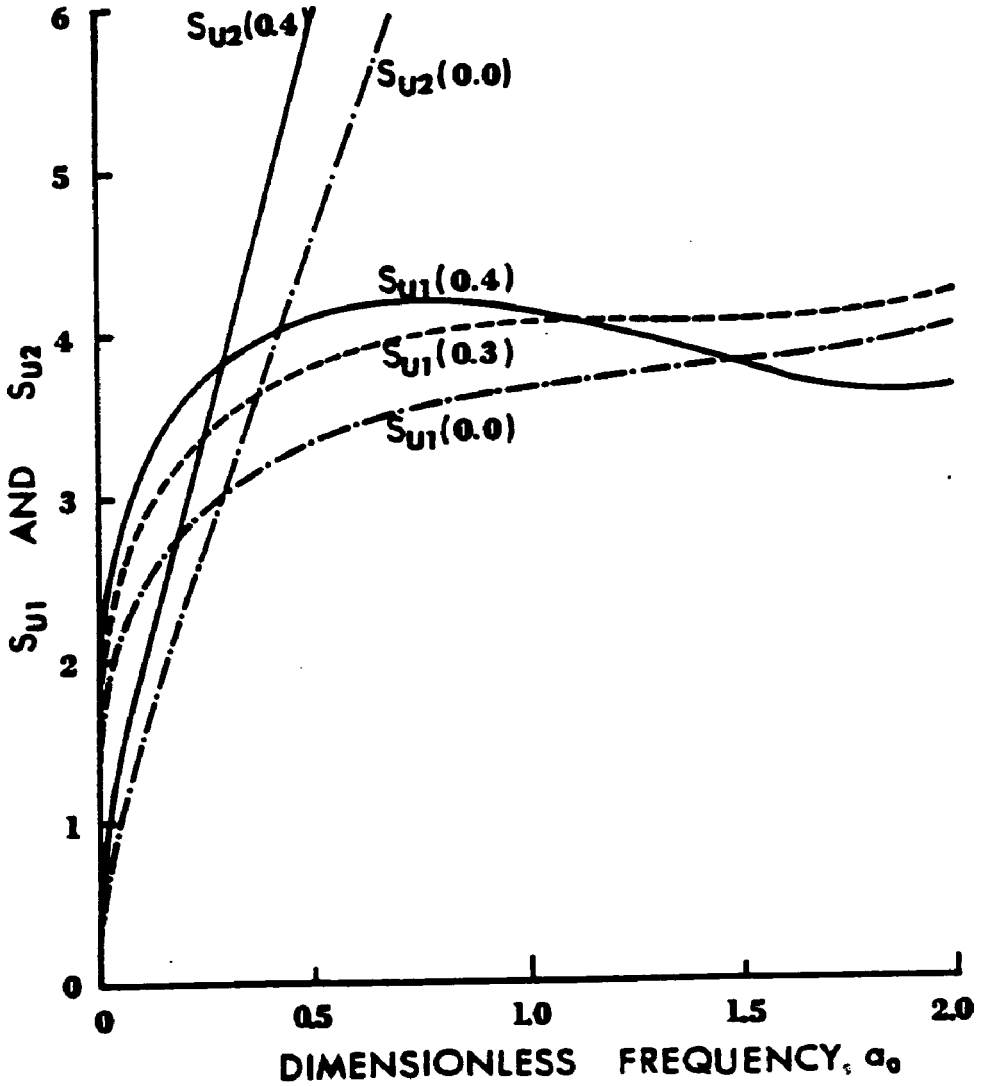

Figure 7.5 Coefficients of side layer reaction for horizontal displacement (after Baranov, 1967). Numbers in parentheses are Poisson's ratio of the soil)

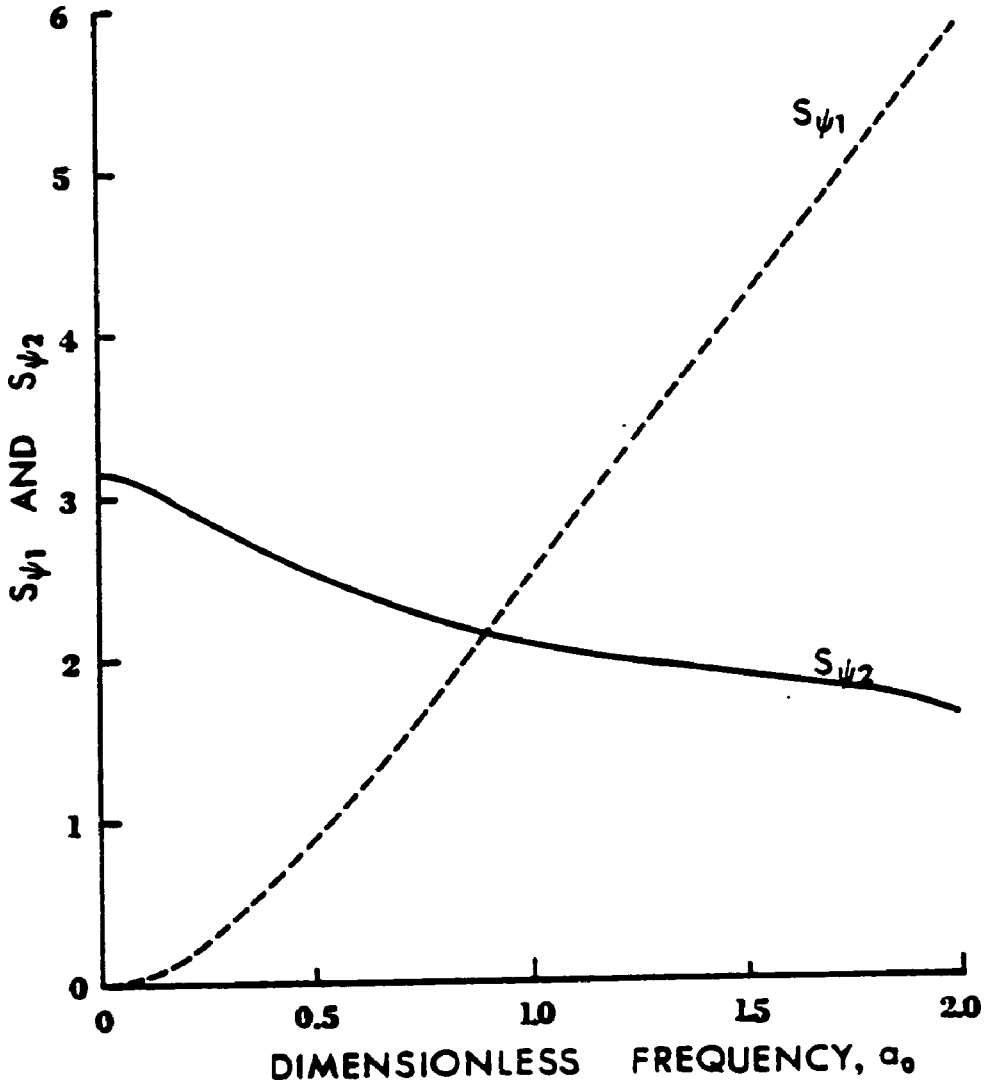

Figure 7.6 Coefficients of side layer reaction for rotation for all Poisson's ratios(after Baranov, 1971)

ground surface, and t = time. U and ϕ are complex numbers when S and M are real numbers.

To calculate the effect of lateral and rotational resistance of a pile, it is necessary to invert the matrix $[F_{ij}]$ and solve for the time dependent force and moment at the pile head. The reactions that act at the top of a single pile are given by:

$$\begin{Bmatrix} Se^{i\omega t} \\ Me^{i\omega t} \end{Bmatrix} = [H_{ij}] \begin{Bmatrix} U\, e^{i\omega t} \\ \phi\, e^{i\omega t} \end{Bmatrix} \tag{7.3.2}$$

in which

$$H_{11} = \frac{F_{22}}{F_{11}F_{22} - F_{12}F_{21}} k_x \tag{7.3.3a}$$

$$H_{12} = \frac{-F_{12}}{F_{11}F_{22} - F_{12}F_{21}} r_o k_x \tag{7.3.3b}$$

$$H_{21} = \frac{-F_{21}}{F_{11}F_{22} - F_{12}F_{21}} \frac{k_\psi}{r_o} \tag{7.3.3c}$$

$$H_{22} = \frac{F_{22}}{F_{11}F_{22} - F_{12}F_{21}} k_\psi \tag{7.3.3d}$$

The terms H_{ij} are, in general, complex numbers. It is assumed the lateral translation spring constant and rotational spring constant are given as

$$k_x = \frac{\pi}{4} E_p r_o \tag{7.3.4a}$$

$$k_\psi = \frac{\pi}{4} E_p r_o^3 \tag{7.3.4b}$$

in which E_p is the modulus of elasticity of pile material. Then, Eq. (7.3.2) can be rewritten as

$$\begin{Bmatrix} Se^{i\omega t} \\ Me^{i\omega t} \end{Bmatrix} = \frac{\pi}{4} E_p r_o \begin{bmatrix} (g_{11}+ia_o h_{11}) & r_o(g_{12}+ia_o h_{12}) \\ r_o(g_{12}+ia_o h_{12}) & r_o^2(g_{22}+ia_o h_{22}) \end{bmatrix} \begin{Bmatrix} U\, e^{i\omega t} \\ \phi\, e^{i\omega t} \end{Bmatrix} \tag{7.3.5}$$

in which a_o is the dimensionless frequency as defined in Eq. (7.2.3).

The values of g_{ij} and h_{ij} are evaluated from F_{ij} through application of Eq. (7.3.3). Note that since velocity and displacement are related by $i\omega$, g_{ij} are the stiffness terms and imaginary terms, h_{ij}, are the damping terms. The values of h_{ij} are equal to zero for the static solution.

If Eq. (7.3.2) is solved for the static case,

$$\frac{(F_{ij})_{st}}{\frac{\pi}{4}E_p} = a_{ij}/E_s \tag{7.3.6}$$

in which $(F_{ij})_{st}$ is equal to F_{ij} evaluated at ω equal to zero. The values of a_{ij} are given in previous static solution.

$$F_{ij} = (F_{ij})_{st}(I_{ij} + iJ_{ij})$$

$$= (E_p/E_s)(\tfrac{\pi}{4})\ a_{ij}(I_{ij} + iJ_{ij}) \qquad (7.3.7)$$

The complex number, $(I_{ij} + iJ_{ij})$; (evaluated as a function of a_o) in conjunction with Eqs. (6.2.5) and (7.3.6), represents the full fundamental solution of the dynamic soil-pile inter-action problem for piles subjected to lateral loads and/or moments. An approximate closed-form expression for I_{ij} and J_{ij} is given as a function of a_o,

$$f(a_o) = c_5 + c_4 a_o + c_3 a_o^2 + c_2 a_o^3 + c_1 a_o^4 \qquad (7.3.8)$$

The values of coefficients of polynomial expansion for the above equation are given in Table 7.1.

Let $F_{ij} = A_{ij} + iB_{ij}$, for convenience, to give, for example,

$$A_{11} = (\tfrac{\pi}{4})(E_p/E_s)\ a_{11}I_{11} \qquad (7.3.9a)$$

and

$$B_{11} = (\tfrac{\pi}{4})(E_p/E_s)\ a_{11}J_{11} \qquad (7.3.9b)$$

Table 7.1. Polynomial Expansion Coefficients for I_{ij} and J_{ij}

Function $f(a_o)$	E_p/E_s	c_1	c_2	c_3	c_4	c_5
I_{11}	100	0.0	4.4512	-4.2924	0.7202	1.0002
	567	0.0	9.0236	-6.4722	0.4832	1.0028
	4000	0.0	15.2862	-11.2626	0.9431	1.0044
J_{11}	100	0.0	-8.4040	3.7805	0.9999	-0.0035
	567	79.9534	-74.8381	20.0969	0.1908	0.0008
	4000	112.681	-93.8280	19.9272	1.0124	-0.0007
I_{12}	100	0.0	-0.4916	0.5876	0.4458	1.0005
	567	0.0	-2.0875	0.9885	0.0300	0.9981
	4000	0.0	6.2155	-6.8635	1.2789	0.9978
J_{12}	100	-21.7249	14.9422	-1.0353	0.1192	0.0000
	567	0.0	-8.7744	6.8672	-0.2978	0.0007
	4000	76.6900	-75.9311	22.4427	-0.7943	0.0028
I_{22}	100	0.0	-0.9091	1.2338	-0.0443	1.0003
	567	0.0	1.0101	0.0	-0.0343	1.0009
	4000	0.0	0.0673	-1.7980	0.6625	0.9971
J_{22}	100	5.3613	0.0544	-0.2885	0.0825	-0.0010
	567	0.0	3.5152	-0.1195	0.0696	0.0009
	4000	0.0	-7.0842	4.2358	-0.0426	-0.0024

Then, the time-dependent lateral displacement, $\bar{U} = Ue^{i\omega t}$, can be expressed as

$$\bar{U} = (A_{11} + iB_{11}) \frac{S}{k_x} e^{i\omega t} + (A_{12} + iB_{12}) \frac{r_o \ell_Q S}{k_\psi} e^{i\omega t} \qquad (7.3.10)$$

$$= (C_1 - iC_2) Se^{i\omega t}$$

in which ℓ_Q = distance to the vibrating external load application point from the ground surface (see Fig. 7.3), and

$$C_1 = \frac{A_{11}}{k_x} + \frac{A_{12} r_o \ell_Q}{k_\psi} \qquad (7.3.11a)$$

$$C_2 = \frac{B_{11}}{k_x} + \frac{B_{12} r_o \ell_Q}{k_\psi} \qquad (7.3.11b)$$

The velocity of lateral displacement is

$$\frac{d\bar{U}}{dt} = iC_1 S \omega e^{i\omega t} + C_2 S \omega e^{i\omega t} \qquad (7.3.12)$$

Multiply Eq. (7.3.10) by $C_1\omega$, and Eq. (7.3.12) by C_2, then adding those two equations gives

$$\bar{U} C_1 \omega + \frac{d\bar{U}}{dt} C_2 = (C_1^2 + C_2^2) \omega S e^{i\omega t} \qquad (7.3.13)$$

Therefore,

$$\bar{S} = k\,\bar{U} + \frac{c}{\omega}\,\dot{\bar{U}} \tag{7.3.14}$$

in which

$$k = C_1/(C_1^2+C_2^2), \quad c = C_2/(C_1^2+C_2^2)\ . \tag{7.3.15}$$

The equation of motion of the pile takes the form of a single-degree-of-freedom, mass-spring-dashpot system as

$$m\ddot{U} + c\dot{U} + kU = Qe^{i\omega t} \tag{7.3.16}$$

A damping ratio for this system can be formed as

$$D = \frac{c}{c_c} = \frac{c}{2(km)^{\frac{1}{2}}} \tag{7.3.17}$$

and the undamped natural frequency is

$$f_n = (\frac{1}{2\pi})\,(k/m)^{\frac{1}{2}} \tag{7.3.18}$$

A computer program for the finite element dynamic solution, is given in Appendix II.

B. Results of Dynamic Tests

1. Displacement-Controlled Tests

The first series of dynamic tests performed were the low frequency displacement-controlled tests using the Gilmore electro-hydraulic actuator as previously described in Chapter III and IV. A total of 36 tests were performed on four different piles (RP3, RP4, SP3, SP4) at three different embedment depths (3, 4 and 5 ft.) and at three frequencies (2, 3 and 5 Hz). Each test consisted of 20 sets of 5 cycles of oscillation. Each set of 5 cycles was performed at a constant displacement amplitude which was controlled by voltage to the power supply of the curve-following programmer. The voltage controlled double displacement amplitude at ground surface varied from 0.004 in. to 0.17 in. Because the curve-follower of the programmer had a limitation in following the curve of 7 in./sec, it was extremely difficult to produce the 5 Hz vibration. Hence, the response for this excitation frequency was generally unreliable and showed a tendency to become random.

Figures 7.7 through 7.9 show the typical hysteresis loops of the pile behavior from the tests. Figure 7.10 shows the averaged hysteresis loops from Figs. 7.7 through 7.9 except for the first half cycle of oscillation. All the other hysteresis loops shown (see Figs. 7.11 through 7.18) were averaged from their original sets of

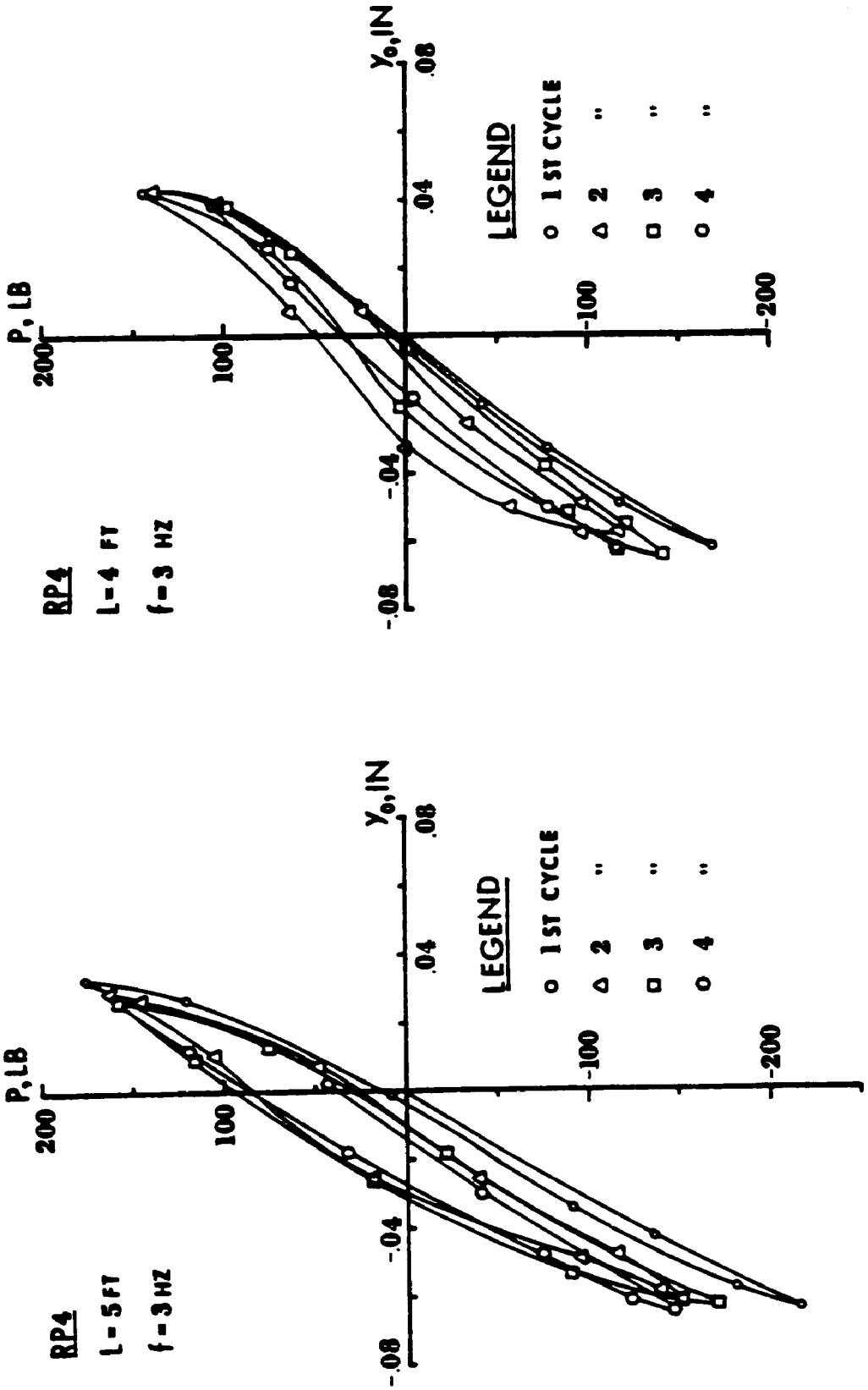

Figure 7.8 Load-displacement curves from displacement-controlled dynamic test

Figure 7.7 Load-displacement curves from displacement-controlled dynamic test

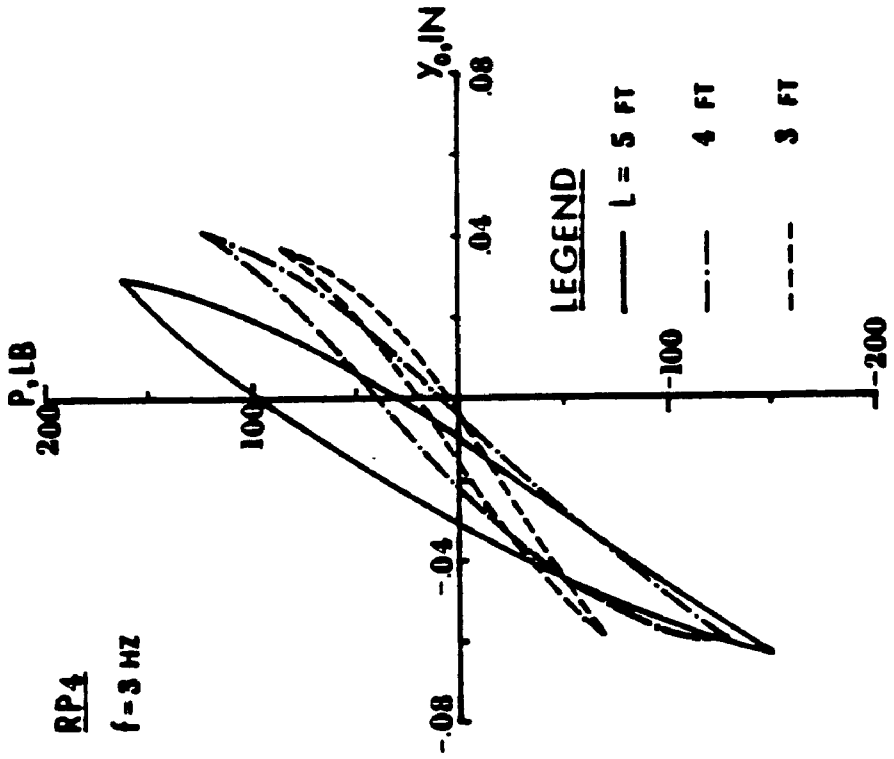

Figure 7.10 Load-displacement curves from displacement-controlled dynamic test

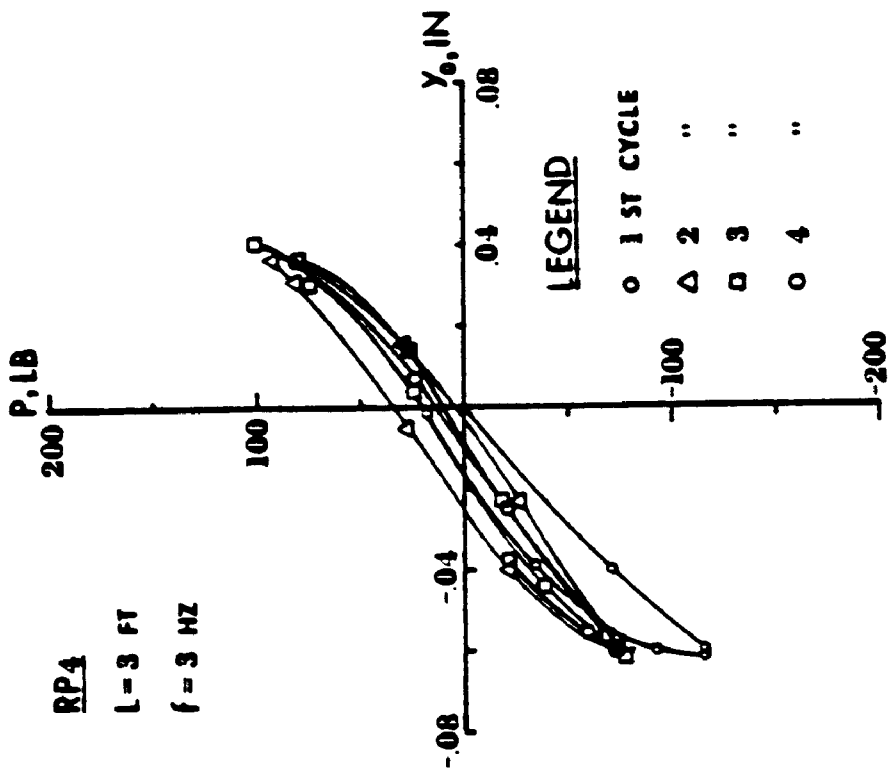

Figure 7.9 Load-displacement curves from displacement-controlled dynamic test

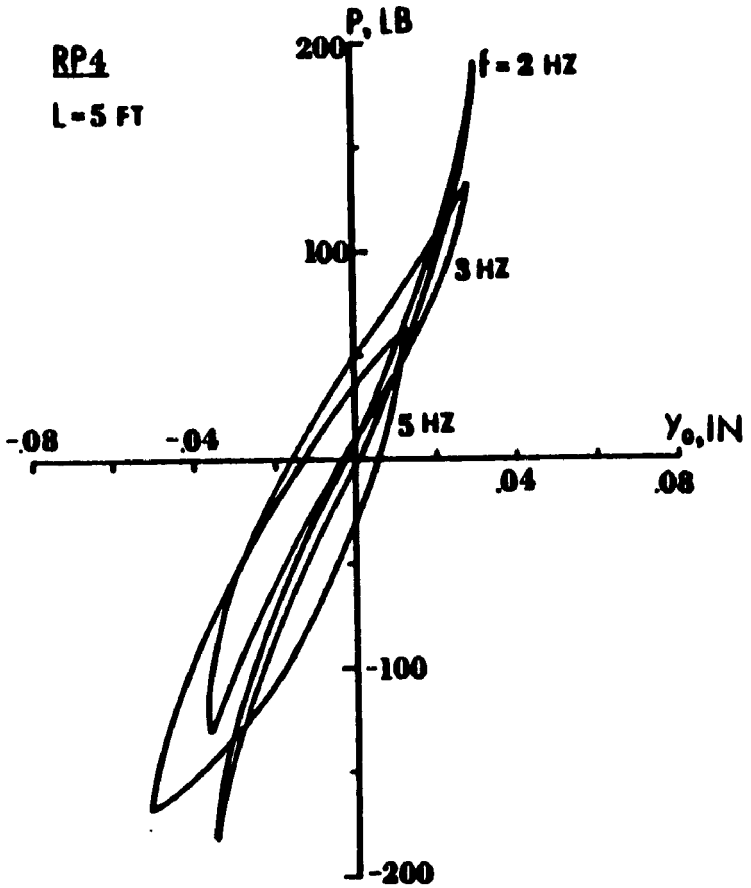

Figure 7.11 Load-displacement curves from displacement-controlled dynamic test

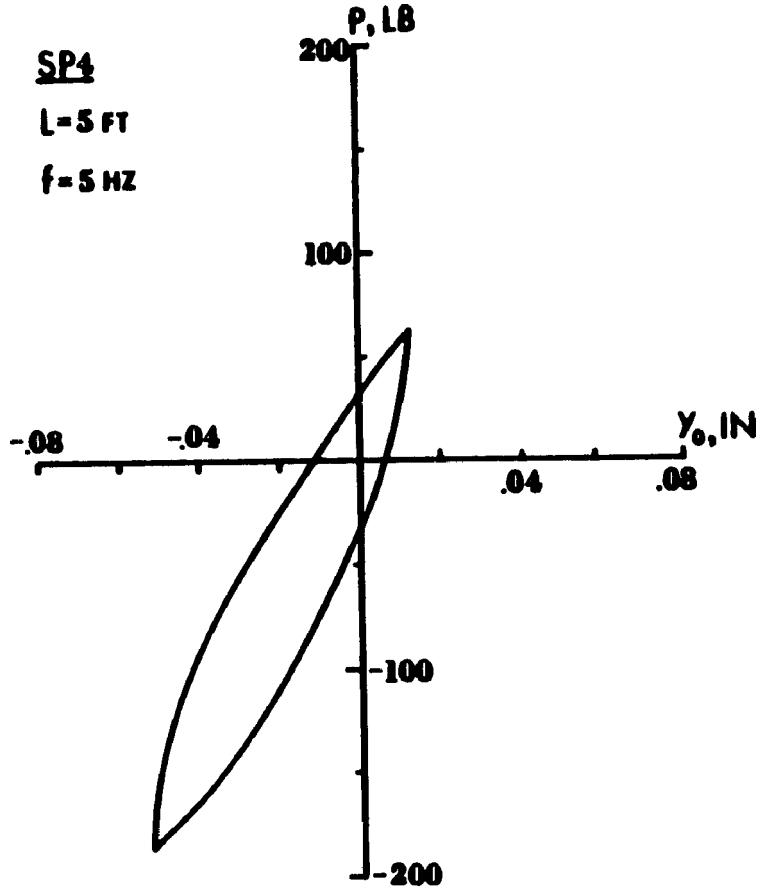

Figure 7.12 Load-displacement curve from displacement-controlled dynamic test

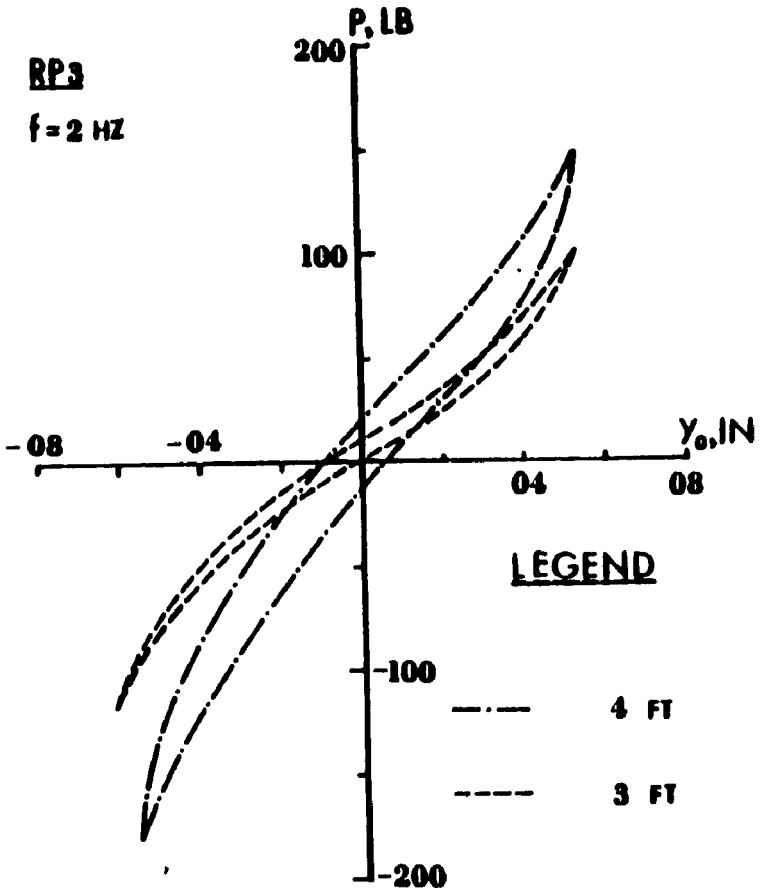

Figure 7.13 Load-displacement curves from displacement-controlled dynamic test

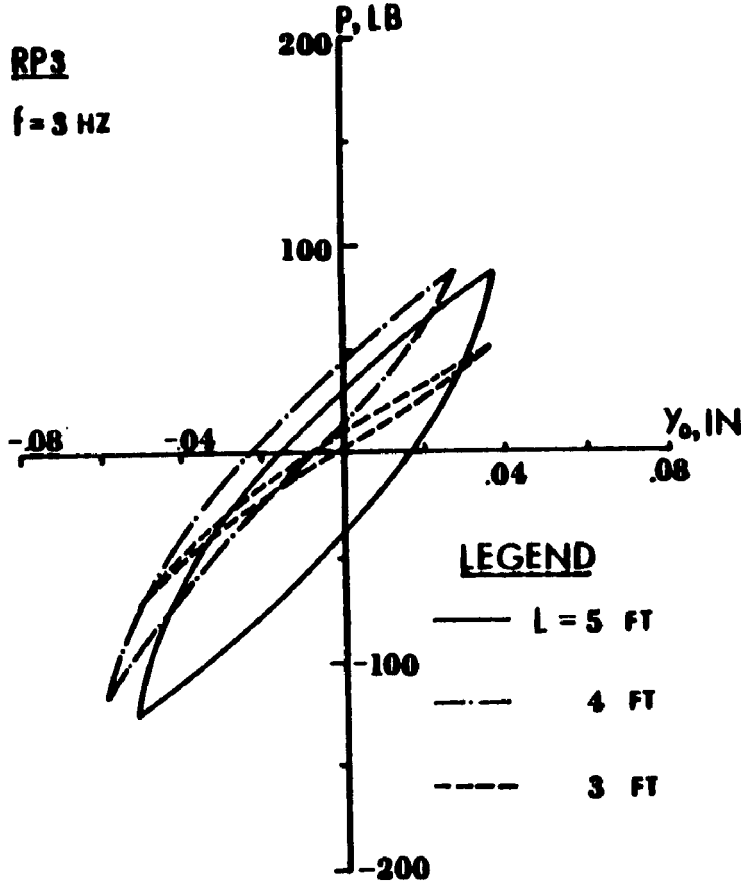

Figure 7.14 Load-displacement curves from displacement-controlled dynamic test

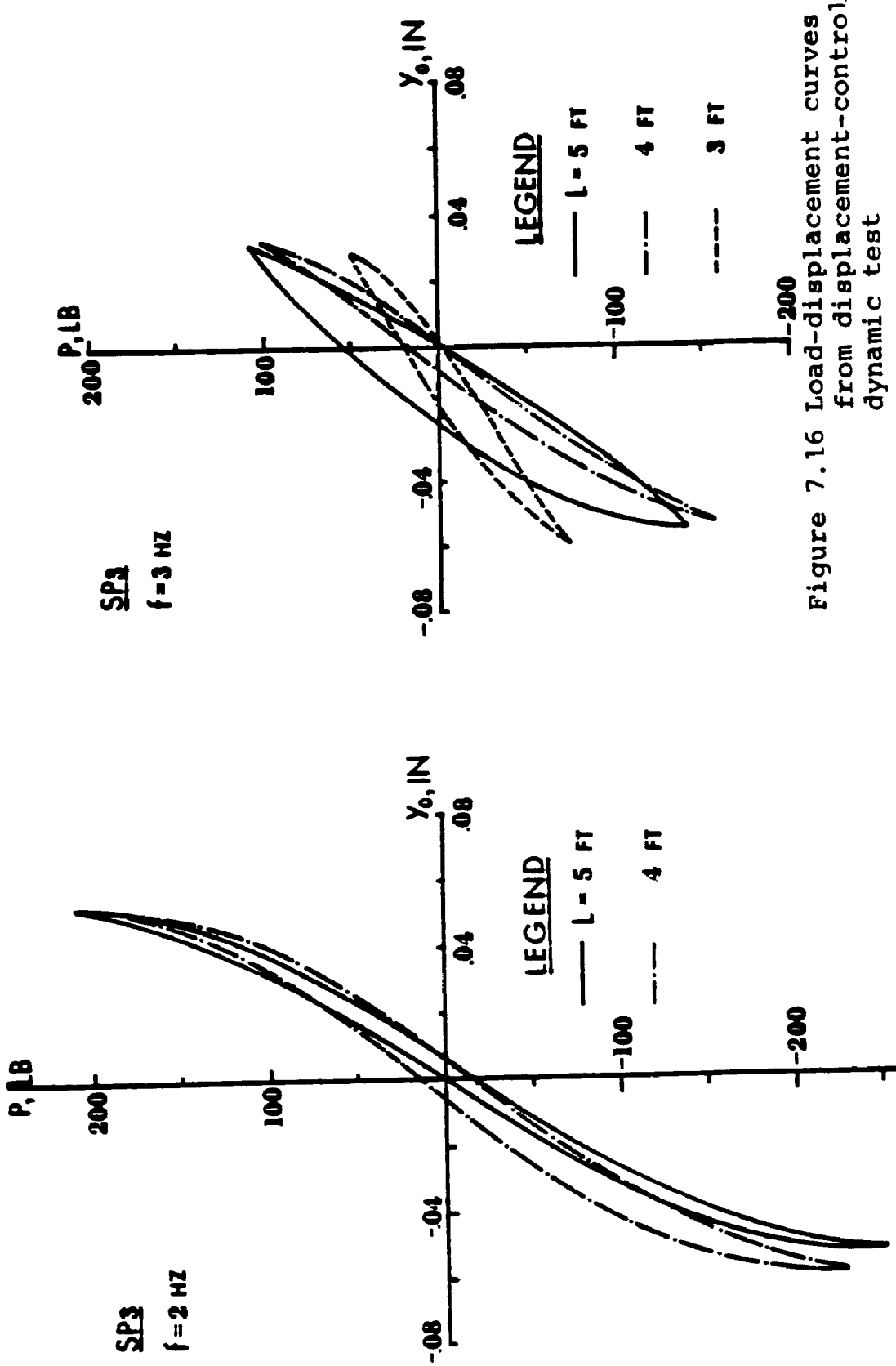

Figure 7.15 Load-displacement curves from displacement-controlled dynamic test

Figure 7.16 Load-displacement curves from displacement-controlled dynamic test

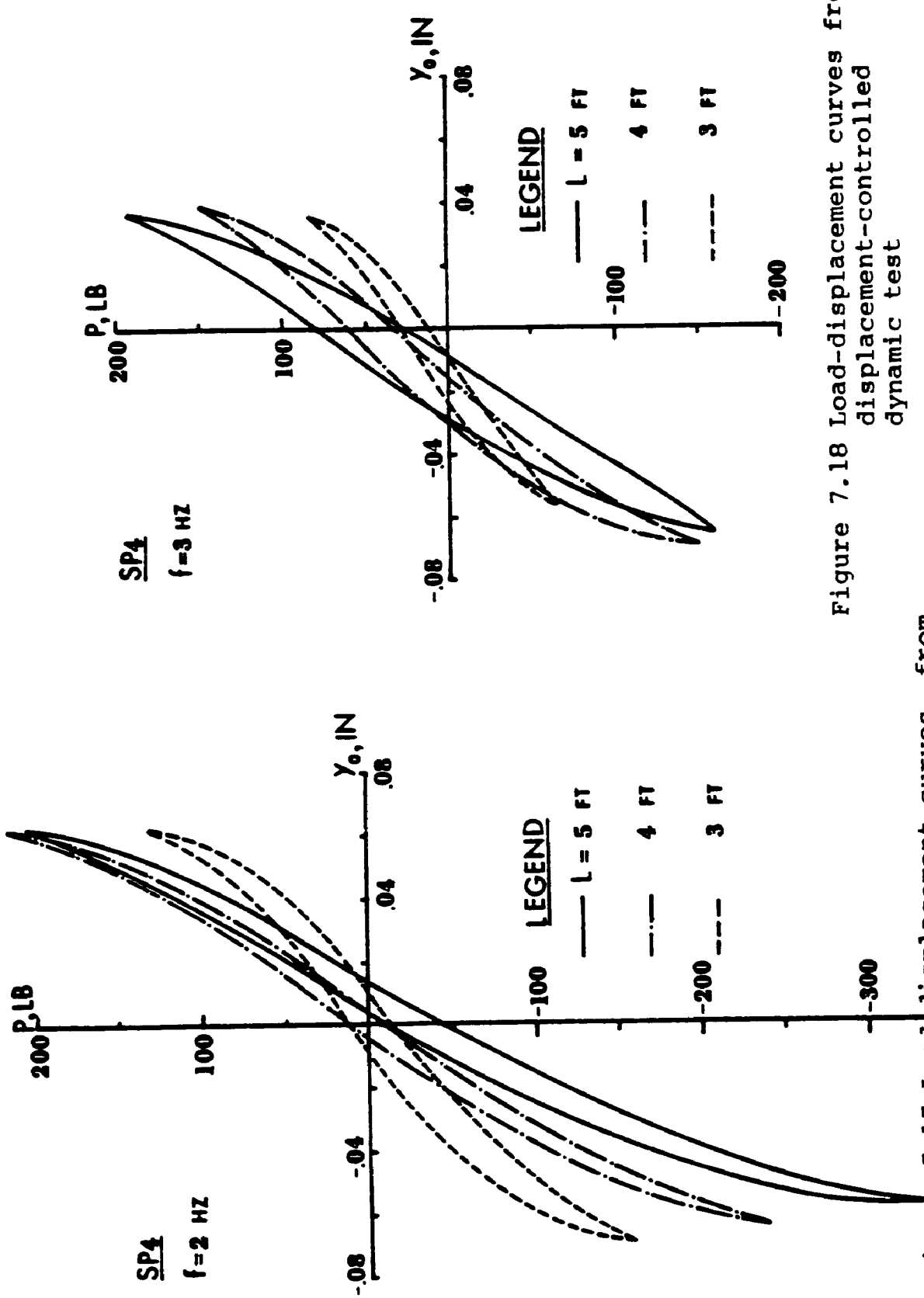

Figure 7.17 Load-displacement curves from displacement-controlled dynamic test

Figure 7.18 Load-displacement curves from displacement-controlled dynamic test

load-displacement curves. Figure 7.11 shows typical load-displacement curves for constant displacement amplitude for the 4½ in. OD round steel pipe pile with forcing frequencies of 2, 3 and 5 Hz.

The load-displacement curves for the 2 Hz and 3 Hz excitation (Fig. 7.11) showed strain-hardening behavior, but a tendency to change into the strain-softening behavior occurred with 5 Hz excitation (see Figs. 7.11 and 7.12). The larger the width of pile and the embedment depth, the larger was the resistance to horizontal load. The horizontal resistance became smaller as the exciting frequency was increased when maintaining the same forcing displacement amplitude (see Figs. 7.13 through 7.18).

2. Load-Controlled Tests

The second series of dynamic test performed were the load-controlled steady-state sinusoidally excited tests using the Lazan rotating eccentric-mass type mechanical oscillator as described in Chapter III and IV. These tests were also performed on four different piles at three different embedment depths as for the displacement-controlled tests, with the angle of eccentricity of the Lazan oscillator at 5, 10, 15 and 20 degrees which produced the forces as shown in Fig. 7.19. The device could not maintain an exactly constant motor speed for any specific excitation frequency, thus it was difficult to obtain the exact peak amplitude at the resonant

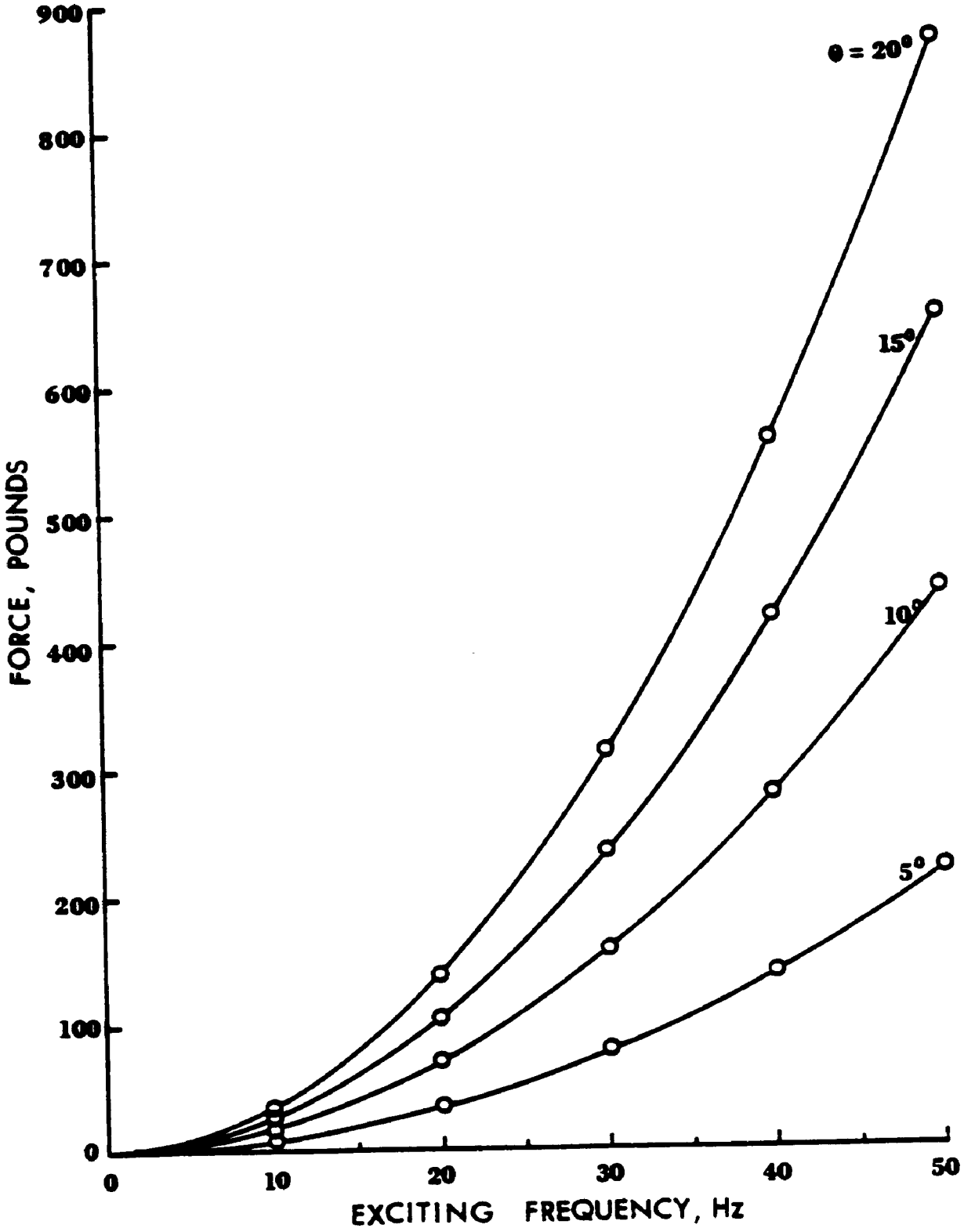

Figure 7.19 The exciting force generated by the Lazan oscillator with different angles of eccentricity of the unbalanced masses

frequency. The Lazan test data were reduced using Novak's (1971) inverse nonlinear solution to find the natural frequency and the damping ratio. Figures 7.20 through 7.22 show typical response curves from Lazan oscillator tests. See Appendix III for additional response curves.

It was found that the size of the pile had a significant effect on the response characteristics. The undamped natural frequency, hence the resonant frequency, increased as the size of the pile increased. However, the shape of the pile did not affect the response characteristics whenever the width of the piles were equal (see Table 7.2). The undamped natural frequency increased as the embedment depth increased. The damping ratio decreased as the amplitude of vibration increased and as the embedment depth increased. Minor inaccuracies occurred in determining the damping ratio for each test, because the resonant amplitude used in the calculation was only the apparent peak response amplitude. It was very difficult to maintain the motor speed at exactly the resonant frequency during these Lazan oscillator tests.

3. Plucking Tests

The transient response of a pile-soil system was observed by performing plucking tests as described in Chapter IV.

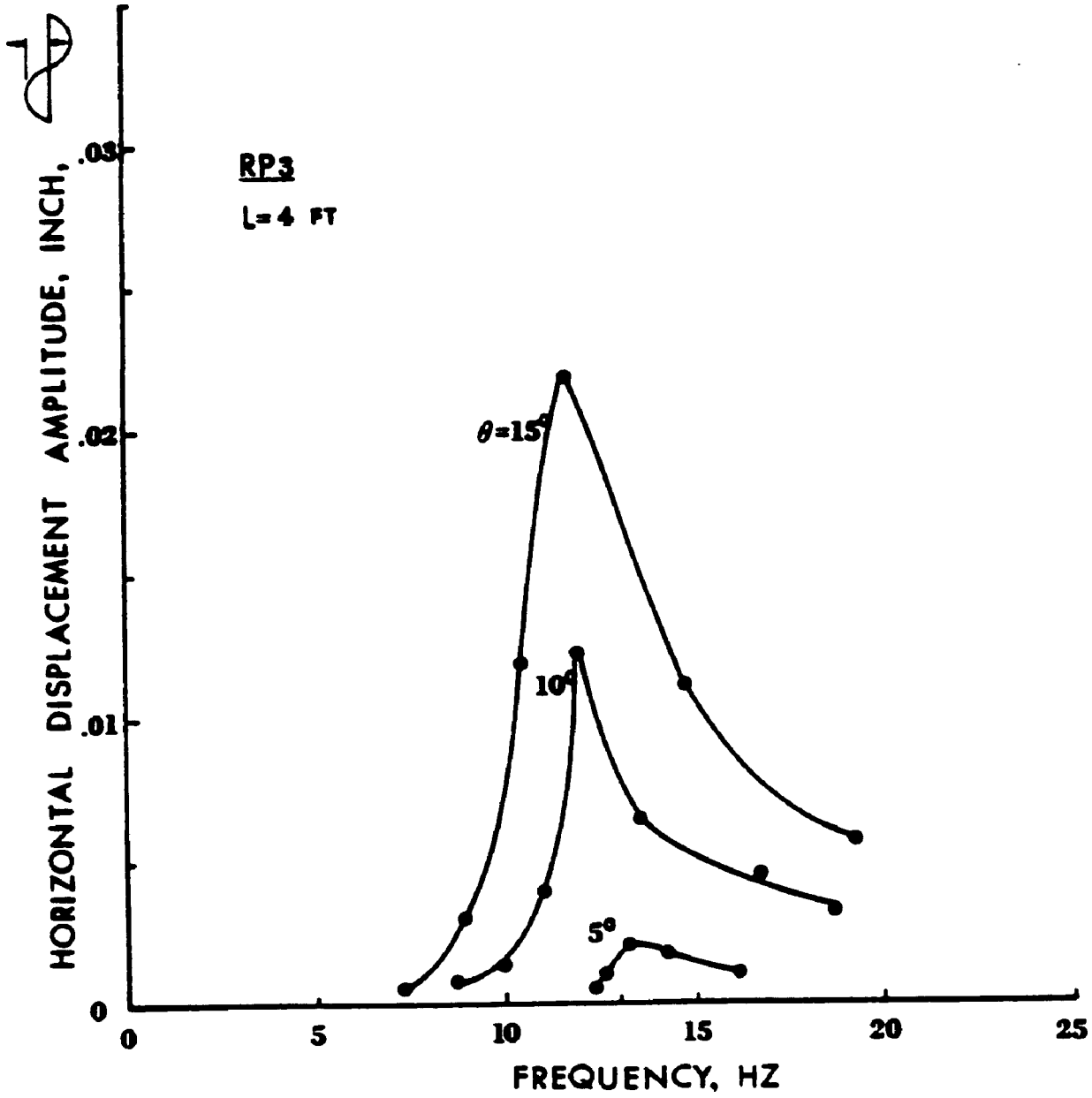

Figure 7.20 Dynamic response curves of load-controlled Lazan test

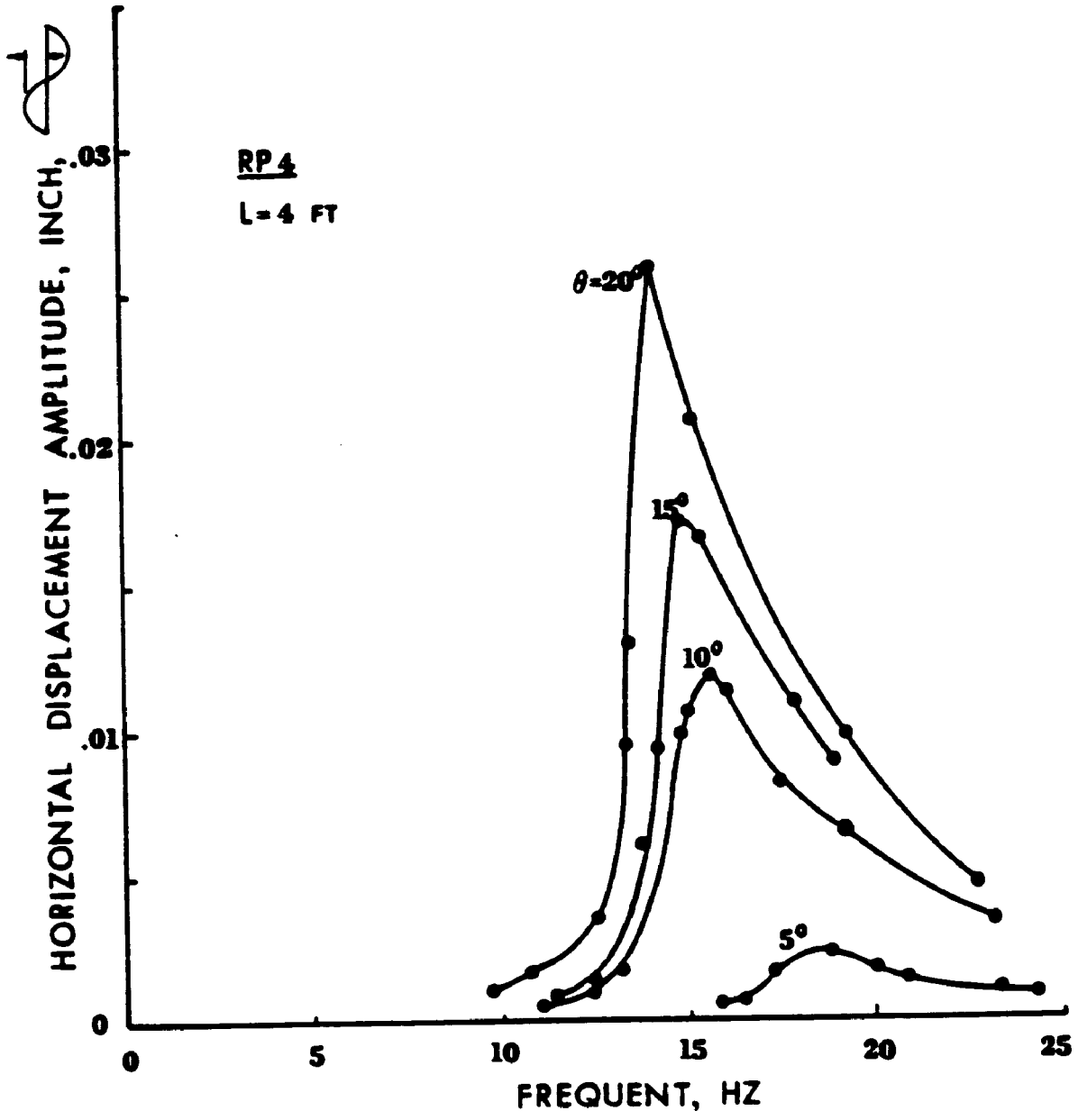

Figure 7.21 Dynamic response curves of load-controlled Lazan test

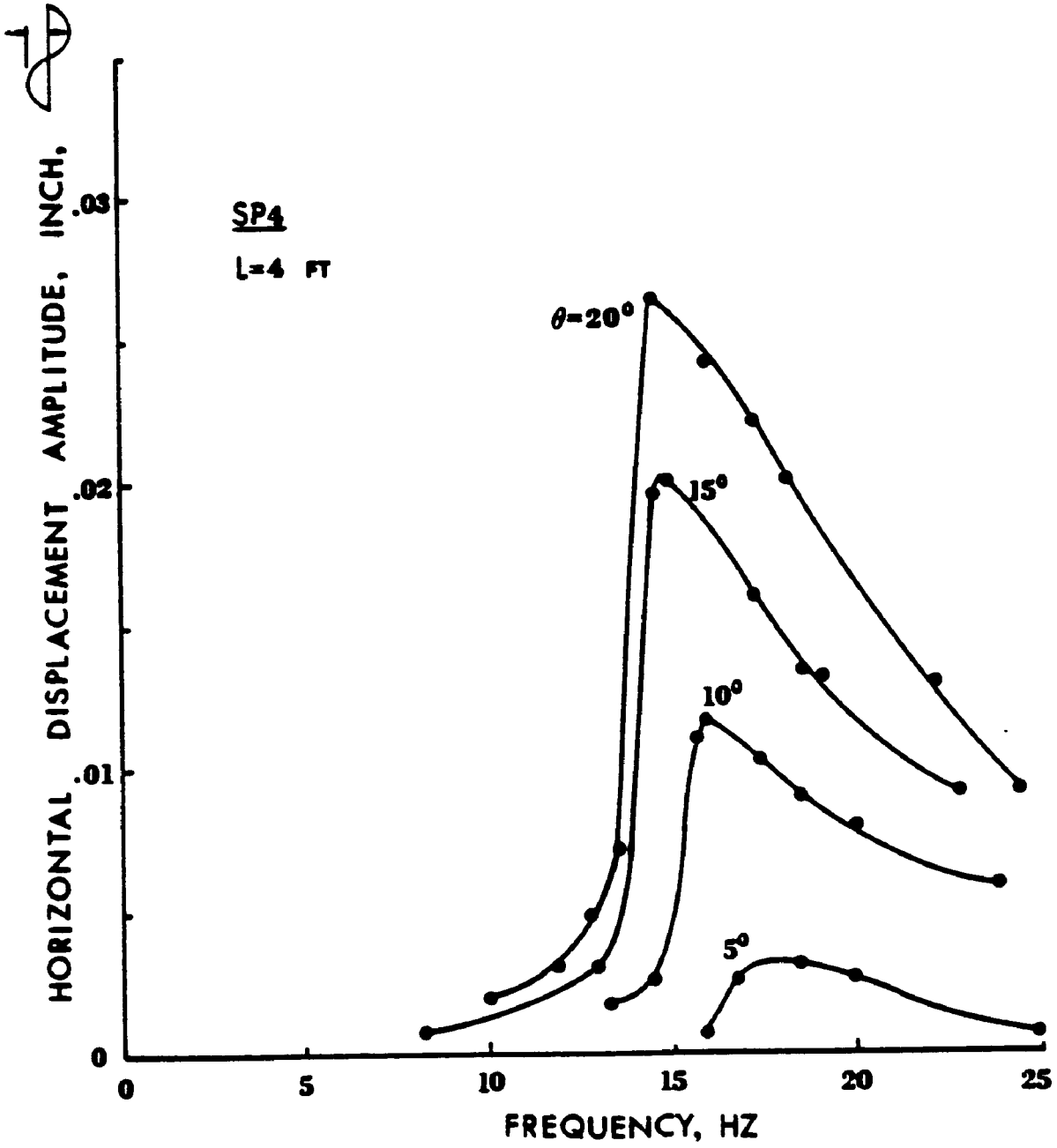

Figure 7.22 Dynamic response curves of load-controlled Lazan test

Table 7.2. Results of Lazan oscillator tests on piles embedded in uniform submerged dense sand (L = 5 ft.).

	RP3		SP3		RP4		SP4	
θ^{o}	A_T (in)	D (%)	A_T (in)	D (%)	A_T (in)	D (%)	A_T (in)	D (%)
5	0.004	25.9	0.004	25.5	0.004	26.0	0.004	25.8
10	0.014	14.0	0.014	13.6	0.014	13.5	0.016	11.4
20	0.033	10.7	0.033	10.4	0.028	11.9	0.033	10.2
f_n, Hz	13.2		13.5		17.5		17.8	

Figures 7.23 and 7.24 show the typical decay curves of the transient loadings on piles in drained dense sand. Damped natural frequencies were obtained from these curves, and the approximate damping ratios were calculated from the logarithmic decrements obtained from the vibration decay curves (see Fig. 4.4). The damping ratio was calculated by the approximate equation,

$$D = \frac{1}{2\pi} \ln(z_1/z_2) \qquad (7.4.1)$$

in which D = damping ratio, z_1, z_2 = consecutive single amplitudes of a transient decay curve.

Table 7.3 shows the tabulated results from plucking tests. The magnitudes of the initial static load for the drained tests were 36, 73 and 111 pounds, while those for submerged tests were 50, 100 and 150 pounds. The reason for using different loads was a matter of convenience.

A weight of 145 pounds was attached to the pile at 30 in. above the sand surface before each plucking test.

The damped natural frequency increased as the amplitude of the vibration decreased in a transient decay curve as shown in Fig. 7.23 for an example. Figure 7.25 shows that the damping ratio for the piles embedded in submerged dense sand was higher than for the piles

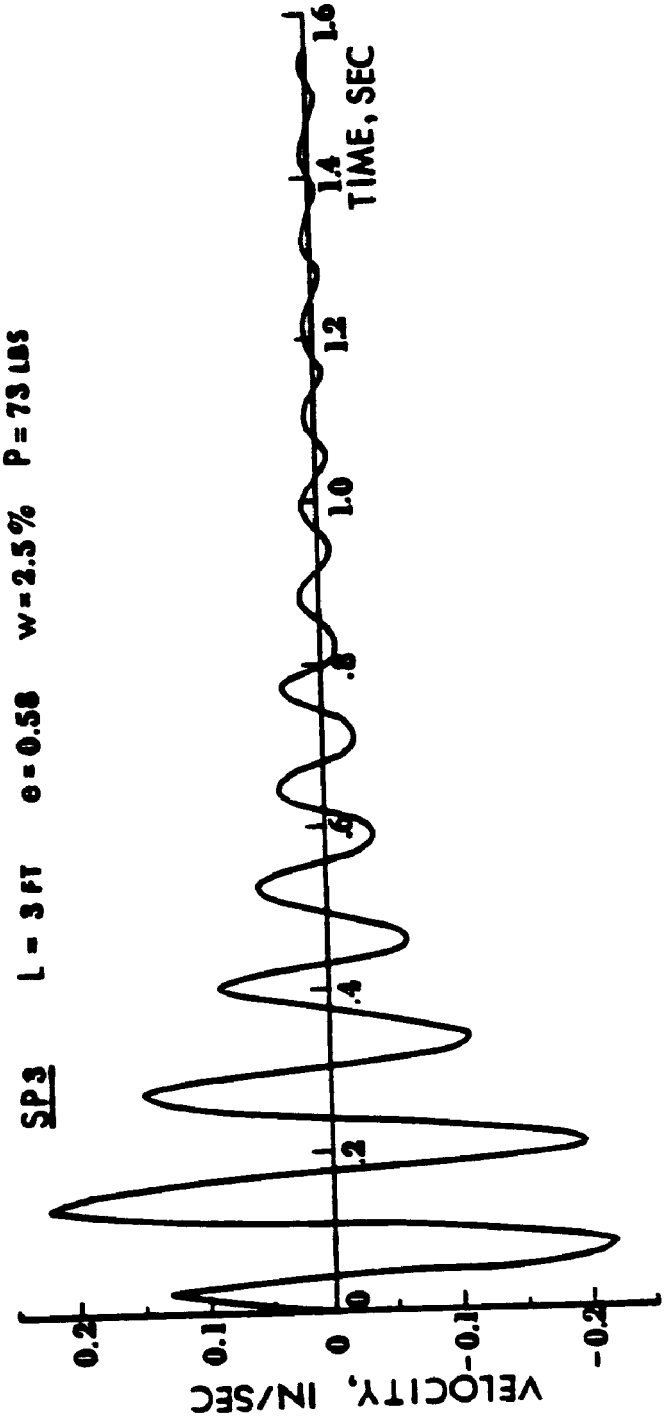

Figure. 7.23 Transient decay curve of plucking test (drained dense sand)

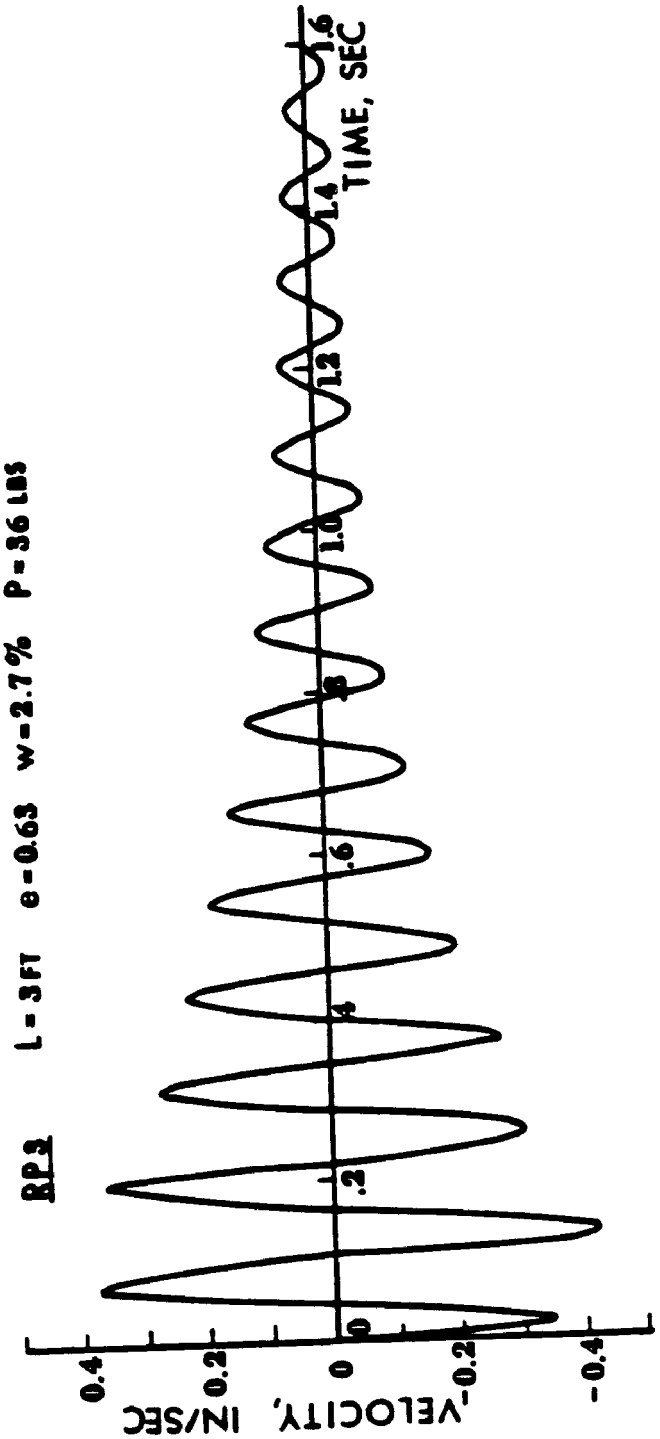

Figure 7.24 Transient decay curve of plucking test (drained dense sand)

Table 7.3. Results of the plucking tests

Piles	Embeded Length (ft)	Initial Static Load P1* f_o,Hz	P1* D,%	P2* f_o,Hz	P2* D,%	P3* f_o,Hz	P3* D,%	Soil Condition
RP3	3'	8.3	5.7	7.4	6.7	5.9	12.8	Drained
	3'	8.3	17.2	9.3	13.4	-	-	Submerged
	4'	7.8	-	6.9	3.8	6.7	2.9	Drained
	5'	-	-	8.1	4.1	7.7	2.7	Drained
RP4	3'	12.5	7.8	10.6	15.6	8.0	17.9	Drained
	3'	9.5	21.4	8.0	13.9	7.4	10.0	Submerged
	4'	11.1	12.1	10.0	14.9	8.0	12.0	Drained
SP3	3'	8.7	4.6	8.1	5.4	-	-	Drained
	4'	10.2	6.2	9.1	7.0	7.4	6.2	Drained
	4'	12.5	21.4	9.8	12.5	9.4	10.6	Submerged
	5'	10.0	5.6	9.1	7.2	7.9	6.6	Drained
SP4	3'	18.2	10.0	11.1	16.6	9.1	17.0	Drained
	4'	-	-	18.2	17.5	11.5	16.6	Drained
	4'	20.0	20.0	15.9	31.2	14.7	53.1	Submerged
	5'	18.2	15.22	16.7	27.3	15.4	32.6	Submerged

*	P1 (lb)	P2 (lb)	P3 (lb)
Drained	36	73	111
Submerged	50	100	150

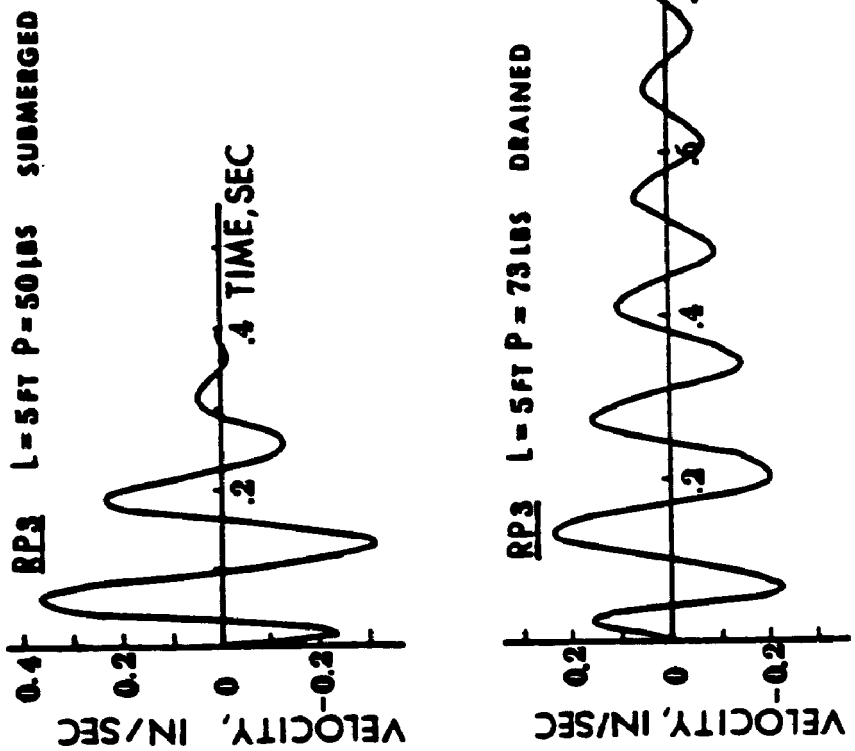

Figure 7.25 Comparison of the transient decay curves of plucking tests in submerged and in drained dense sand

embedded in drained sand. The damped natural frequency decreased as the initial static displacement increased. The damping ratio increased as the static load was increased in drained tests, while it decreased in submerged condition.

The increase of the embedment length of piles increased the damped natural frequency and the damping ratio. Larger piles showed a higher damped frequency and damping ratio than those for the smaller piles. Square piles showed higher damped natural frequency and damping ratio than for round piles.

C. Parametric Study

1. Baranov's Solution

The solution for pure rotation of short rigid piles, which was presented in Section VII. A. 2. using Baranov's (1967) side layer reaction theory, has many variables. These include the dynamic shear modulus of the soil, size of the pile, depth of embedment of the pile, the height of the load application point from the ground surface, weight of the mass located on top of the pile, Poisson's ratio, and the magnitude of the exciting force. A parametric study was performed to observe the effects of these variables on the dynamic response of a pile using the computer program provided in Appendix I. The calculations involved in the computation of the coefficients of

side layer reaction, stiffness and damping coefficients of the pile, and the dynamic response of the pile. It was assumed that the pile was free at the top. The computer output included the exciting frequency, dimensionless frequency, undamped natural frequency, damping ratio, displacement amplitude at ground surface, rotational amplitude, phase shift, dimensionless rotational amplitude, and the depth to zero displacement.

The dimensionless rotational amplitude was calculated using the equation

$$A_{\psi} = \frac{I_{\psi}}{m_e \bar{e} h_Q} \psi_o \qquad (7.5.1)$$

in which A_{ψ} = dimensionless rotational amplitude, I_{ψ} = mass moment of inertia of the pile and mass on top of the pile about the point 0 in Fig. 7.3, ψ_0 = rotational amplitude about the point 0, h_Q = height of excitation above the point 0. The natural frequency was calculated from Eq. (7.2.42), and the damping ratio was calculated from Eq. (7.2.44). All the amplitudes calculated using this solution were single amplitudes.

The input data used in the calculations were from the present experimental work except that the dynamic shear modulus was considerably reduced compared with the shear modulus discussed in Chapter V.

Figure 7.26 shows that the larger pile yielded the smaller resonant amplitude and higher resonant frequency. Force levels, i.e., eccentricity angles in Fig. 7.26, were same as for the Lazan tests in experimental phase. The damping ratio for the larger pile at the resonant condition was slightly higher than for the smaller pile (see Fig. 7.27). These values were 25 and 28 percent for 3½ in. and 4½ in. OD round pile, respectively. The increase in exciting force resulted in a proportional increase in the resonant amplitudes without changes in damping ratio and resonant frequency, as would be expected for an elastic solution.

Figure 7.28 shows the effect of increase of the height of excitation from the ground surface as it was changed from 0.5 ft. to 5.0 ft. for the 3½ in. OD round pile embedded 5 ft. into submerged dense sand. A weight of 111.6 pounds was located at the same height as the dynamic excitation. The angle of oscillator eccentricity was 5 degrees. For the sand, Poisson's ratio was assumed as 0.25, and the submerged unit weight was 63.6 pounds per cubic foot. The resonant frequency decreased from 19.1 Hz to 7.92 Hz, the dimensionless rotational amplitude at resonant condition increased from 1.786 to 2.273, and the damping ratio decreased from 28.9 percent to 22.3 percent as the height of the weight and excitation increased from 0.5 ft. to 5.0 ft.

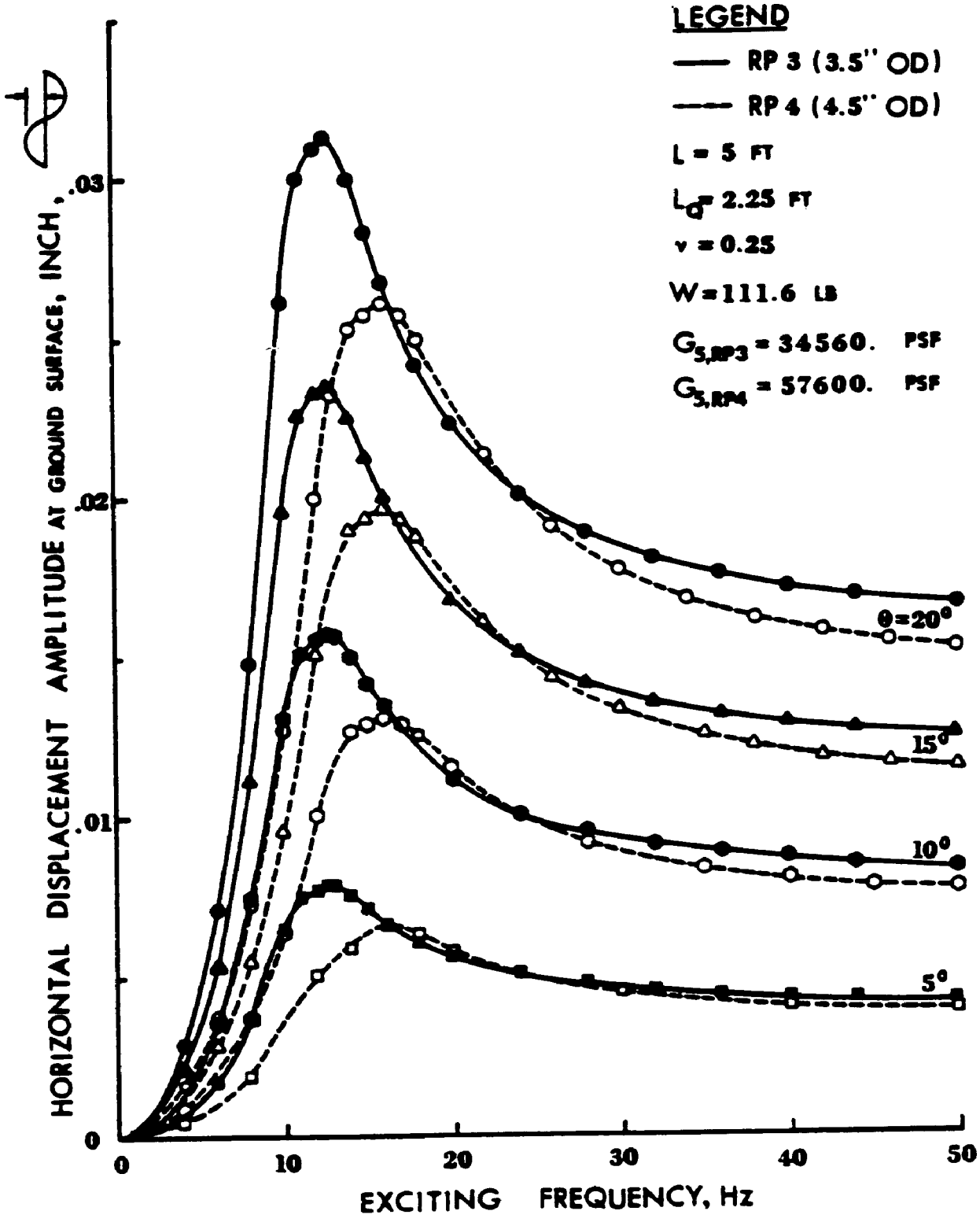

Figure 7.26 Effects of increase of the exciting force, and pile size (Theoretical results after Baranov, 1967)

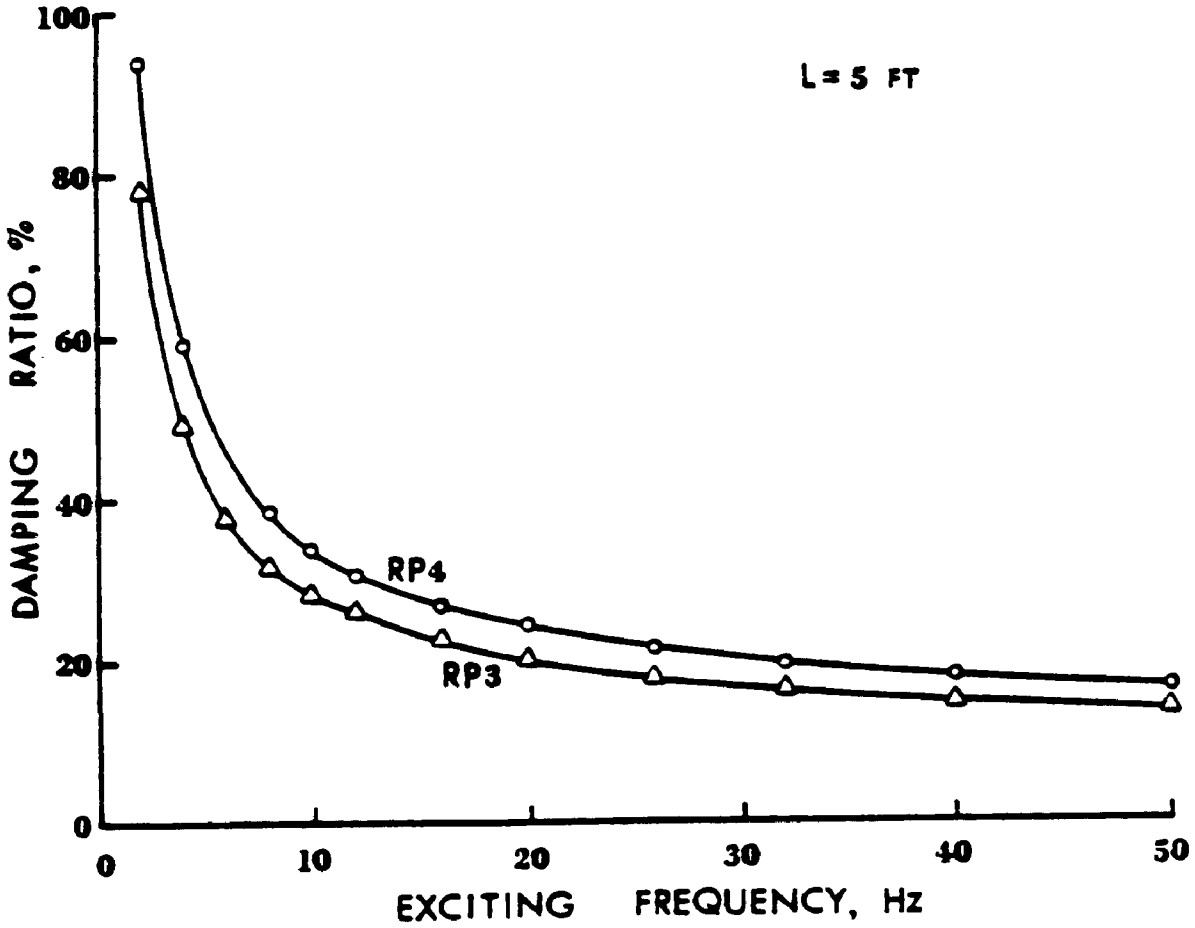

Figure 7.27 Damping ratio curves calculated from Baranov's solution for 3½ in. and 4½ in. OD round steel pipe piles

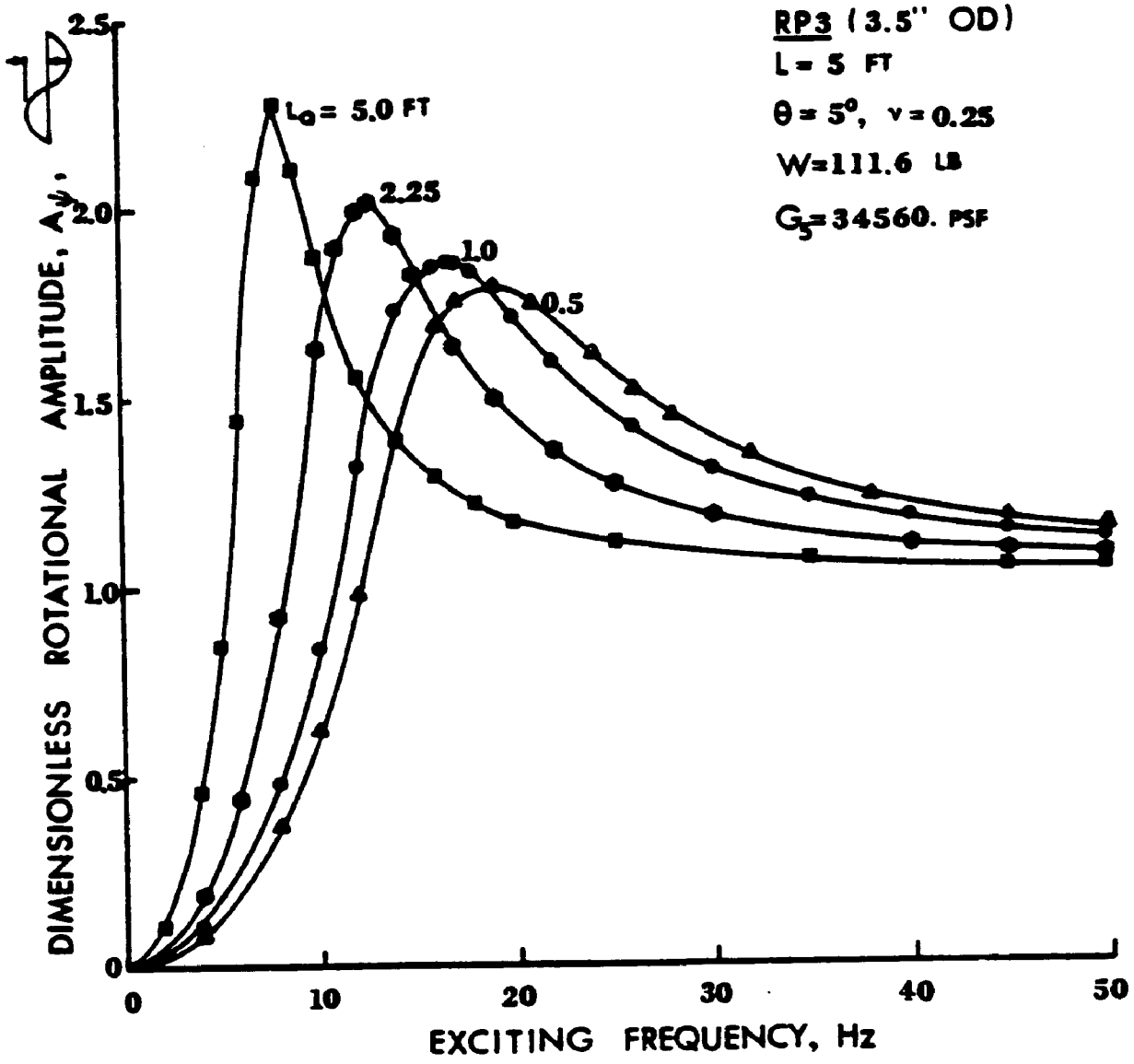

Figure 7.28 Effect of the height of the excitation from the ground surface (Theoretical results after Baranov, 1967)

The effect of a mass on top of the pile is shown in Fig. 7.29. It shows that as the weight increased from 10.0 pounds to 2000 pounds located at 2.25 ft. from the ground surface, the resonant frequency decreased from 36.0 Hz to 2.4 Hz, the damping ratio also decreased from 28.8 percent to 17.1 percent, and the dimensionless rotational resonant amplitude increased from 1.48 to 2.96. Figure 7.29 was plotted for the same pile and soil data as used for Fig. 7.28.

Table 7.4 shows the effect of Poisson's ratio of the soil on the dynamic response of a 3½ in. OD round pile embedded 5 ft. into submerged dense sand with a weight of 111.6 pounds located at 2.25 ft. above the ground surface. The effect of increasing Poisson's ratio from 0.25 to 0.40 is to increase the natural frequency by 8 percent, to increase the damping ratio by approximately 3 percent, and to decrease by 3 percent the resonant horizontal displacement amplitude at ground surface and the dimensionless rotational resonant amplitude. But differences were small.

An increase of the dynamic shear modulus increased the resonant frequency considerably without affecting the resonant horizontal displacement amplitude at ground surface. However, as shown in Table 7.5, an increase of shear modulus increased the stiffness and damping coefficients. The dimensionless frequency did not change

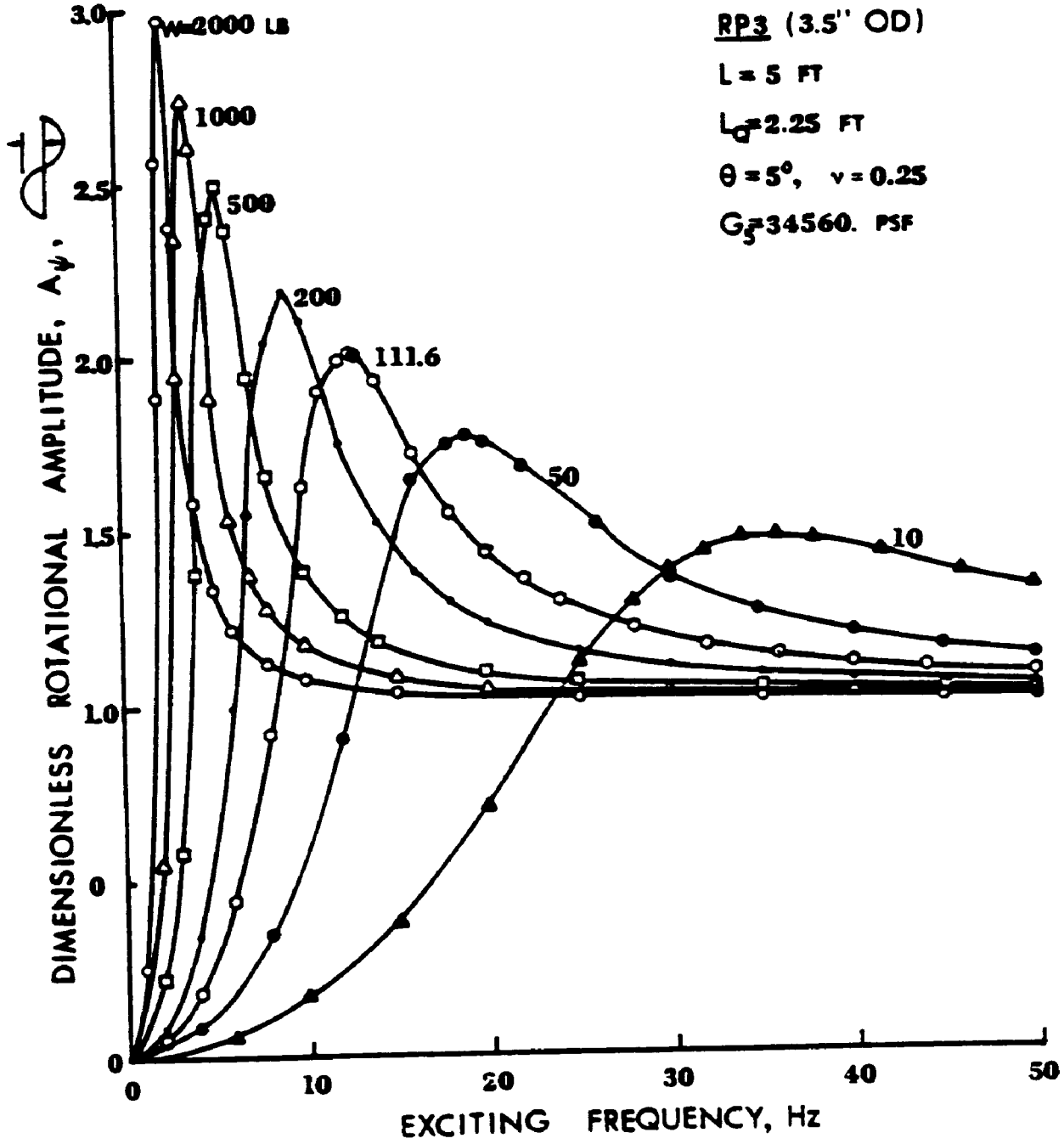

Figure 7.29 Effect of the mass located on the top of the pile (Theoretical results after Baranov, 1967)

Table 7.4. Effect of the change of Poisson's ratio of soil (RP3, L = 5 ft., $\theta = 5^{o}$, $G_{s,5} = 34560.$ psf, $\ell_Q = 2.25$ ft., W = 111.6 lb)

ν	f_n, Hz	A_T, in.	D, %	A_ψ
0.25	11.20	0.007862	25.38	2.0116
0.30	11.42	0.007816	25.54	1.9997
0.35	11.70	0.007749	25.78	1.9827
0.40	12.06	0.007649	26.14	1.9570

Table 7.5. Effect of the change of dynamic shear modulus in Baranov's solution (RP3, L = 5 ft., $\theta = 5^{o}$, $\nu = 0.25$, $\ell_Q = 2.25$ ft., w = 111.6 lb, $\gamma = 63.6$ pcf, $A_T = 0.007862$ in.)

G_z, pcf	a_o	k_ψ, in-lb/rad	C_ψ, $\frac{\text{in-lb-sec}}{\text{rad}}$	f_n, Hz
21600.	0.087116	331025	18985	9.94
34560.	0.087094	529613	24017	12.57
43200.	0.087133	662077	26846	14.06
57600.	0.087106	882713	31004	16.23
72000.	0.087078	1103319	34668	18.14

much because the increase of resonant frequency with increase of shear modulus essentially cancelled this effect on the dimensionless frequency. The shear moduli shown in Table 7.5 were the values at depth of 5 ft. below the sand surface. Other pile and soil data used were the same as for the Table 7.4 except that the Poisson's ratio used was 0.25.

The increase in embedment length of a 3½ in. OD round pile from 3 ft. to 5 ft. in a submerged dense sand increased the undamped natural frequency from 5.8 Hz to 11.2 Hz, increased the damping ratio from 21.2 percent to 25.4 percent, and decreased the dimensionless rotational amplitude at the resonant condition from 2.4 to 2.0.

The damping ratio obtained from this solution decrease continuously as the exciting frequency increased.

2. Kuhlemeyer's Solution

Kuhlemeyer's solution as presented in Section VII. A. 3. includes the same variables as Baranov's solution except for Poisson's ratio. The most important parameter in Kuhlemeyer's solution is the ratio of the moduli of elasticity of the soil and the pile. A computer program presented in Appendix II was used for this parametric study. It includes the computations of the pile flexibility coefficients, flexibility coefficient factors, dynamic flexibility coefficients, and the dynamic response

at ground and mass level. The input data were the same as for the Baranov's solution except that the modulus of elasticity and dynamic shear modulus were assumed to conform with Poulos' suggested numbers (see Table 7.6). The flexibility coefficient factors were computed for the condition:

$$E_p/E_s < 333.,$$

$$333. \leq E_p/E_s \leq 2283.,$$

$$E_p/E_s > 2283.$$

Table 7.6. Average Values of E_s for Cohesionless Soils, Poulos (1971)

Soil Density	E_s, psi	Avg. E_s, psi
Loose	130-300	250
Medium	300-600	500
Dense	600-1400	1000

The output of the computer solution includes the exciting frequency, dimensionless frequency, damping ratio, undamped natural frequency, horizontal displacement at ground surface, and dimensionless amplitude. It also writes the horizontal displacement, damping ratio, undamped natural frequency, and the dimensionless amplitude of the

pile at the mass level. The dimensionless amplitude for the horizontal displacement was calculated from the equation

$$A_u = \frac{m}{m_e \bar{e}} u_o \qquad (7.6.1)$$

in which A_u = horizontal dimensionless amplitude, m = mass located on top of the pile, m_e = rotating eccentric mass, $\bar{e}$ = eccentricity of the rotating mass, u_o = horizontal displacement at ground surface, or at mass level. The amplitudes calculated from Kuhlemeyer's solution were double amplitudes. However, the results presented in Figs. 7.30 through 7.34 and in Table 7.7 are single amplitudes for easy comparison with the Baranov's solution. The damping ratios and undamped natural frequencies were calculated by the Eqs. (7.3.17) and (7.3.18).

Figure 7.30 shows that an increase of the exciting force yields a proportional increase in the resonant horizontal displacement amplitude at ground surface. It also indicates that the larger pile gives the higher resonant frequency, lower resonant amplitude, and a larger damping ratio (see Fig. 7.31) for the same level of the exciting force compared with those of the smaller pile.

The effect of increase of the weight of mass located on top of the pile is shown in Fig. 7.32. It shows that the dimensionless resonant displacement amplitude increased

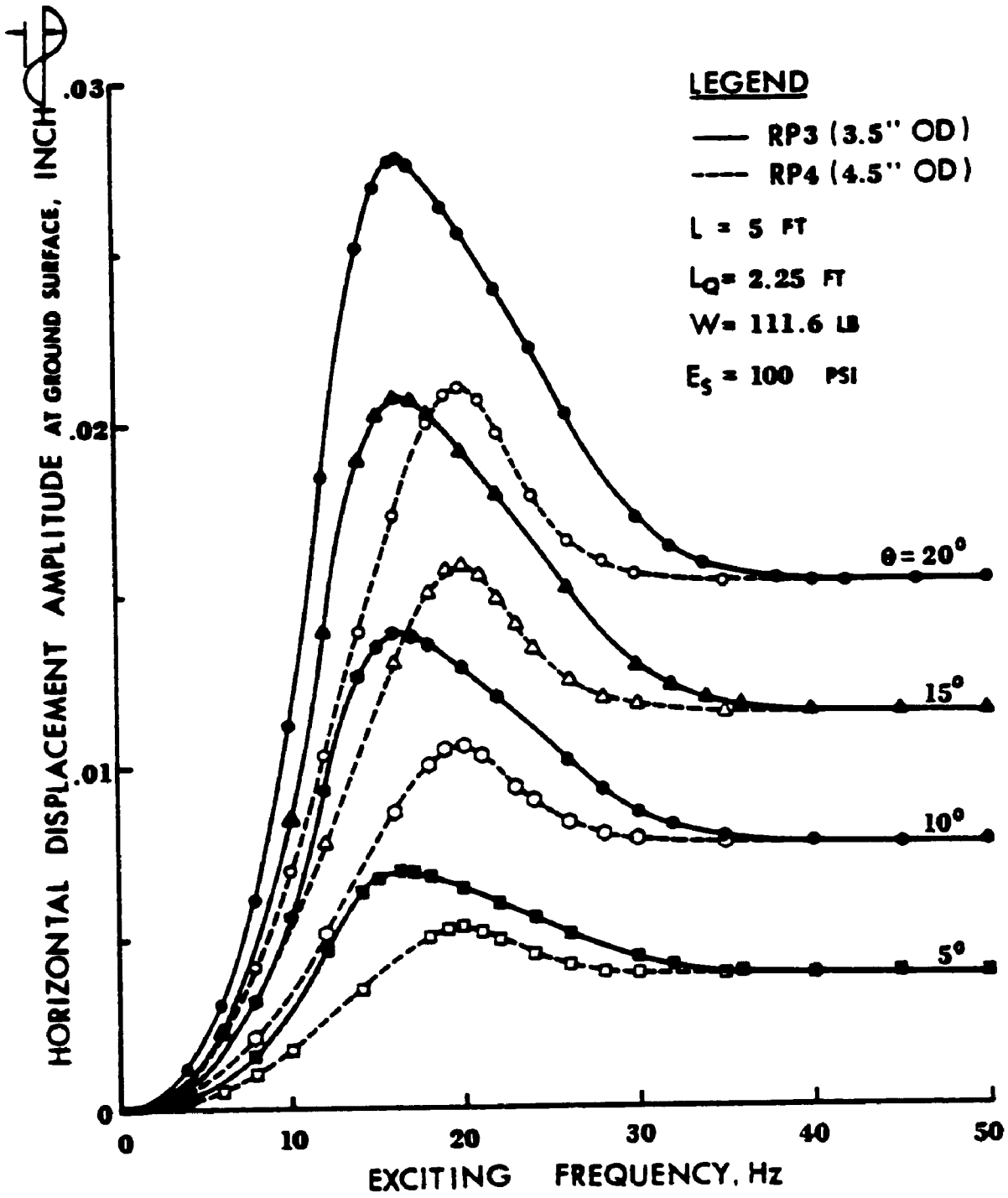

Figure 7.30 Effect of increase of the exciting force, and pile size (Theoretical results after Kuhlemeyer, 1976)

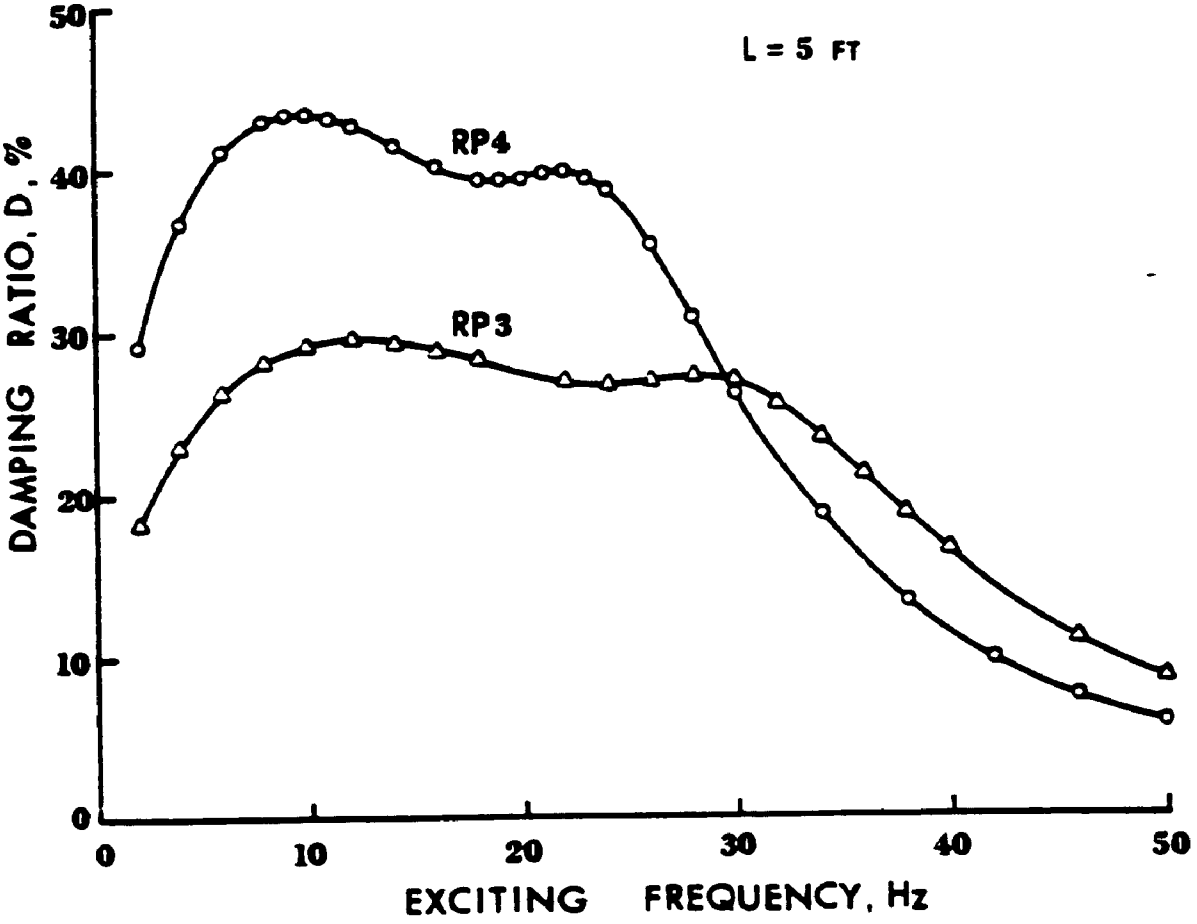

Figure 7.31 Damping ratio curves calculated from Kuhlemeyer's solution for 3½ in. and 4½ in. OD round steel pipe piles

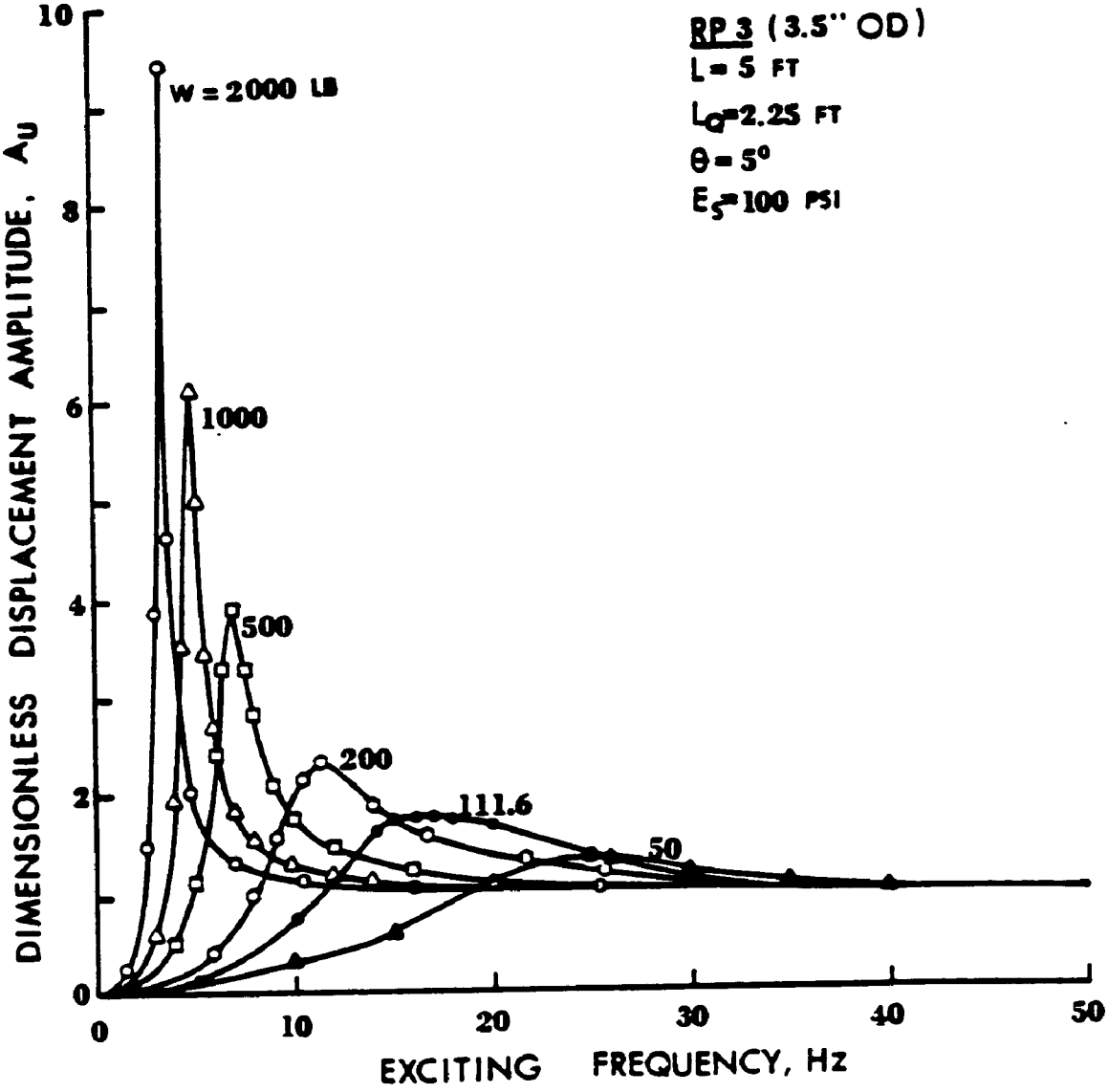

Figure 7.32 Effect of the mass located on top of the pile (Theoretical results after Kuhlemeyer, 1976)

from 1.36 to 9.5, and the resonant frequency decreased from 26.0 Hz to 3.5 Hz as the oscillating weight increased from 50.0 pounds to 2000 pounds. This weight acted at 2.25 ft. above the soil surface and was attached to a 3½ in. OD round pile embedded 5 ft. into submerged dense sand. The value of modulus of elasticity of the soil used was 100 psi which resulted in a pile flexibility factor of K_R = 0.1705. The damping ratio decreased from 40.1 percent to 5.2 percent at the ground level, and from 38.1 percent to 4.8 percent at the mass level when the system reached its resonant condition.

Table 7.7 shows the effect of the modulus of elasticity of soil for 3½ in. OD round pile embedded 5 ft. into submerged dense sand and excited with the rotating eccentric mass type oscillator, with the angle of eccentricity of 5 degrees. It shows the same effect as for Baranov's solution. An increase of the modulus of elasticity of soil increased the resonant frequency, decreased the pile flexibility factor, K_R, and increased the stiffness and damping coefficients.

Figures 7.33 and 7.34 show the effect of the increase of the height of the excitation from the ground surface for values calculated at the ground level and at the mass level, respectively. A weight of 111.6 pounds was located on top of the pile. Figure 7.33 shows that the increase of the height of the excitation from 0.5 ft.

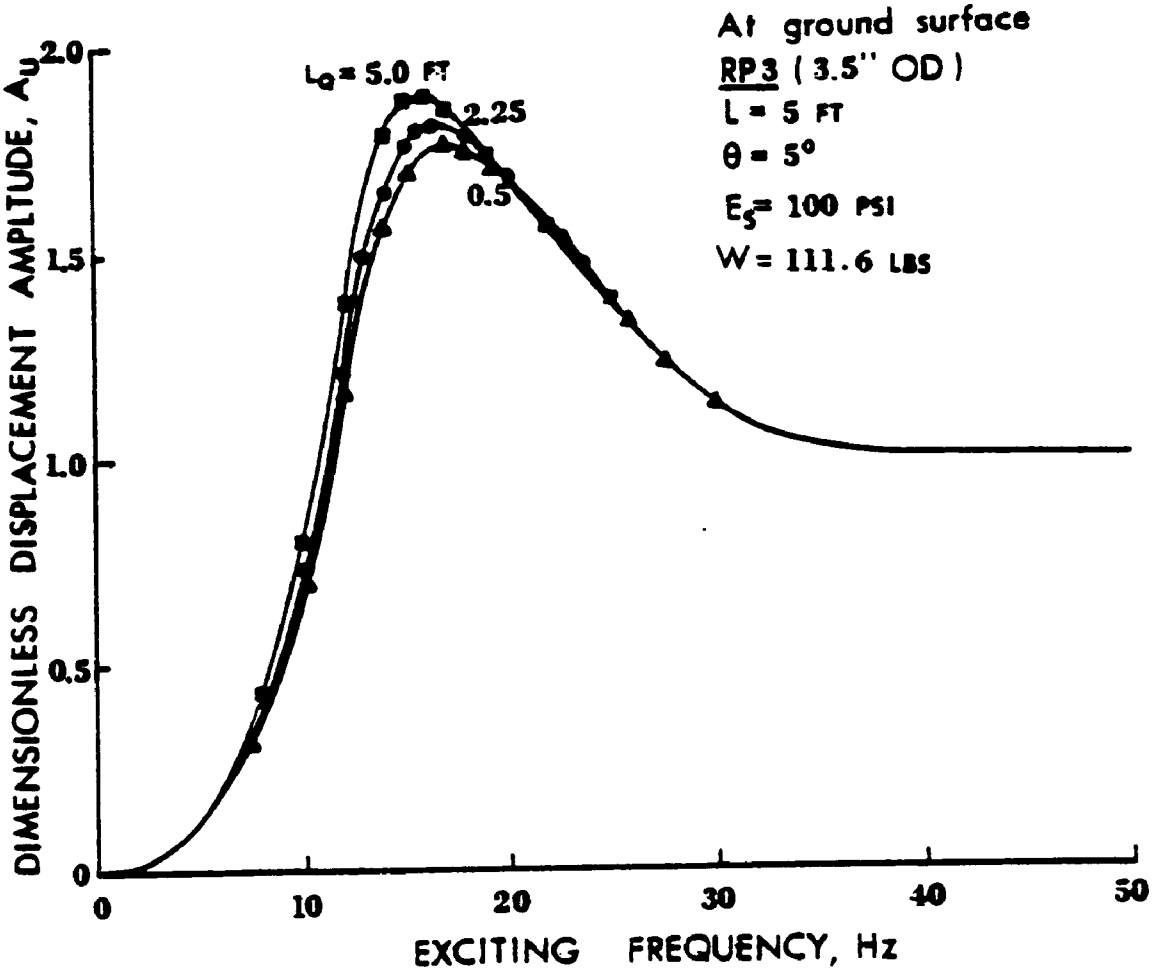

Figure 7.33 Effect of the height of the excitation from the ground surface. (Theoretical results after Kuhlemeyer, 1976)

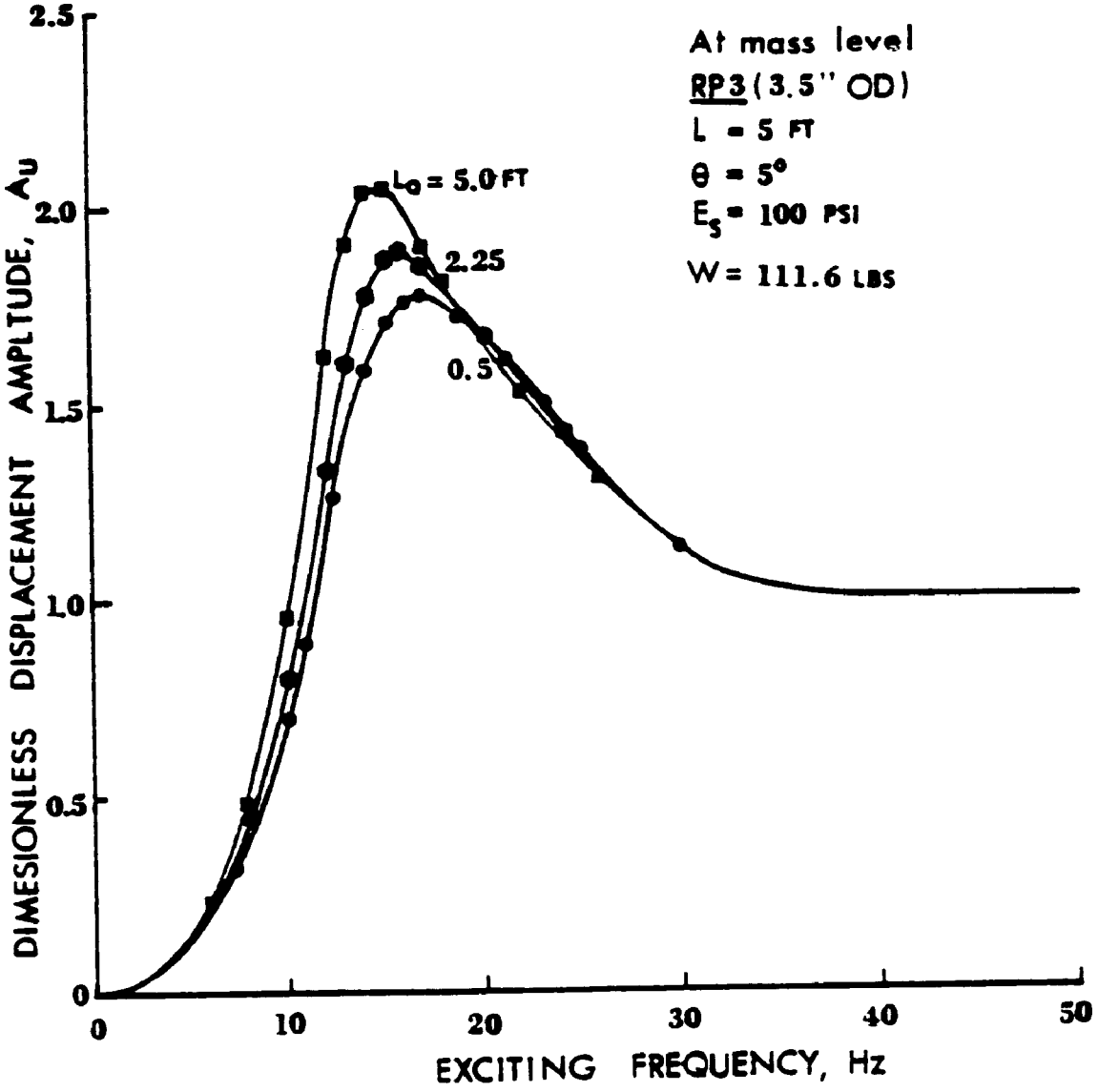

Figure 7.34 Effect of the height of the excitation from the ground surface (Theoretical results after Kuhlemeyer, 1976)

to 5.0 ft. decreased the resonant frequency from 17.0 Hz to 15.8 Hz and increased the dimensionless resonant displacement amplitude from 1.8 to 1.89 at the ground level. The damping ratio decreased from 29.4 percent to 27.5 percent. Figure 7.34 shows the changes in the dynamic response at the mass level for the same parameters as in Fig. 7.33. The resonant frequency decreased from 17.0 Hz to 14.5 Hz and the dimensionless resonant displacement amplitude increased from 1.78 to 2.06. The damping ratio decreased from 29.4 percent to 25.1 percent.

Table 7.7. Effect of the Change of Modulus of Elasticity of Soil in Kuhlemeyer's Solution. (RP3, $L = 5$ ft., $\theta = 5°$, $\gamma = 63.6$ lb., $W = 111.58$ lb., $\ell_Q = 2.25$, $A_T = 0.00693$ in.)

Es, psi	a_o	K_x, lb/in.	C_x, $\frac{\text{lb-sec}}{\text{in.}}$	K_R	f_R, Hz
100.	0.2767	2432.	15.2	0.1705	16.30
150.	0.2627	3352.	17.4	0.1137	18.95
200.	0.2529	4215.	19.0	0.0853	21.07
300.	0.2406	5835.	21.6	0.0768	25.56

D. Comparisons and Discussions

1. Comparison of Results

The results of the load-controlled steady-state dynamic test using the Lazan oscillator were compared with

the calculated results obtained from Baranov's pure rotational solution and from Kuhlemeyer's finite element method. The embedment length of the pile studied was 5 ft. The sand had a submerged unit weight of 63.6 pcf and provided complete contact between soil and pile during the tests. The Lazan oscillator which weighed 111.6 pounds was attached on top of the pile at 2.25 ft. above the sand surface and the angle of the eccentricity considered was 5 degrees. Table 7.8 shows the results of the dynamic tests and the calculated values for the 3½ in. OD and 4½ in. OD round steel piles for the resonant condition.

Baranov's solution showed the largest horizontal displacement amplitude at ground surface and the smallest natural frequency for both piles. The finite element solution (Kuhlemeyer) also showed a larger displacement amplitude than the experimental results, and gave better agreement with other experimental values than the pure rotational solution did, except for the damping ratios. The damping ratios for the larger pile obtained from the Kuhlemeyer's solution showed the largest values.

2. Selection of the Shear Modulus and the Modulus of Elasticity of Soil

The determination of the shear modulus and/or modulus of elasticity is the most important and difficult factor in solving dynamic problems of the pile response. Baranov's solution assumes a square root distribution of

Table 7.8. Comparison of test results with theoretical analysis, (RP3 and RP4, L = 5 ft., W = 111.6 lb, ℓ_Q = 2.25 ft., γ = 63.6 pct, $\theta = 5^o$)

Pile Method	RP3			RP4		
	A_T (in)	D (%)	f_n (Hz)	A_T (in)	D (%)	f_n (Hz)
Lazan test	0.004	25.9[1]	13.2	0.004	26.0	17.8
Baranov's	0.0079	25.4[2]	11.2	0.0065	27.9	13.9
Kuhlemeyer's	0.0067	28.7[3]	14.6	0.0053	39.4	16.6

Note: 1 Nonlinear Data Reduction

$$D = \frac{1}{2} \frac{m_e \bar{e}}{m} \frac{1}{A_T} \frac{\omega_T}{\omega_o}$$

in which $m_e\bar{e}$ = exciting force, m = mass on top of the pile, A_T = resonant amplitude at ground surface, ω_T = resonant frequency, ω_o = natural frequency.

2 Baranov's (Pure rotational solution, short rigid pile)

$$D = C_\psi / 2 \sqrt{k_\psi I_\psi}$$

in which C_ψ = damping coefficient, k_ψ = stiffness coefficient, I_ψ = mass moment of inertia of pile and mass about the point of rotation.

3 Kuhlemeyer's (Long pile)

$$D = C_x / 2 \sqrt{k_x m}$$

in which C_x = damping coefficient, k_x = stiffness coefficient, m = mass on top of the pile.

the shear modulus along the embedded pile length and requires the determination of the shear modulus at the tip of the pile. The shear moduli used in calculating the dynamic response of the piles using Baranov's theory were significantly lower than the values obtained from the cross-hole test and the resonant column test. This was also mentioned by Novak (1976), and he used the factor of 3/4 or 2/3 to reduce the measured shear modulus. The shear modulus for 3½ in. OD round pile was reduced approximately to 4 percent of the shear modulus obtained from the tests, and 6.8 percent for 4½ in. OD round pile. The upper part of the embedded portion of the pile participates actively in the motion and determines the pile stiffness and damping. The shear wave velocity diminishes at the same time with decreasing depth which yields a much lower shear modulus near the soil surface in a sand deposit. In the tests the embedment depth of the piles was small, which resulted in extremely small confining pressures compared to the usual field condition. The separation of piles from the tension part of the soil cannot be the reason for such reduction in shear modulus for this study because the submerged condition of the sand assured a perfect contact between the soil and the pile surface during the tests.

In Kuhlemeyer's solution the modulus of elasticity of the soil was the important factor in determining the

dynamic response of the pile. The value of the modulus of elasticity of soil used in the parametric study was 100 psi which yielded a reasonably good agreement in dynamic response compared with the experimental results. The value used was about ½ of the value suggested by Poulos (1971) for the loose cohesionless soil. It is believed that the previous reasoning for the reduction of shear modulus can be also true for this solution.

It was attempted to compare the values of E_s obtained using Dutch Cone test results and the equation suggested by Schmertmann (1970)

$$E_s = 28.45\ q_c \qquad (7.7.1)$$

(lb/in^2) (kg/cm^2)

Table 7.9 shows that the E_s used in Kuhlemeyer's solution is approximately ½ of the Poulos' value for loose soil near to the surface, and the G_s value for Baranov's solution is ½ of the value from the Eq. (7.7.1) for the smaller pile and 4/5 of the same value for the larger pile. For the tests reported here, the best correlation occurred when the E_s in the finite element solution was assumed by taking ½ of the value suggested by Poulos (1971), and for the pure rotational solution the G_s was assumed by taking the lower limit of the values for the dense sand for the smaller pile and the average value for the dense sand for the smaller pile and the average value

for the dense soil for the larger pile and use the equation,

$$G_s = \frac{E_s}{2\ (1+\nu)} \quad . \tag{7.7.2}$$

Table 7.9. Values of E_s for Analytical Solutions

Depth (ft.)	q_c, Kg/cm^2	E_s, psi (EQN 7.5.1)	Poulos (1971)	Used
1	6	171	250	100 (Kuhlemeyer)
5	42	1195	1000	600 (RP3) 1000 (RP4) (Baranov)

CHAPTER VIII

PULL-OUT CAPACITY OF PILES

A. Review of Previous Work

The load-carrying capacity of a vertical friction pile is determined by the shearing stresses which act at the pile-soil interface. In cohesionless soils these shearing stresses depend upon the normal stresses which act upon this interface. Variations in the magnitude or distribution of these normal stresses along the pile will affect the vertical load-deflection behavior of the pile.

It has long been recognized that driving of displacement piles in sands increases the relative density of loose soils in a zone approximately seven times the diameter of the pile (Meyerhof, 1959; Kishida, 1967). Both model tests and full-scale tests have shown that the bearing capacity of piles driven into loose sands is increased because of densification produced by piles driven previously. Kishida (1967) found that the increase of bearing capacity depended on the original relative density of the sand, the pile spacing, the number of piles, and the position and sequence of driving of the pile in the pile group.

Densification of a zone of sand around a driven pile sets up residual shearing stresses in the soil around the pile. These residual shearing stresses permit the development of horizontal static stresses on the pile face which correspond to K_o values from 1.0 to nearly the value of the coefficient of passive earth pressure K_p (Ireland, 1957). Repeated vertical and/or lateral motions of the pile may considerably reduce the load-carrying capacity of the piles.

It has been observed by many workers that vertical pile motions on the order of 8 to 10 percent of the pile length are required to develop the full point bearing capacity, whereas motions of the order of 0.25" to 0.40" appear to be adequate to develop full skin friction on piles and caissons (Vesic, 1968). Thus it would be anticipated that under normal design vertical loads, the major part of the load would be carried by skin friction. Any factor which reduced this skin friction, or caused major redistribution of these stresses along the pile would undoubtedly cause additional settlement of the pile under static load. Therefore vertical or lateral load-patterns produced by earthquakes could cause additional settlement of structures supported by piles.

Previous studies (see Richart, 1959) have shown that horizontal arching developed around an expanding pile will reduce considerably the pull-out resistance capacity.

It was observed that a contraction of about 0.002 x Radius reduced the pull-out resistance capacity by about 50 percent in both loose and dense sands. Therefore it is evident that any motion of a pile against the soil that tends to increase the size of the hole will generate an arching action in the soil which reduces the load-carrying ability. Vertical motions of tapered piles or lateral motions of piles may develop this arching effect in cohesionless soils. The concept described above has been applied practically by anyone who has wiggled a nail laterally in order to pull it out of a board or by anyone who has shoved horizontally on a fencepost before beginning to pull it out of the ground.

B. Experimental Results

When a pile is subjected to a purely axial pull, the resistance to movement is provided only by skin friction developed between pile surface and the soil. The moisture content of soils, the roughness of pile surface, the composition of soils, and the intensity of normal load are the most important factors in determining skin friction.

Ireland (1957) has proposed an equation for friction piles in cohesionless soils.

$$P_u = \pi d\, L_f(\gamma z + q)\, K \tan\phi \qquad (8.1.1)$$

in which,

z = depth to center of gravity of embedded portion of pile (or of the corresponding L_f of any strata),

q = surcharge load,

L_f = length of embedment for pile in any stratum or total length for a uniform soil deposit,

K = lateral earth pressure coefficient ($K_a < K < K_p$),

d = average pile diameter,

P_u = ultimate pull-out capacity of pile.

The pull-out capacity tests were performed on piles embedded in drained and submerged dense sand after each static and dynamic test. Pull-out tests on undisturbed piles were also performed for comparison of results with those from pretested piles. The surface of the square piles were sand blasted and left untreated which caused the pile to rust immediately upon contact with the moisture in the sand and formed a rough surface condition. The round piles were left with the initial protective coating as black steel pipe and presented smoother surfaces than those for the square piles.

It was observed that a certain amount of vertical displacement (less than ¼ in.) was required to develop the ultimate shearing resistance against axial pull-out motion all along the embedded portion of the pile. The round piles developed a smaller pull-out capacity than the square piles due to the smaller surface area and due to their

smoother surface. The pull-out capacity increased considerably as the depth of embedment of the pile increased.

The moisture content in drained sand was in the range of 2.4 and 3.5 percent. Pull-out capacity decreased approximately 60 to 80 percent for the embedment depth of 3 ft. and 5 ft. respectively when the relative density of the drained sand changed from 80 percent to 10 percent for all piles. The smaller piles embedded in drained sand showed a decrease of the pull-out capacity of approximately 15 percent after plucking tests, compared with values obtained from undisturbed piles, while the larger piles showed approximately 20 percent decrease. The K-values calculated from the Eq. (8.1.1) were in the range of 1.5 and 2.2.

The pull-out capacities of piles in submerged dense sand showed approximately 55 percent and 40 percent of those of the test results in drained sand for smaller and larger piles respectively. The data from the square piles after dynamic tests in submerged dense sand were too scattered to derive any meaningful conclusions.

The average pull-out capacities of piles after the quasi-static tests in submerged sand were 33 lb/ft^2 for the round piles and 65 lb/ft^2 for the square piles, which showed a decrease of 77 percent and 60 percent respectively compared with the undisturbed piles.

After the low frequency displacement-controlled dynamic tests, the pull-out capacity of the round piles embedded in submerged sand decreased approximately 40 percent. The test results also showed a decrease of 16 percent of the pull-out capacity after plucking test for the round piles. The pull-out capacity after the load-controlled Lazan dynamic tests decreased 50 percent for the round piles.

The K-values for the pull-out capacity of undisturbed piles embedded in submerged sand was in the range of 1.0 and 1.7, which showed a lower range than that of the drained sand.

Table 8.1 shows the pull out-test results tabulated for the round piles.

Table 8.1. Pull-out capacity, Lb/Ft^2

Pile Size	Embedded Depth, Ft	Drained		Submerged						
							After Dynamic Tests			
		Undisturbed	After Plucking	Undisturbed	After Static	After Plucking	2 Hz	3 Hz	5 Hz	Lazan
RP3	3'	209 (0.60)*	177 (0.63)	111	27	83	49	60	58	-
	4'	282 (0.56)	239 (0.60)	134	37	-	79	78	108	67
	5'	-	362 (0.61)	143	34	-	133	-	117	-
RP4	3'	214 (0.60)	177 (0.59)	89	32	84	57	44	68	-
	4'	356 (0.56)	271 (0.56)	145	37	-	92	74	95	-
	5'	398	-	154	32	-	101	95	144	75
Lateral Displacement (in)			0.005 (typical)		0.25 (max)	0.008 (typical)	0.090 (avg)	0.090 (avg)	0.090 (avg)	0.033 (max)

*Void ratio of sand.

CHAPTER IX

SUMMARY AND CONCLUSIONS

The static and dynamic behavior of a single rigid friction pile was studied experimentally and theoretically. Four steel piles of different sizes and shapes were used as model piles, embedded 3, 4, and 5 ft. into poorly graded fine Muskegon dune sand. The sand was contained in a watertight, galvanized, corrugated steel tank 7½ ft. in diameter and 10 ft. high, which operated as a quicksand tank. The quicksand operation of the tank and subsequent densification provided approximately the same density within the tank for each test. For many tests, the sand was left in a submerged condition to assure perfect contact between soil and pile surface. The piles were tested in dense sand for which the average void ratio was 0.60 and the relative density was 76 percent. Table 9.1 shows the list of all the tests performed in this study.

Static tests were performed using a Gilmore actuator to produce 1 cycle per minute sinusoidal motion. Dynamic tests were performed using the Gilmore actuator for displacement-controlled low-frequency tests and the

Table 9.1. List of tests performed

Test		Number of Tests Performed	Condition of Sand
Static:	Quasi-static (1 cpm) horizontal load test	12	Submerged, dense
Dynamic:	Displacement-controlled test	36	Submerged, dense
	Load-controlled test	15	"
	Plucking test	9	"
		23	Drained, dense
Pull-Out Capacity:	Vertical axial pull-out resistance capacity test	22	Drained, dense
		73	Submerged, dense
Miscellaneous:	Dutch Cone test	73	Drained, dense & loose
	Cross-hole test	12	Drained, dense
	Resonant-column test	6	Dry, dense

Lazan mechanical oscillator was used for the load-controlled, steady-state high frequency vibration tests. Plucking tests were also performed to study the response of the piles to transient vibrations. A series of pull-out capacity tests was performed to study the effects of static or dynamic motion of the pile on the pull-out resistance capacity.

Analytical solutions for static and dynamic response of the pile were also studied. Kubo's nonlinear solution and Kuhlemeyer's finite element solution were adopted for evaluating the static behavior of the pile, and Baranov's elastic side layer reaction theory and Kuhlemeyer's finite element method were used to analyze the dynamic response of the pile.

The static resistance of the pile against the horizontal load can be reasonably well estimated by using Kubo's nonlinear solution. However, this solution requires lengthy calculations. On the other hand, Kuhlemeyer's solution yields quick and easy firsthand values, which may be used for a first estimate of pile motions.

Novak's (1971) inverse nonlinear solution to reduce the dynamic test data was found convenient and was adopted for comparison of test results with theoretical solutions.

Because the sand was not surcharged, the confining pressure near the surface was low. This established low values of the shear modulus, G, in the zone where pile

motions were greatest. Consequently, it was necessary to reduce the values of G, as found from cross-hole tests, to a lower value in order to fit Baranov's and Kuhlemeyer's theoretical solutions to the test data. If the shear modulus and the modulus of elasticity can be assumed or provided, both of the above dynamic solutions will yield a reasonably good but conservative dynamic response of the pile. Kuhlemeyer's solution tends to overestimate the damping ratio. Baranov's solution was studied for the pure rotational motion of short rigid piles and Kuhlemeyer's solution assumed a pile with $L/r_o > 25$.

The pull-out capacity of piles embedded in submerged sand decreased about 70 percent after the quasi-static tests and 40 to 50 percent after the dynamic tests compared to the values obtained from the undisturbed piles. Piles in drained soil showed a much larger pull-out capacity than for piles in submerged soil. The amount of the horizontal displacement the pile experienced during the test was found to be a very important factor in determining the pull-out capacity.

APPENDIX I

COMPUTER PROGRAM FOR BARANOV'S SOLUTION

```
C  THIS PROGRAM IS TO CALCULATE THE DYNAMIC RESPONSE OF A SHORT
C RIGID PILE EMBEDDED IN AN ELASTIC HALF-SPACE AND SUBJECTED
C TO LATERAL STEADY-STATE HARMONIC EXCITATION BASED ON BARKAN'S
C SLIP LAYER DEFINITION.
C    FREQUENCY OF EXCITATION SPECIFIED = C.S.
C    FREQUENCY-INCREMENT OF EXCITATION FREQUENCY,CPS
C    FREQSTP-FREQUENCY AT WHICH CALCULATION IS TO BE TERMINATED
C    GMS-UNIT WEIGHT OF SOIL, PCF
C    NU-POISSON'S RATIO
C    LO-HEIGHT OF THE LOAD APPLICATION POINT FROM THE
C       GROUND SURFACE, FT
C    W-WEIGHT OF MASS ACTING ON TOP OF PILE, LB
C    GS-SHEAR MODULUS OF SOIL AT THE LOWER END OF PILE, PSF
C    WP-WEIGHT OF PILE, LB
C    IPRT-PRINT OR NOT PRINTING OUT ROTATING MASSES, D=O
C    EO-UNIFORM DIAMETER OF PILE, FT
C    E1-INSIDE DIAMETER OF PILE, FT
C    L-EMBEDDED LENGTH OF PILE, FT
C    LP-LENGTH OF PILE, FT
C
      INTEGER EXP
      REAL J0,J1,J2,Y0,Y1,Y2,LAMDA,L,LP,NU,NPSI,IPSI,MEE,MAG,LO
      J0(XX)=1.-2.25*(XX/3.)**2+1.25542*(XX/3.)**4-0.31438*(XX/3.)**6+
     A0.4448*(XX/3.)**8
      J1(XX)=XX*(0.5-0.5625*(XX/3.)**2+0.21936*(XX/3.)**4-0.03954*
     A(XX/3.)**6+0.00433*(XX/3.)**8)
      J2(XX)=J1(XX)*2./XX-J0(XX)
      Y0(XX)=2./PI*(ALOG(XX/2.)*J0(XX)+0.36746+0.60559*(XX/3.)**2-
     A0.74350*(XX/3.)**4+0.253*(XX/3.)**6-0.04261*(XX/3.)**8
      Y1(XX)=(1./XX)*(2./PI)*ALOG(XX/2.)*XX*J1(XX)-0.6366+0.2212*
     A(XX/3.)**2+2.1682*(XX/3.)**4-1.31648*(XX/3.)**6+0.31239*(XX/3.)
     B**8)
      Y2(XX)=Y1(XX)*2./XX-Y0(XX)
```

```
   45 READ(5,100,END=99) FREQ,FRQINC,FRQSTP
      READ(5,101) UWS,NU,LP,W
      READ(5,102)GS
      READ(5,103)THETA
      READ(5,104)R0, RI,UP,L,LP
      KAP=1
   13 G=32.17
      PI=4.*ATAN(1.)
      OM=FREQ*2.*PI
      MEE=2.*SIN(THETA/2.)
      Q0=MEE*FREQ**2
      Q=(1.-2.*NU)/(2.*(1.-NU))
      A0=OM*R0*SQRT(UWS/G/GS)
      X0=A0*SQRT(Q)
C
C CALCULATION OF THE COEFFICIENTS OF SIDE LAYER REACTION
      E=J0(A0)*J2(X0)+J0(X0)*J2(A0)-Y0(A0)*Y2(X0)-Y0(X0)*Y2(A0)
      F=J0(A0)*Y2(X0)+J0(X0)*Y2(A0)+J2(A0)*Y0(X0)+J2(X0)*Y0(A0)
      A=(J1(X0)*J2(A0)-Y1(X0)*Y2(A0))/SQRT(Q)+J1(A0)*J2(X0)-Y1(A0)*
     1Y2(X0)
      B=(J1(X0)*Y2(A0)+J2(A0)*Y1(X0))/SQRT(Q)+J2(X0)*Y1(A0)+J1(A0)*
     1Y2(X0)
      SU1=2.*PI*A0*(A*E+B*F)/(E*E+F*F)
      SU2=2.*PI*A0*(A*F-B*E)/(E*E+F*F)
      SPSI1=PI*(1.-A0*((J0(A0)*J1(A0)+Y0(A0)*Y1(A0))/(J1(A0)**2+Y1(A0)
     A**2)))
      SPSI2=(-1.)*PI*A0*((J0(A0)*Y1(A0)-J1(A0)*Y0(A0))/(J1(A0)**2+
     AY1(A0)**2))
C
C COMPUTING LAMBDA WHICH MAXIMIZES PSID
      PSIDI=0.
      TEL=0.
   34 LAMDA=3.*L/5.+TEL*0.0005*L
      KPSI=GS*L*(2.*R0**2*SPSI1/3.+SU1*(2.*L**2/7.-4.*LAMDA*L/5.
     1+2.*LAMDA**2/3.))
```

```
      OMCPSI=GS*L*(2.*R0**2*SPSI2/3.+SU2*(2.*L**2/7.-4.*LAMDA*L/5.
     1+2.*LAMDA**2/3.))
      IPSI=(WP/3./G)*(LP+LAMDA-L)**2+W*(LQ+LAMDA)**2/G
      PSIC=Q0*(LQ+LAMDA)/SQRT((KPSI-OM**2*IPSI)**2+OMCPSI**2)

      DIF=PSIDI-PSIC
      IF (DIF.GT.0.) GO TO 34
      PSIDI=PSIC
      TEL=TEL+1.
      GO TO 34
C
C CALCULATIONS OF DYNAMIC RESPONSE
C   PSID-ROTATIONAL AMPLITUDE, RAD
C   DELD-LATERAL DISPLACEMENT AT GROUND SURFACE, INCH
C   MAG-DIMENSIONLESS AMPLITUDE
C   FRQNAT-NATURAL FREQUENCY, CPS
C   DAMP-DAMPING RATIO
C   PHI-PHASE SHIFT, RAD
C
   34 PSID=(PSIDI*PSIC)/2.
      DELD=12.*LAMDA*PSID
      MAG=IPSI*4.*PI**2*PSID/ACE/(LQ+LAMDA)
      FRQNAT=SQRT(KPSI/IPSI)/(2.*PI)
      DAMP=OMCPSI/(2.*OM*SQRT(KPSI*IPSI))
      PHI=ATAN(OMCPSI/(KPSI-IPSI*OM**2))
C
      IF(KAP.GT.1.) GO TO 47
      WRITE(6,205)
      WRITE(6,210)L,R0,RI,WP,W,LQ,THETA
      WRITE(6,215)
      WRITE(6,220)UWS,NU,GS
      WRITE(6,225)
   47 WRITE(6,300)FREQ,A0,FRQNAT,DAMP,DELD,PSID,PHI,MAG,LAMDA
  100 FORMAT(3F10.2)
  101 FORMAT(4F10.3)
```

```
102 FORMAT(F10.0)
103 FORMAT(F10.0)
104 FORMAT(5F10.5)
205 FORMAT('1',[illegible]'PILE AND LOADING DATA*'///)
210 FORMAT(' ',[illegible]'EMBEDDED LENGTH,FT=',20X,[illegible]/' ',5X,'RADIUS OF PIL
   1E(OUTSIDE,FT)=',12X,F5.4/' ',5X,'RADIUS OF PILE(INSIDE,FT)=',13X,F
   28.1/' ',5X,'WEIGHT OF PILE(LB)=',1[illegible],F10.2/' ',5X,'DEAD WEIGHT ATT
   3ING ON PILE(LB)=',4X,F10.2/' ',5X,'WEIGHT OF LOAD APPLICATION'/' '
   4,5X,'POINT FROM THE GROUND SURFACE(FT)=',5X,F6.2/' ',5X,'ANGLE OF
   [illegible]
215 FORMAT(' ',[illegible]'SOIL PROPERTIES*'///)
220 FORMAT(' ',[illegible]'UNIT WEIGHT OF SOIL(LB/FT**3)=',5X,F10.2/' ',5X,'PO
   1ISSONS RATIO',25X,F[illegible]/' ',5X,'SHEAR MODULUS AT THE LOWER '/' ',5
   2X,'END OF PILE(LB/FT**2)=',11X,F12.2///)
225 FORMAT(' ',[illegible]'[illegible] RESPONSE*'/////' ',1X,'FREQ          [illegible]
   1   [illegible] FREQ    [illegible]    AMPLITUDE      [illegible]ATION          [illegible]
   2    [illegible]
300 FORMAT(' ',[illegible]F10.[illegible],F10.[illegible],F10.[illegible],F10.[illegible]
   1[illegible],F10.[illegible]
    FREQ FREQ[illegible]
    KAP=KAP+1
    IF(FREQ.GT.[illegible]) GO TO [illegible]
    GO TO 17
 99 STOP
    END
```

APPENDIX II

COMPUTER PROGRAM FOR KUHLEMEYER'S SOLUTION

```
C  DAMPING RATIO AND DAMPED NATURAL FREQUENCY
C  OF LATERALLY LOADED PILE-SOLUTION BY KUHLEMEYER'S THEORY
       INTEGER FAP
       DIMENSION CT1(3,5),CT2(3,5),CJ1(3,5),CJ2(3,5)
       COMPLEX FII,FI1,FI2,A2,A3,A4,A44,D1
C  POLYNOMIAL EXPANSION COEFFICIENTS
       DATA CT1/3.0,-.02,-1.284,-1.2824,-.4722,-11.2e21,
      1 .7262,0.42?,0.512,1.0002,1.0028,1.005/
       DATA CJ1/0.0,.72,-.313,-.231,-2.2036,-24.0321,-92.308,
      1 3.7805,20.6959,1.,.9773,.999,.1269,1.0124,-.0035,.0008,-.00077
       DATA CT2/3.0,-.1916,-2.0875,6.2157,.5874,.9885,-6.8475,
      1.4458,.0309,1.078(,.0003,.7931,.9978/
       DATA CJ2/-21.7209,0.0,-1.1000,1A .423,-2.7744,-75.9311,
      1-1.0753,6.857,.7  .4,.1121,- .7  ,  .7113,6 ,, 0.07, .0029/
       DATA CJ2/3.0,  ,  ,-1.0101, 0.72,1 .1.,0,, 1.7024,
      1-.0315,-.031,  ,  .1 .0004,1 .0001,  ,  /
       DATA CJ2/3.,1 ,  ,0,  ,  ,  ,  ,  .7  .883,  .705,  .1101,  ,
      1,.0075,.6696,-.0171,-.0011, .0015,-.0017/
C  VARIABLE PARAMETERS
C   RADO-OUTSIDE RADIUS OF PILE, INCH
C   RADI-INSIDE RADIUS OF PILE, INCH
C   PELM-PILE EMBEDMENT LENGTH, FEET
C   PLNS-HEIGHT OF CENTER OF GRAVITYOF DEAD WEIGHT ABOVE
C        GROUND SURFACE, FEET
C   WO-DEAD WEIGHT ACTING ON PILE, LB
C   EPH-MODULUS OF ELASTICITY OF PILE MATERIAL, PSI
C   ESS-MODULUS OF ELASTICITY OF SOIL, PSI
C   GSMS-SHEAR MODULUS OF SOIL, PSI
C   DENSOL-DENSITY OF SOIL, LB/FT**3
C   FREQV-FREQUENCY OF VIBRATION, CYCLES/SEC
C   FMEE-ECCENTRIC MASS EXCITATION FORCE, MEXE, IN-LB
    45 READ(5,100,END=99) FREQV, FRQINC,FRQSTP
       READ(5,101)RADO,RADI,PELM,PLNS,WO,EPH
```

```
      READ(5,102)ESS,GSMS,DENSOL
      READ(5,103)FMEE
      KAP=1
   13 G=32.17
      PI=4.*ATAN(1.)
      FMASS=WQ/12./G
      RHO=FMEE/(FMASS*4.*PI**2)
      OM=2.*PI*FREQV
      FIPP=PI/4.*(RADO**4-RADI**4)
      FISP=PI/4.*RADO**4
      ESP=EPM*FISP/FISP
C PILE FLEXIBILITY FACTOR
      FKP=ESP*FISP/ESS/(12.*PELN)**4
C SHEAR WAVE VELOCITY
      VSHEAR=SQRT(GSMS/9.144/DENSOL)
C DIMENSIONLESS FREQUENCY
      A0=OM*RADO/VSHEAR/12.
C FLEXIBILITY COEFFICIENTS FOR STATIC LATERAL LOADING
      EFFE=ESP/ESS
      A11=.567*EFFE**(-.170)
      A12=.[illegible]*EFFE**(-.[illegible])
      A22=.585*EFFE**(-.[illegible])
C COMPUTE FLEXIBILITY COEFFICIENT FACTORS
      I=1
      IF (EFFE-333.) 10,10,11
   11 I=2
      IF(EFFE-2283.)10,10,12
   12 I=3
   10 FI11=CI11(I,1)*A0**4+CI11(I,2)*A0**3+CI11(I,3)*A0**2+
     1CI11(I,4)*A0+CI11(I,5)
      FJ11=-(CJ11(I,1)*A0**4+CJ11(I,2)*A0**3+CJ11(I,3)*A0**2+
     1CJ11(I,4)*A0+CJ11(I,5))
      FI12=CI12(I,1)*A0**4+CI12(I,2)*A0**3+CI12(I,3)*A0**2+
     1CI12(I,4)*A0+CI12(I,5)
```

```
      FJ12=-(CJ12(I,1)*A0**4+CJ12(I,2)*A0**3+CJ12(I,3)*A0**2+
     1CJ12(I,4)*A0+CJ12(I,5))
      FI22=CI22(I,1)*A0**4+CI22(I,2)*A0**3+CI22(I,3)*A0**2+
     1CI22(I,4)*A0+CI22(I,5)
      FJ22=-(CJ22(I,1)*A0**4+CJ22(I,2)*A0**3+CJ22(I,3)*A0**2+
     1CJ22(I,4)*A0+CJ22(I,5))
      FK1=PI/4.*EBBE
      FII11=A11*FI11
      FJJ11=A11*FJ11
      FII12=A12*FI12
      FJJ12=A12*FJ12
      FII21=A12*FI12
      FJJ21=A12*FJ12
      FII22=A22*FI22
      FJJ22=A22*FJ22
C [illegible] LATERAL LOADING
      FF11=FK1*CMPL(FII11,FJJ11)
      FF12=FK1*CMPL(FII12,FJJ12)
      FF22=FK1*CMPL(FII22,FJJ22)
C COMPUTE COMPLEX TERMS FOR EQUATION 32
      AAA=FF11*FF22-FF12*FF12
      A2=FF22/AAA
      A3=FF12/AAA
      A4=FF11/AAA
      FK2=PI/4.*ESS*RADO
      U1=(A4-PLMS/RADO/A3)/FK2/(A2*A4-A3*A3)
      CC1=REAL(U1)
      CC2=AIMAG(U1)
      CCCC=CC1*CC1+CC2*CC2
      CU32=CC1/CCCC
      CDU32=CC2/CCCC/OM
C CHECK WITH EQUATION 27
      CC3=(FII11/RADO+PLMS*FII12/RADO/RADO)/ESS
      CC4=(FJJ11/RADO+PLMS*FJJ12/RADO/RADO)/ESS
```

```
C FOR DETERMINATION OF [illegible]
      CO=-(FI*2*PI*SIN(PHI)/(2*PI*SIN(PHI)+2*PI*COS(PHI)))
      CO=-(FI*2*PI*SIN(PHI)/(2*PI*SIN(PHI)+2*PI*COS(PHI)))
C [illegible]
C [illegible]
C [illegible]
```

```
      FNX=1./2./PI*SQRT(FKX/FMASS)
      DISPX=FMEE*FREQV**2/SQRT((FKX-FMASS*OM**2)**2+(OM*CX)**2)
      DLSMPX=DISPX/RHO
      IF(KAP.GT.1) GO TO 47
      WRITE(6,300)
      WRITE(6,310)PELN,RADO,RADI,FMEE,WO,PLNS
      WRITE(6,320)
      WRITE(6,330)DENSOL,ESS,GSMS
      WRITE(6,335)FKR
      WRITE(6,338)CU32,CDU32,CU27,CDU27,CUX27,CDUX27
      WRITE(6,340)
   47 WRITE(6,350)FREQV,AO,DMPO,UDMFRO,DISPO,DLSMPO,DX,FNX,DISPX,DLSMPX
  100 FORMAT(3F10.5)
  101 FORMAT(5F10.4,F10.2)
  102 FORMAT(3F10.4)
  103 FORMAT(F10.5)
  300 FORMAT('1 [illegible] FILE AND LOADING DATA'/' ',4X,'*****************
     1*'///)

  310 FORMAT(' ',5X,'[illegible]'/' ',5X,'RADIUS OF PIL
     1E(OUTSIDE,IN) [illegible]'/' ',5X,'RADIUS OF PILE(INSIDE,IN)=',1X,F5.
     22/' ',5X,'MEE(IN-LB) [illegible]'/' ',5X,'DEAD WEIGHT ACTING ON PI
     3LE(LB)=',1X,F8.2/' ',5X,'HEIGHT OF CENTER OF GRAVITY OF DEAD'/' ',
     45X,'WEIGHT ABOVE GROUND SURFACE(FT)=',1X,F5.2////)
  320 FORMAT(' ',4X,'SOIL PROPERTIES'/' ',4X,'*****************'///)
  330 FORMAT(' ',4X,'UNIT WEIGHT OF SOIL(LB/FT**3)=',5X,F8.2/' ',5X,
     1'MODULUS OF ELASTICITY OF SOIL(PSI)=',1X,F8.2/' ',5X,'SHEAR MODULU
     2S OF SOIL(PSI)=',[illegible],F8.2///)
  335 FORMAT(' ',4X,'*FILE FLEXIBILITY FACTOR,KR=',2X,F10.5///)
  338 FORMAT(' ',4X,'*COMPARISON OF VALUES FROM EQ. 27 & 32!'//' ',5X,'C
     1U32  =',5X,F12.5/' ',5X,'CDU32 =',5X,F12.5/' ',5X,'CU27  =',5X,F12
     2.5/' ',5X,'CDU27 =',5X,F12.5/' ',5X,'CUX27 =',5X,F12.5/' ',5X,'CDU
     3X27=',5X,F12.5///)
  340 FORMAT(' ',4X,'DYNAMIC RESPONSE!'/' ',4X,'*****************'//' ',
     115X,'MOTION AT GROUND LEVEL                                    M
```

APPENDIX III

ADDITIONAL DYNAMIC RESPONSE CURVES FROM LAZAN TESTS

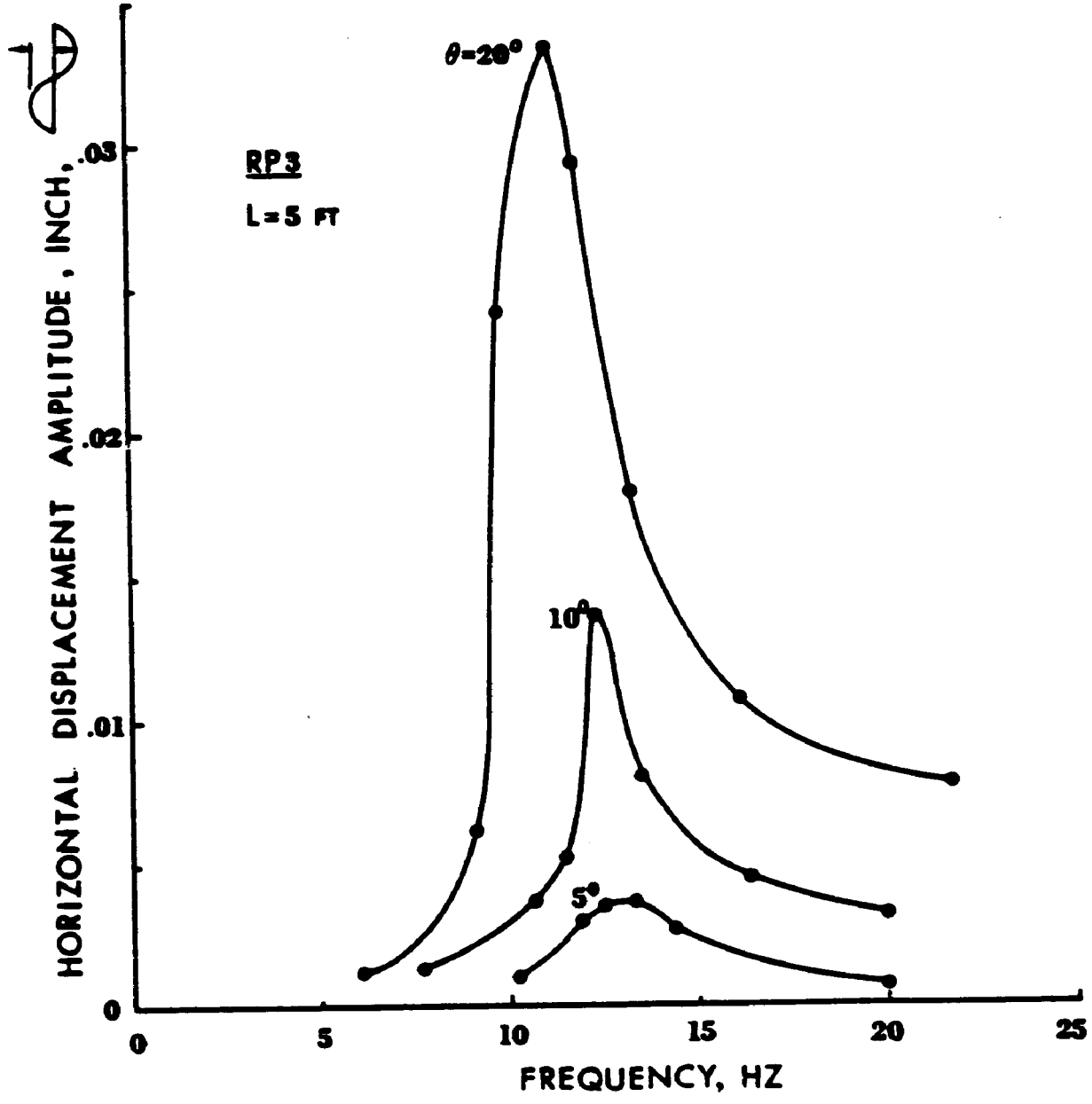

Figure A.3.1 Dynamic response curves of load-controlled Lazan test

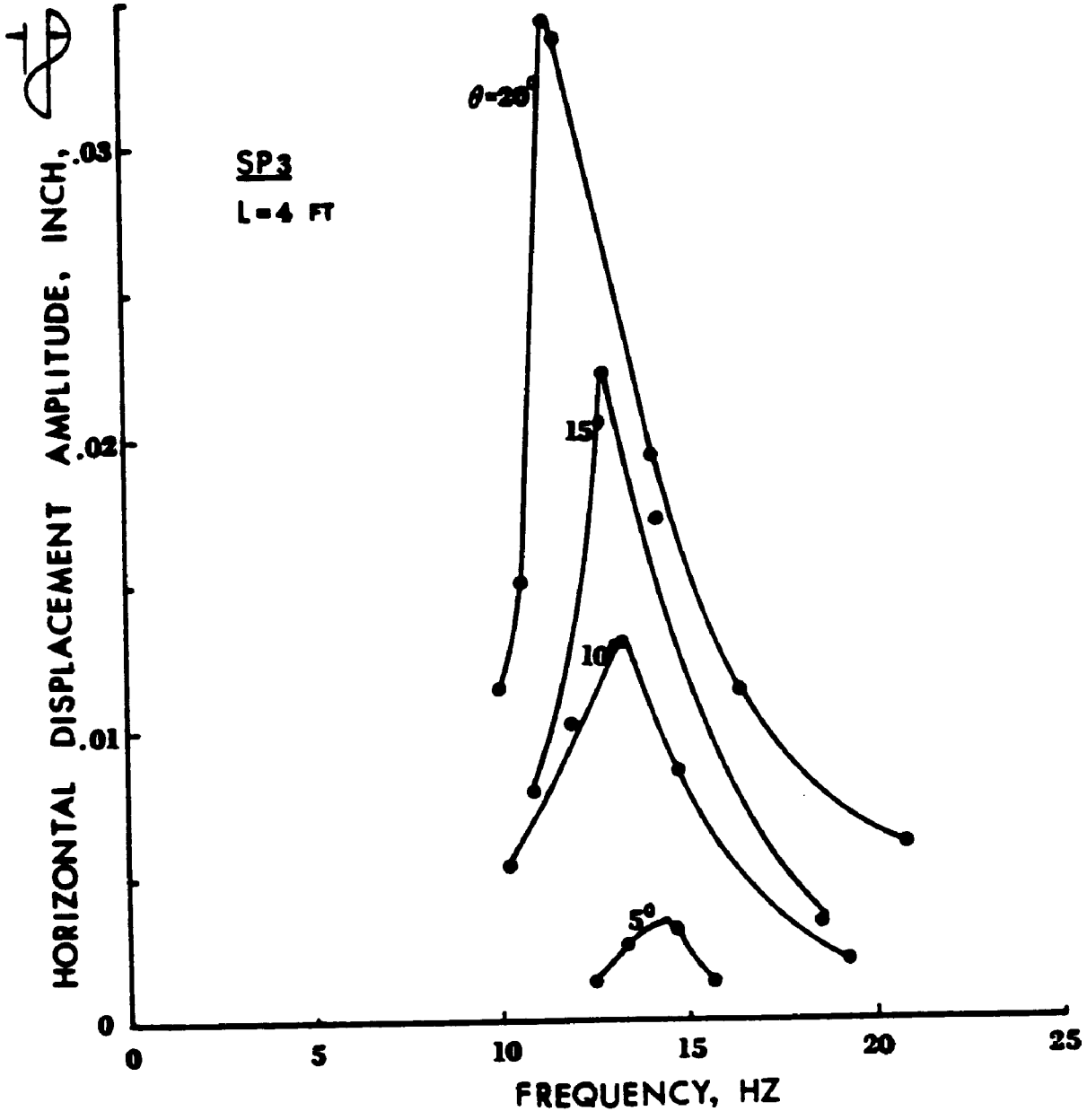

Figure A.3.2 Dynamic response curves of load-controlled Lazan test

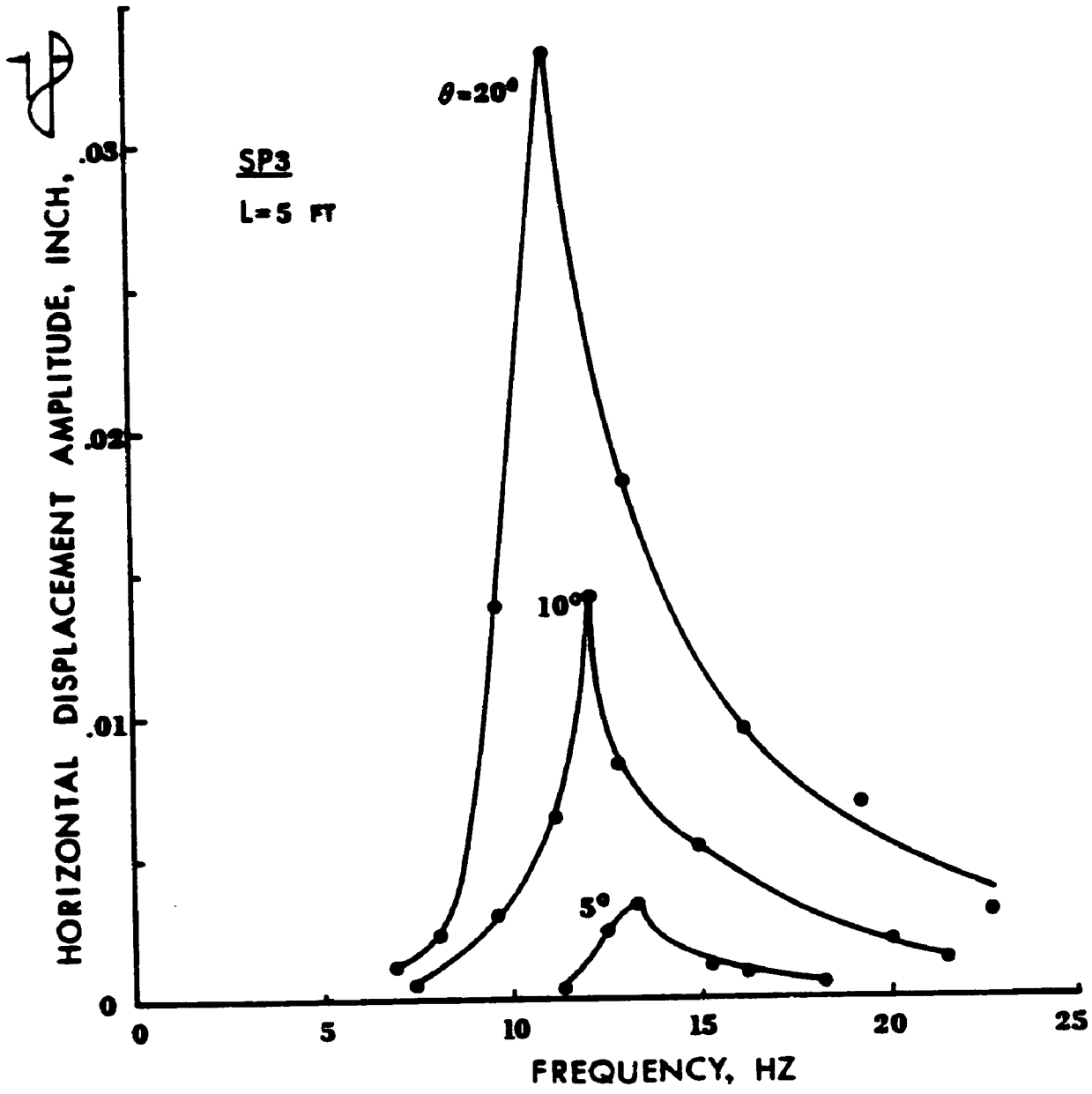

Figure A.3.3 Dynamic response curves of load-controlled Lazan test

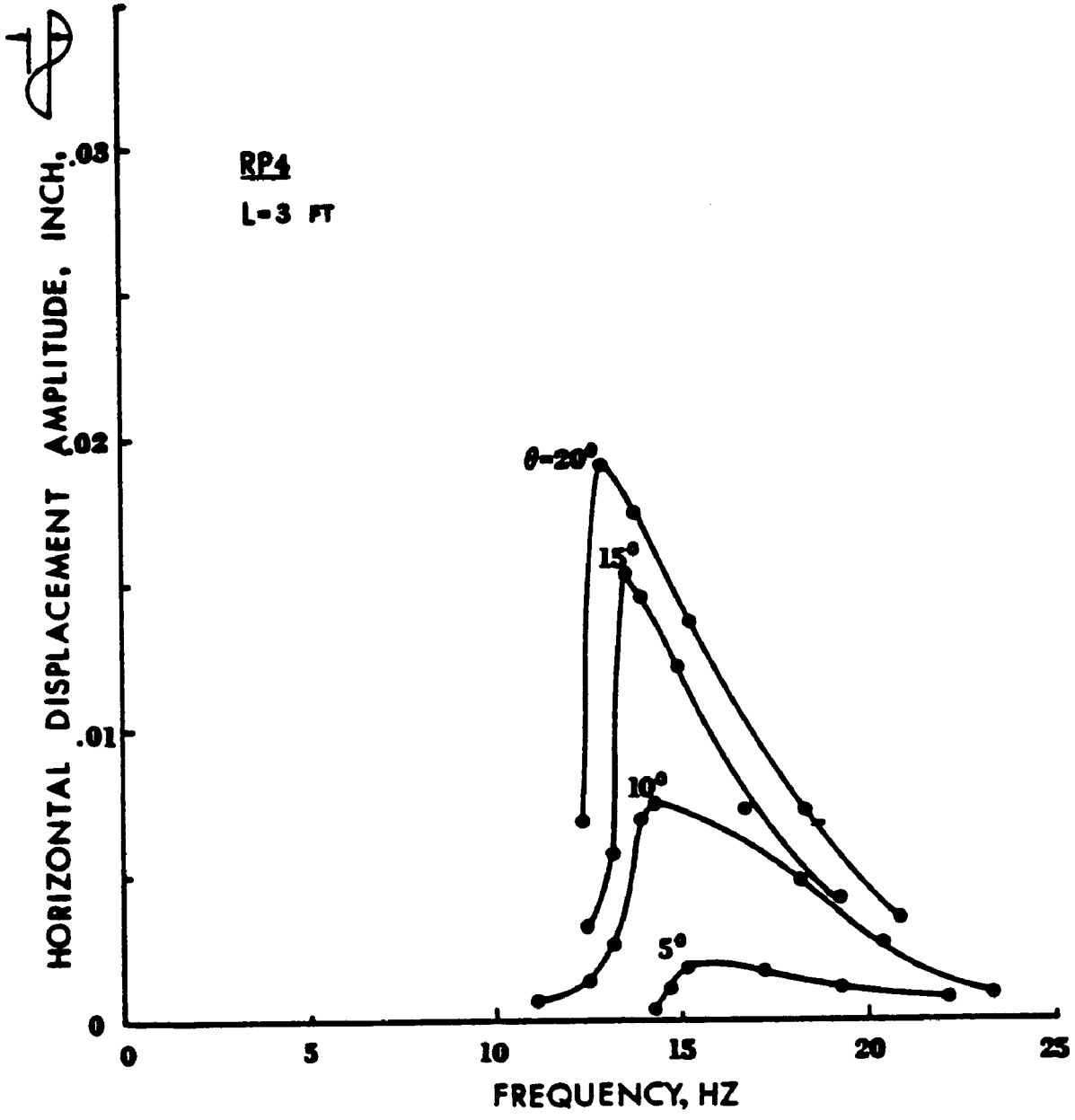

Figure A.3.4 Dynamic response curves of load-controlled Lazan test

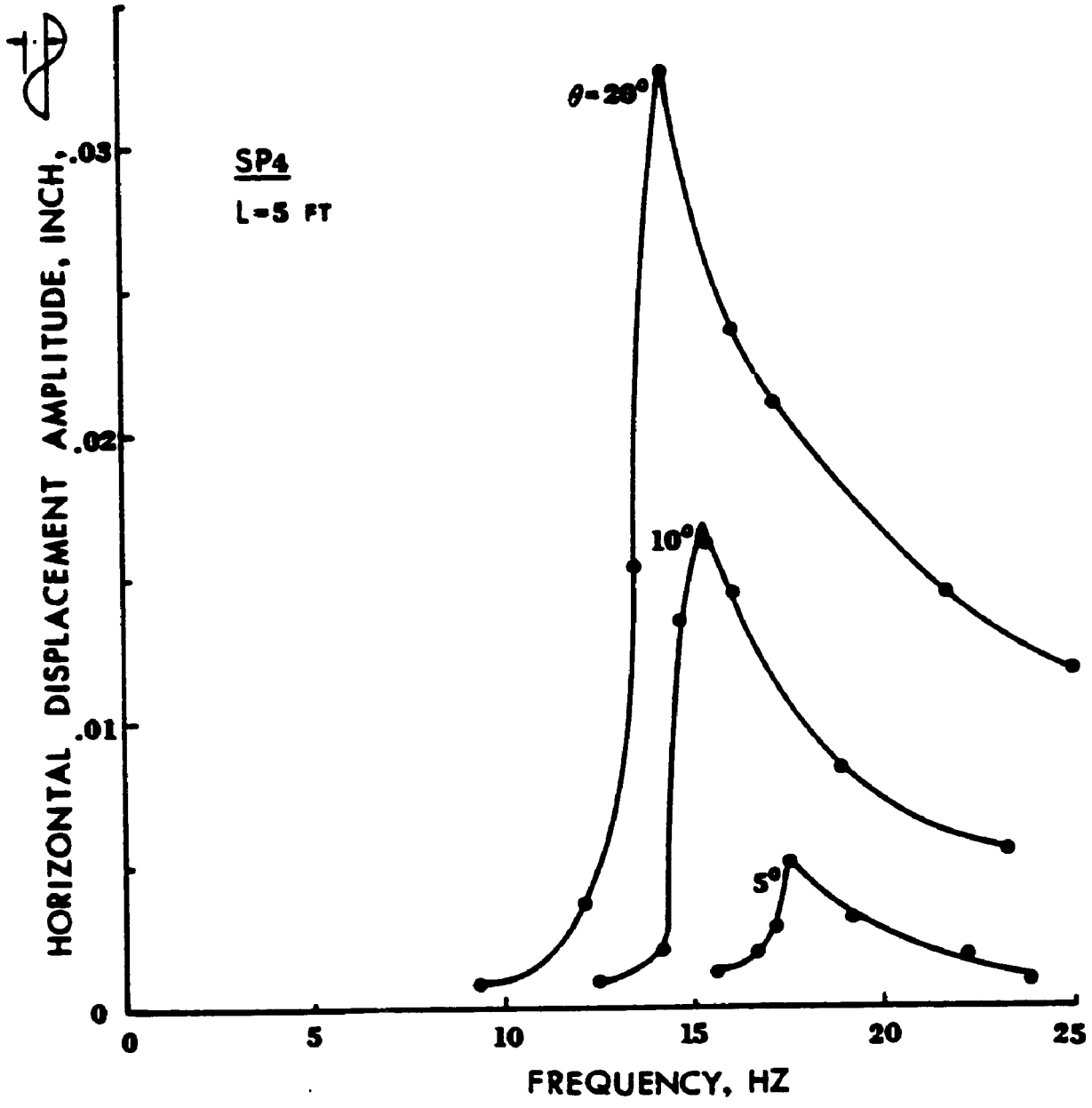

Figure A.3.5 Dynamic response curves of load-controlled Lazan test

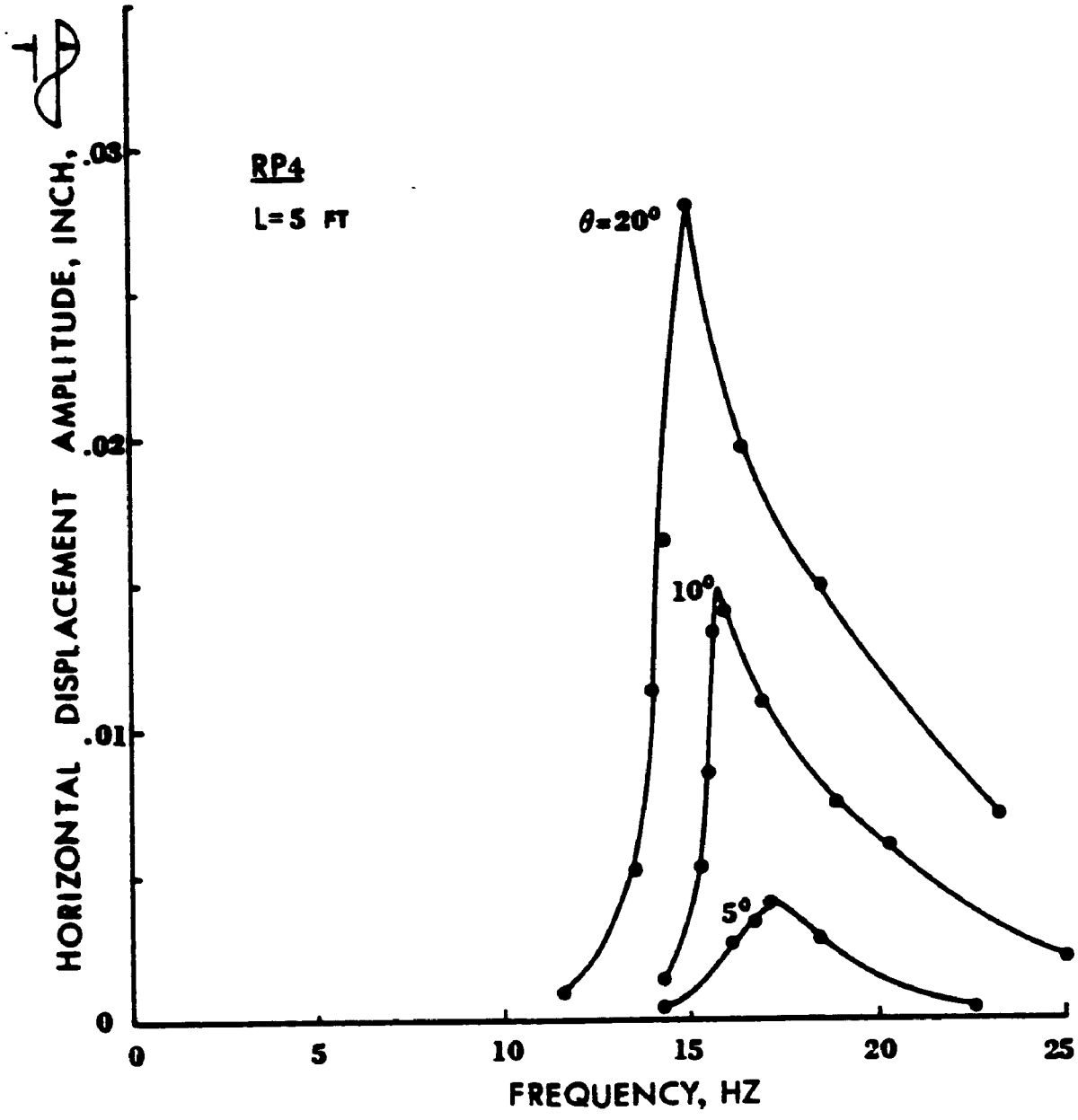

Figure A.3.6 Dynamic response curves of load-controlled Lazan test

REFERENCES

Abramowitz, M. and Stegun, I. A. (1964), Handbook of Mathematical Functions, National Bureau of Standards, Applied Mathematics Series 55, United States Department of Commerce, June, 1964.

Afifi, S. E. A. (1970), Effects of Stress History on the Shear Modulus of Soils, Ph. D. Thesis, University of Michigan, Ann Arbor, 1970.

Agarwal, S. L. (1973), "Discrete Element Method for vertical piles under Dynamic Lateral Loads," Symposium on Earth and Earth Structures under Earthquakes and Dynamic Loads, March, 1973, pp. 159-164.

Anderson, D. G. (1974), Dynamic Modulus of Cohesive Soils, Ph. D. Thesis, University of Michigan, Ann Arbor, 1974.

Baranov, V. A. (1967), "On the Calculation of Excited Vibrations of an Embedded Foundation," (in Russian) Voprosy Dynamiki i Prochnocti, No. 14, Polytechnical Institute of Riga, 1967, pp. 195-209.

Beaton, J. L., Nordlin, E. F., and Field, R. N. (1967), "Dynamic Tests of Corrugated Metal Beam Guardrail," Highway Research Record No. 174, Highway Research Board, Washington, D.C., pp. 42-87.

Beredugo, Y. O. (1971), Vibrations of Embedded Symmetric Footings, Ph. D. Thesis, University of Western Ontario, London, Canada, August, 1971.

Beredugo, Y. O., and Novak, M. (1971), "The Effect of Embedment on Footing Vibrations," First Canadian Conf. on Earthquake Eng. Research, University of British Columbia, Vancouver, Canada, May, 1971.

Beredugo, Y. O., and Novak, M. (1972), "Coupled Horizontal and Rocking Vibration of Embedded Footings," Canadian Geotech. Journal, no. 9, 1972, pp. 447-497.

Bowles, J. E. (1974), Analytical and Computer Methods in Foundation Engineering, McGraw Hill Publishing Co., 1974.

Broms, B. B. (1964b), "Lateral Resistance of Piles in Cohesionless Soils," Journal of the Soil Mech. and Found. Eng. Div., Proc. ASCE, Vol. 90, No. SM5, May, 1964, pp. 123-156.

Broms, B. B. (1972), "Stability of Flexible Structures (Pile and Pile Groups)," Proc. 5th European Conf. of Soil Mech. and Found. Eng., Vol. 2, pp. 239-269.

Christensen, N. H. (1961), "Model Test with Transversally Loaded Rigid Piles in Sand," Danish Geotech. Inst. Bulletin, No. 12, Copenhagen, pp. 10-16.

Coyle, H. M., and Sulaiman, I. H. (1967), "Skin Friction for Steel Piles in Sand," Journal of the Soil Mech. & Found. Eng. Div., Proc. ASCE, Vol. 93, November, 1967, pp. 261-278.

Davisson, M. T. (1960), Behavior of Flexible Vertical Piles Subjected to Moment, Shear, and Axial Load, Ph. D. Thesis, University of Illinois, Urbana, Ill.

Davisson, M. T., and Gill, H. (1963), "Laterally Loaded Piles in a layered Soil System," Journal of the Soil Mech. & Found. Eng. Div., Proc. ASCE, Vol. 89, No. SM3, May, 1963, pp. 63-94.

Davisson, M. T. (1970), "Lateral Load Capacity of Piles," Highway Research Record No. 333, Highway Research Board, Washington, D.C., pp. 104-112.

Davisson, M. T., and Salley, J. R. (1970), "Model Study of Laterally Loaded Piles," Journal of the Soil Mech. & Found. Eng. Div., Proc. ASCE, Vol. 96, No. SM5, Sept., 1970, pp. 1605-1627.

Drnevich, V. P., and Richart, F. E., Jr. (1970), "Dynamic Prestraining of Dry Sand," Journal of the soil Mech. & Found. Eng. Div., Proc. ASCE, Vol. 96, No. SM2, March, 1970, pp. 453-469.

Ehler, O. M. C. (1968), "Nonlinear Parameters of Vibrating Foundations," Journal of the Soil Mech. and Found. Eng. Div., Proc. ASCE, Vol. 94, No. SM6, Nov., 1968 pp. 1199-1214.

Fellenius, B. H. (1973), "Bending of Piles Determined by Inclinometer Measurements," Swedish Geotech. Inst., No. 53, pp. 25-32.

Forrestal, M. J., and Alzheimer, W. E. (1968), "Transient Motion of a Rigid Cylinder Produced by Elastic and Acoustic Waves," Journal of Applied Mechanics, ASME, March, 1968, pp. 134-138.

Gaul, R. D. (1958), "Model Study of a Dynamically Laterally Loaded Piles," Journal of the Soil Mech. & Found. Eng. Div., Proc. ASCE, Vol. 84, No. SM1, Feb., 1958, pp. 1535-32.

Gill, H. (1968), Soil Behavior Around Laterally Loaded Piles, Technical Report R-571, Naval Civil Eng. Laboratory, Port Hueneme, California, April, 1968.

Gill, H., and Demars, K. (1970), Displacement of Laterally Loaded Structures in Nonlinearly Responsive Soil, Technical Report R-670, Naval Civil Eng. Lab., Port Hueneme, California, April, 1970.

Gleser, Sol M. (1953), "Lateral Load Tests on Vertical Fixed-head and Free-head Piles," Special Technical Publication 154, American Society for Testing Materials, 1953, pp. 75-.

Hakuno, M. (1973), "Evaluation of Dynamical Properties of Pile Foundation Based on Wave Dissipation Theory," Proc. Fifth World Conf. on Earthquake Eng., Rome, No. 334, 1973.

Hardin, B. O., and Richart, F. E., Jr. (1963), "Elastic Wave Velocities in Granular Soils," Journal of the Soil Mech. & Found. Eng. Div. Proc. ASCE, Vol. 89, No. SM1, Feb., 1963, pp. 33-65.

Haupt, W. A. (1973), "In Situ Shear Wave Velocity by Cross-Hole Method,"-Discussion Journal of the Soil Mech. & Found. Eng. Div., Proc. ASCE, Vol. 99, No. SM2, Feb., 1973, pp. 224-228.

Hayashi, S., Miyazawa, N., and Yamashita, I. (1965), "Horizontal Resistance of Steel Piles Under Static and Dynamic Loads," Proc. Third World Conf. on Earthquake Engineering, Vol. 2, 1965.

Hayashi, S. (1973), "A new Method of Evaluating Seismic Stability of Steel Pile Structures," Proc. Fifth World Conf. on Earthquake Eng., Rome, No. 329.

Hetenyi, M. (1964), Beams on Elastic Foundation, Univ. of Michigan Press, Ann Arbor, Michigan, 1946.

Ireland, H. O. (1957), "Pulling Tests on Piles in Sand," Proc. Fourth International Conf. on Soil Mech. and Found. Eng., London, Vol. II, pp. 43-45.

Jamiolkowski, M. B., and Marchetti, S. (1972), "Discussion of Lateral Load Tests on Full-scale Pile Groups," Proc. Purdue Conf. on Performance of Earth and Earth supported Structures, Vol. III, 1972, pp. 237-240.

Jennings, P. C. (1967), "Force-Deflection Relations from Dynamic Tests," Journal of the Engineering Mechanics Div., Proc. ASCE, Vol. 93, No. EM2, April, 1967, pp. 115-129.

Jennings, P. C. (1968), "Equivalent Viscous Damping for Yielding Structures," Journal of the Eng. Mech. Div., Proc. ASCE, Vol. 94, No. EM1, Feb., 1968, pp. 103-115.

Kajima Institute of Construction Tech. (1973), Dynamic Response of Buildings Supported on Piles Extending Through Soft Alluvial Subsoil Layers, May 14, 1973.

Kim, J. B., and Brungaber, R. J. (1974), "Measuring Pile Deflections with Inclinometer," Journal Geotech. Eng. Div., Proc. ASCE, Vol. 100, No. GT7, July, 1974, pp. 867-869.

Kinoshita, K., and Kishida, H. (1973), "Experimental Study on Vibrational Characteristics of the Structures with Embedded Foundation," Proc. Fifth World Conf. on Earthquake Eng., Rome, 1973, No. 335.

Kishida, H. (1967), "Ultimate Bearing Capacity of Piles Driven into Loose Sand," Soil and Foundations, Journal of Japanese SMFE, Vol. VII, No. 3, August, 1967, pp. 20-29.

Konder, R. L., and Zelasko, J. S. (1963), "A Hyperbolic Stress-Strain Formulation for Sands," Proc. Second Pan American Conf. on Soil Mech. and Found. Eng., Brazil, Vol. 1, 1963, pp. 289-

Kondner, R. L., Pfister, P., and Zelasko, J. S. (1966), "Void Ratio Effects on Lateral Stability of Rigid Poles Partially Embedded in Sands," Highway Res. Record No. 108, Higheay Research Board, Washington, D.C., pp. 42-53.

Koscis, P. (1968), Lateral Loads on Piles, Bureau of Engineering, Chicago, Illinois, 1968, pp. 1-68.

Kubo, K. (1962a), "Experimental Study on the lateral Resistance of Piles-Part 2," (in Japanese) Monthly Reports of Transportation Tech. Research Inst., Vol. 11, No. 12, Ministry of Transportation, Japan, Feb., 1962, pp. 533-559.

Kubo, K. (1962b), "Experimental Study on the Lateral Resistance of Piles-Part 3," (in Japanese) Monthly Reports of Transportation Tech. Res. Inst., Vol. 12, No. 2, Ministry of Transportation, Japan, March, 1962, pp. 181-205.

Kubo, K. (1964), "A New Method for the Estimation of Lateral Resistance of Piles," (in Japanese) Report of Port and Harbour Technical Research Institute Vol. 2, No. 3, Ministry of Trans., Japan, March, 1964, pp. 1-37.

Kubo, K. (1965), "Experimental Study of the Behavior of Laterally Loaded Piles," Proc. Sixth ICSMFE, Montreal, Canada, Vol. II, September, 1965, pp. 275-279.

Kubo, K., Saigusa, P., and Suzuki, A. (1967), "Lateral Resistance of Vertical Anchor Piles," Proc. Third Asian Reg. Conf. Soil Mech. & Found. Eng., Vol. 1, Haifa, pp. 205-209.

Kuhlemeyer, R. L. (1976), Static and Dynamic Laterally Loaded Piles, Research Report No. CE76-9, Dep't of Civil Eng., The University of Calgary, Canada, March 1976, pp. 1-65.

Madhav, M. R., and Kameswara, Rao, N. S. V., and Madhavan K. (1971), "Laterally Loaded Pile In Elasto-plastic Soil," Soils and Foundations, Tokyo, Vol. 11, No. 2, pp. 1-15.

Masao, T., Suzuki, T., Suzuki, S., and Hirasawa, M. (1973), "Dynamic Analysis on Caisson," Symposium on Earth & Earth Structures Under Earthquakes and Dynamic Load," March, 1973, pp. 195-199.

Mathews, P. M. (1958), "Vibrations of a beam on elastic foundation," Zeitschrift fur Angewandte Mathematik und Mechanik, Vol. 38 and 39, 1958 and 1959.

Matlock, H., Ripperger, E. A. (1956), "Procedure and Instrumentation for tests on a Laterally Loaded Pile," Proc. Eighth Texas Conf. on Soil Mech. and Found. Eng., Austin, Texas, 1956.

Matlock, H., Ripperger, E. A., and Fitzgibbon, D. (1956), Static and Cyclic Lateral Loading of an Instrumented Pile, Report to Shell Oil Co., Austin, Texas, July, 1956.

Matlock, H., and Reese, L. C. (1960), "Generalized Solutions for Laterally Loaded Piles," Journal of the Soil Mech. & Found. Eng. Div., Proc. ASCE, Vol. 86, No. SM5, October, 1960 pp. 63-91.

Matlock, H., and Reese, L. C. (1961), "Foundation Analysis of Offshore Pile-supported Structures," Proc. Fifth ICSMFE, Paris, Vol. 2, 1961, pp. 91-

Matlock, H. (1970), "Correlations for Design of Laterally Loaded Piles in Soft Clay," Proc. Offshore Tech. Conf., Vol. I, No. OTC 1204, April, 1970, pp. 577-594.

Matthewson, C. (1969), The Elastic Behavior of Laterally Loaded Piles, Ph. D. Thesis, University of Canterbury, Christchurch, New Zealand, 1969.

Maxwell, A. A., Fry, Z. B., and Poplin, J. K. (1969), "Vibratory Loading of Pile Foundations," Symposium on Performance of Deep Foundations, Proc. ASTM, Special Tech. Publ. No. 444, pp. 338-361.

Mazurkiewicz, B. K. (1968), "Skin Friction on Model Piles in Sand," Bulletin No. 25, Danish Geotech. Inst., Copenhagan, 1968.

McClelland, B., and Focht, J. A., Jr. (1958), "Soil Modulus for Laterally Loaded Piles," Transactions, ASCE, Vol. 123, 1958, pp. 1049-

Medearis, K. and Young, D. (1964), "Energy Absorption of Structures Under Cyclic Loading," Journal of the Soil Mech. & Found. Eng. Div., Proc. ASCE, Vol. 90, No. ST1, Feb., 1964, pp. 61-91.

Meyerhof, G. G. (1959), "Compaction of Sands and Bearing Capacity of Piles," Journal of the Soil Mech. & Found. Eng. Div., Proc. ASCE, Vol. 85, No. SM6, 1959, pp. 1-29.

Mironov, V. V. (1973), "Analysis of Piles of Finite Length Subjected to Horizontal Loads," Osnovanija, Fundamenty i Mekhanika Gruntov, No. 1, pp. 3-6, Jan., 1973.

Mitchell, R. A. (1957), Behavior of Single Piles in Sand due to Horizontal Loads, Master Thesis, University of Florida, Gainsville, Florida, June, 1957.

Mohan, D., and Shrivastava, S. P. (1971), "Nonlinear Behavior of Single Vertical Pile Under Lateral Loads," Third Annual Offshore Tech. Conf., Houston, Texas, April 1971, Vol. 2, No. OTC 1458, pp.

Mononobe, N., and Matso, H. (1932), "Experimental Investigation of Lateral Earth Pressure During Earthquakes," Earthquake Research Institute, Bulletin, No. 10, Tokyo.

Morison, J. R., Johnson, J. W., and O'brien, M. P. (1954), "Experimental Studies of Forces on Piles," Proc. 4th Conf. on Coastal Eng., The Eng. Found. Council on Wave Research, 1954.

Muga, B. J., and Wilson, J. F. (1970), Dynamic Analysis of Ocean Structures, Plenum Press, New York, 1970.

Murthy, V. N. S. (1971), "Non-dimensional Solutions for Laterally Loaded Vertical and Batter Piles Embedded in Cohesionless Soils," Proc. 4th Asian Reg. Conf. Soil Mech. and Found. Eng., Vol. 1, July, 1971, pp. 295-300.

Nair, K. (1969), "Dynamic and Earthquake Forces on Deep Foundations," Performance of Deep Foundations, ASTM Special Technical Publication No. 444, Philadelphia, 1969, pp. 229-263.

Nishida, Y. (1975), "State-of-the-Art and Bibliography for Lateral Resistance of Pile Foundations," (in Japanese) Japanese Association for Steel Pipe Piles, Report No. 1, Tokyo, Japan, 1975, pp. 1-107.

Novak, M. (1971), "Data Reduction From Non-linear Response Curves," Journal of the Eng. Mech. Div., Proc. ASCE, Vol. 97, No. EM4, August, 1971, pp. 1187-1204.

Novak, M. (1973), "The Effect of the Embedment on Vibration of Footings and Structures," Proc. Fifth World Conf. on Earthquake Eng., Rome, 1973, No. 337.

Novak, M. (1974), Dynamic Stiffness and Damping of Piles, Soil Mech, Research Report SM-1-74, University of Western Ontario, London, Canada, 1974.

Novak, M., and Grigg, R. F. (1976), "Dynamic Experiments with Small Pile Foundations," Canadian Geotechnical Journal, Vol. 13, No. 4, 1976, pp. 372-385.

Oteo, C. S. (1972), "Displacements of Vertical Pile Group Subjected to Lateral Loads," Proc. Fifth European Conf. Soil Mech. & Found. Eng., Vol. 1, 1972, pp. 397-406.

Parker, F., Jr., and Cox, W. R. (1969), A Method of Analysis of Pile Supported Foundations Considering the Nonlinear Soil Behavior, Center for Highway Research, Res. Report No. 117-1, Univ. of Texas, Austin, June, 1969.

Parker, F., Jr., and Reese, L. C. (1971), "Lateral pile-Soil Interaction Curves for Sand," Proc. International Symposium on the Engineering Properties of Seafloor Soils and Their Geophysical Identification, Univ. of Washington, Seattle, Washington, July, 1971.

Parmelee, R., Penzien, J., Scheffey, C., Seed, H., and Thiers, G. (1964), Seismic Effects on Structures Supported on Piles Extending Through Deep Sensitive Clays, University of California, Institute of Eng. Research, Berkeley, California, August, 1964.

Penzien, J. (1970), "Soil-Pile Foundation Interaction," Chapter 14, of Earthquake Engineering, Edited by Wiegel, F. L., Prentice-Hall, 1970.

Petrasovits, G. and Awad, A. (1972), "Ultimate Lateral Resistance of a Rigid Pile in Cohesionless Soil," Proc. Fifth European Conf. on Soil Mech. and Found, Eng., Madrid, 1972.

Petrovski, J., and Jurukovski, D. (1975), "Static and Dynamic Test of Piles Under Horizontal Load," Proc. Fifth European Conf. on Earthquake Engineering, Vol. 1, Istanbul, Turkey, Sept., 1975.

Popov, E., and Pinkney, R. (1968), "Behavior of Steel Building Connections Subjected to Inelastic Strain reversals," American Iron and Steel Institute, Bulletin No. 13, Nov., 1968.

Potyondy, J. G. (1961), "Skin Friction Between Various Soils and Construction Materials," Geotechnique, Vol. 11, No. 4, Dec., 1961, pp. 339-353.

Poulos, H. (1971a), "Behavior of Laterally Loaded Piles-Part I, Single Piles," Journal of the Soil Mech. & Found. Eng. Div., Proc. ASCE, Vol. 97, No. SM5, May, 1971, pp. 711-731.

Poulos, H. (1971b), "Behavior of Laterally Loaded Piles-Part II, Group Piles," Journal of the Soil Mech. & Found. Eng. Div., Proc. ASCE, Vol. 97, No. SM5, May, 1971, pp. 733-751.

Poulos, H. G. (1973), "Analysis of Piles in Soil Undergoing Lateral Movements," Journal of the Soil Mech. & Found. Eng. Div., Proc. ASCE, Vol. 99, No. SM5, May, 1973, pp. 391-406.

Prakash, S. (1961), Behavior of Pile Groups Subjected to Lateral Loads, Ph. D. Thesis, University of Illinois, Dec., 1961, pp. 1-229.

Prakash, S., and Agarwal, S. L. (1965), "Study of Vertical Pile Under Dynamic Lateral Load," Proc. Third World Conf. on Earthquake Eng., Vol. 1, 1965, pp. 215-229.

Prakash, S., and Agarwal, S. L. (1966), "Predicting Displacements of Laterally Loaded Piles in Non-cohesive Soils," Journal of the Institution of Engineers (India), Vol. XLVII, No. 1 and 3, pts. CI1 - CI2, Sept. and Nov., 1966.

Prakash, S., and Gupta, L. P. (1970), "A study of Natural Frequency of Pile Groups," Proc. Second Southeast Asian Conf. Soil Eng., Singapore, June, 1970, pp. 401-410.

Prakash, S., and Chandrasekaran, V. (1970), "Deflections of Battered Pile Groups Under Cyclic Lateral Loads," Proc. 2nd Southeast Asian Conf. on Soil Eng., Singapore, June, 1970, pp. 411-421.

Prakash, S., and Singh, A. (1971), "Model Pile Group Subjected to Cyclic Lateral Load," Soils and Foundations, Vol. 11, No. 2, Tokyo, June, 1971, pp. 51-60.

Prakash, S., and Agarwal, H. P. (1971), "Effect of Vibrations on Skin Friction of Piles," Proc. Fourth Asian Reg. Conf. Soil Mech. and Found. Eng., Bangkok, Vol, 1, July, 1971, pp. 203-208.

Prakash, S., and Chandrasekaran, V. (1971), Seismic Analysis of Pile Foundations, Research Report for Khosla Res. and Incentive Award, June, 1971, School of Res. and Training in Earthquake Eng., Univ. of Roorkee, India.

Prakash, S., and Chandrasekaran, V. (1973), "Pile Foundations Under Dynamic Loads," Symposium Earth & Earth Structures Under Earthquakes and Dynamic Loads, March, 1973, pp. 165-173.

Ramanathan, T. S., and Aiyer, P. G. (1970), "Pull out Resistance of Piles in Sand," Journal of the Indian National Soc. of Soil Mech. and Found. Eng., 1970, pp. 189-202.

Reese, L., and Matlock, H. (1956), "Nondimensional Solutions for Laterally Loaded Piles with Soil Modulus Assumed Proportional to Depth," Proc. Eighth Texas Conf. on Soil Mech. and Found. Eng., Univ. of Texas, Austin, Texas, 1956.

Reese, L. C., and Matlock, H. (1960), "Numerical Analysis of Laterally Loaded Piles," Proc. Second Struc. Div. Conf. on Electronic Computation, ASCE, Pittsburg, Sept., 1960, pp. 657-

Reese, L. C., O'Neill, M. W., and Smith, R. E. (1970), "Generalized Analysis of Pile Foundations," Journal of the Soil Mech. & Found. Eng. Div., Proc. ASCE, Vol. 96, No. SM1, Jan., 1970, pp. 235-250.

Reese, L. C. (1973), "A Design Method for an Anchor Pile in a Mooring System," Proc. Annual Offshore Tech. Conf., Houston, Texas, Vol. 1, April, 1973, pp. 209-218.

Richart, F. E., Jr. (1957), "Analysis for Sheet-Pile Retaining Walls," Transactions, ASCE, Vol. 122, 1957, pp. 1113-1138.

Richart, F. E., Jr. (1959), Arching in Granular Elastic Media, Final Report on NSF Grant-G4797, Dep't of Civil Eng., Univ. of Florida, Gainsville.

Richart, R. E. Jr., Hall, J., Jr., and Woods, R. D. (1970), Vibrations of Soils and Foundations, Prentice-Hall, 1970.

Richart, F. E., Jr. (1975), Some Effects of Dynamic Soil Properties on Soil-Structure Interaction, The 10th Terzaghi Lecture, ASCE, Report of Civil Eng. Dep't, Univ. of Michigan, UMEE-75R1, April, 1975, pp. 1-81.

Rowe, P. W. (1956), "The Single Pile Subject to Horizontal Force," Geotechnique, Vol. 6, No. 2, 1956, pp. 70-85.

Sabzvari, A., and Ghahramani, A. (1971), "Dynamic Interaction Between Piles and Dry Sand," Proc. Fourth Asian Reg. Conf. on Soil Mech. and Found. Eng., Bankok, Vol. 1, July, 1971, pp. 209-213.

Sainsbury, R. N. (1973), "Oscillation of Piles-Some Marine Experience," Ground Engineering, Vol. 6, No. 3, 1973, pp. 44-51.

Saul, W. (1968), "Static and Dynamic Analysis of Pile Foundations," Journal of the Structural Div., Proc. ASCE, Vol. 94, No. ST5, May, 1968, pp. 1077-1099.

Schwarz, S. D., and Musser, J. M., Jr. (1972), "Various Techniques for making In-Situ Shear Wave Velocity Measurements-A Description and Evaluation," Proc. International Conf. on Microzonation for Safer Construction, Research and Application, Seattle, Washington, Vol. II, 1972, pp. 593-608.

Schmertmann, J. H. (1970), "Static Cone to Compute Static Settlement Over Sand," Journal of the Soil Mech. and Found. Eng. Div., Proc. ASCE, Vo. 96, No. SM3, May, 1970, pp. 1013-1043.

Shilts, W. L., Graves, L. D. and Driscoll. G. G. (1948), "A Report of Field and Laboratory Tests on the Stability of Posts Against Lateral Loads," Proc. of the 2nd ICSMFE, Rotterdam, 1948.

Shinohara, T., and Kubo, K. (1961), "Experimental Study on the Lateral Resistance of Piles (part 1)," (in Japanese) Monthly Reports of Transportation Tech. Res. Inst., Vol. 11, No. 6, Ministry of Transportation, Japan, July, 1961, pp. 169-242.

Singh, J. P., Donovan, N. C., and Jobsis, A. C. (1975), "Design Procedures for Dynamically Loaded Pile-supported Foundations," Shock and Vibration Problems in Geotechnical Eng., ASCE, National Convention, Denver, Colo., 1975, pp. 1-30.

Singh, A., Hu, R. E. W., and Cousineau, R. D. (1971), "Lateral Load Capacity of Piles in Sand and Normally Consolidated Clay," Civil Engineering, ASCE, Vol. 41, No. 8, August, 1971, pp. 52-54.

Siva Reddy, A., and Ramasamy, G. (1973), "Analysis of an Axially and Laterally Loaded Tapered Pile in Sand," Soils and Foundations, Vol. 11, No. 4, Dec., 1973, Tokyo, pp. 15-28.

Spiller W. R., and Stoll, R. D. (1964), "Lateral Response of Pile," Journal of the Soil Mech. and Found. Eng. Div., Proc. ASCE, Vol. 90, No. SM6, pp. 1-9.

Susbielles, G. G., Bunt, J. R. van den Deluci, G., and Michel, D. (1971), "Wave Forces on Pile Sections due to Irregualr and Regular Waves," Third Annual Offshore Tech. Conf., Houston, Texas, April, 1971, Vol. 1, No. OTC 1379, 12 pp.

Stavnitzer, L. P., and Shekhter, O ya (1971), "Forced Horizontal Pile Vibrations Under the Action of Seismic Waves," Soil Mechanics and Foundation Eng., Vol. 13, No. 5, May, 1971.

Stokoe, K. H. II (1972), Dynamic Response of Embedded Foundations, Ph. D. Thesis, University of Michigan, Ann Arbor, Michigan, 1972.

Stokoe, K. H. II, and Woods, R. D. (1972), "In-Situ Shear Wave Velocity by Cross-Hole Method," Journal of the Soil Mech. and Found. Eng. Div., Proc. ASCE, Vol. 98, No. SM5, May, 1972, pp. 443-460.

Stokoe, K. H. II, and Woods, R. D. (1973), "In-Situ Shear Wave Velocity by Cross-Hole Method,"-Closure, Journal of the Soil Mech. and Found. Eng. Div., Proc. ASCE, Vol. 99, No. SM11, Nov., 1973, pp. 1014-1016.

Tadashi, K. (1974), "Studies on Lateral Resistance of Single Piles Considering Non-linear Properties of Soils," (in Japanese) Japanese Society of Civil Eng., Reports, No. 223, March, 1974, pp. 39-49.

Tajimi, H. (1969), "Dynamic Analysis of a Structure Embedded in an Elastic Stratum," Proc. Fourth World Conf. on Earthquake Engineering, Santiago, Chile, 1969, pp. 54-69.

Takeda, T., and Tachikawa, H. (1969), "Effect of Displacement Rate on Horizontal Soil Reaction in Sand," Soils and Foundations, Vol. 9, No. 2, Tokyo, June, 1969, pp. 15-34.

Terzaghi, K. (1955), "Evaluation of Coefficients of Subgrade Reaction," Geotechnique, Vol. 5, 1955, pp. 297-326.

Tucker, R. L. (1964), "Lateral Analysis of Piles with Dynamic Behavior," Proc. Conf. on Deep Foundations, Mexico, 1964, pp. 151-171.

Valsankar, A. J., and Reddy, A. S. (1970), "Generalized Solutions for Laterally Loaded Pile in Elaso-Plastic Soil" Soil and Foundations, Vol. X, No. 3, Tokyo, Sept., 1979, pp. 66-80.

Valsankar, A. J., and Kameswara Rao, N. S. V. (1973), "Generalized Solutions of Axially and Laterally Loaded Piles in Elasto-Plastic Soil," Soils and Foundations, Vol. 13, No. 4, Tokyo, Dec., 1973, pp. 1-14.

Vesic, A. S. (1964), "Investigation of Bearing Capacity of Piles in Sand," Proc. Conf. on Deep Foundations, Mexico, Vol. 1, 1964, pp. 197-

Vesic, A. S. (1968), "Load Transfer, Lateral Loads and Group Action of Deep Foundations," General Report, Session I, ASTM, Symposium on Deep Foundations, San Francisco, California, 1968.

Waller, R. and Thomas, R. (1970), "Dynamic Behavior of Piled Foundations," Proc. Symposium on Structural Dynamics, Loughborough Univ. of Tech. Dep't of Trans. Tech., England, March, 1970.

Watanabe, N., Harii, K., and Terasaka, M. (1970), "Combined Steel Batter Pile Foundation Method and Its Seismic Properties," Roads, Annual Report, 1970, pp. 17-29.

Winkler, E. (1867), Die Lehre von Elastizität, Prague, 1867.

Wright, D. A., and Coyle, H. M. (1971), "Soil Parameters Required to Simulate the Dynamic Lateral Response of Model piles in Sand," Report of Texas A & M Univ., TAMU-sg-71-219, August, 1971.

Yamamoto, S. (1966-67), "Rocking Vibration of Structures with Piles," Transactions Architectural Institute of Japan,
Part 1: No. 125, July, 1966
Part 2: No. 129, Nov., 1966
Part 3: No. 130, Dec., 1966
Part 4: No. 131, Jan., 1967
Part 5: No. 132, Feb., 1967

Yamamoto, S., and Kometani, N. (1968), "Horizontal Resistance of Pile for Rapidly Reduced Spring System Near Top of Pile," Trans. Architectural Institute of Japan, 1968.

Yamamoto, S., and Kometani, N. (1968), "Rocking Vibration of Structure with Piles placed on Elastic Two Layer System Against Ground Motion," Trans., Architectural Institute of Japan, 1968.

Yamamoto, S., and Seki, T. (1970), "Earthquake Response of Multi-story Building Supported on Piles," Trans., Architectural Institute of Japan
Part 1: No. 177, Nov., 1970 pp. 69-76.
Part 2: No. 178, Dec., 1970 pp. 55-60.

Yamamoto, S., Seki, T., and Suzuki, N. (1971), "Effects of Vibro-Composer and Preloading on the Elastic Modulus of Soil," Trans., Architectural Inst. of Japan, No. 188, Oct., 1971.

Yamashita, I., Inatomi, T., Ogura, K., and Okuyama, Y. (1971), "New Standard Curves in the Port and Harbour Research Institute Method," (in Japanese) Report of the Port and Harbour Research Institute, Vol. 10, No. 1, Ministry of Trans., Japan, March, 1971, pp. 107-168.

Yegian, M., and Wright, S. G. (1973), "Lateral Soil Resistance-Displacement Relationships for Pile Foundations in Soft Clays," Annual Offshore Tech. Conf., Vol. 2, No. OTC 1893, 1973, pp. 663-676.

Yoshida, I., and Yoshinaka, R. (1972), "A Method of Estimate Modulus of Horizontal Subgrade Reaction of Pile," Soils and Foundations, Vol. 12, No. 3, Tokyo, Sept., 1972, pp. 1-17.

Yoshimi, Y. (1964), "Piles in Cohesionless Soil Subject to Oblique Pull," Journal of the Soil Mech. and Found. Eng. Div. Proc. ASCE, Vol. 90, No. SM6, June, 1964, pp. 11-24.